PLETHORA-autophagy axis in plant regeneration

विद्या वाचस्पति की
उपाधि की अपेक्षाओं की आंशिक पूर्ति में प्रस्तुत शोध प्रबंध

A thesis submitted in partial fulfillment of the requirements of the degree of Doctor of Philosophy

द्वारा / By
छात्र का नाम / Name of Student:
आकांशा गांगुली / Akansha Ganguly

पंजीकरण सं. / Registration No.:
२०२०३७११ / 20203711

शोध प्रबंध पर्यवेक्षक / Thesis Supervisor:

प्रो. कालिका प्रसाद / Prof. Kalika Prasad

भारतीय विज्ञान शिक्षा एवं अनुसंधान संस्थान पुणे

INDIAN INSTITUTE OF SCIENCE EDUCATION AND RESEARCH PUNE

2026

"All we have to decide is what to do with the time that is given us."

— Gandalf, The Lord of the Rings, by J.R.R. Tolkien

I dedicate this thesis to

Ms. Sabita Bandyopadhyay

Ms. Binapani Ganguly

Mr. Nitibhushan Bandyopadhyay

Padma Shri Prof. Anil Kumar Ganguly

Baba

"Whatever you are is because of what your ancestors have done."

-Li Lu

Declaration by Student

Name of Student: AKANSHA GANGULY

Reg. No.: 20203711

Thesis Supervisor(s): PROF. KALIKA PRASAD

Department: BIOLOGY

Date of joining program: 01-01-2020

Date of Pre-Synopsis Seminar: 03-12-2025

Title of Thesis: PLETHORA-autophagy axis in plant regeneration

I declare that this written submission represents my idea in my own words and where others' ideas have been included; I have adequately cited and referenced the original sources. I declare that I have acknowledged collaborative work and discussions wherever such work has been included. I also declare that I have adhered to all principles of academic honesty and integrity and have not misrepresented or fabricated or falsified any idea/data/fact/source in my submission. I understand that violation of the above will be cause for disciplinary action by the Institute and can also evoke penal action from the sources which have thus not been properly cited or from whom proper permission has not been taken when needed.

The work reported in this thesis is the original work done by me under the guidance of

Prof. **KALIKA PRASAD**

Date: **27-02-2026** (Signature of the student)

Place: IISER Pune

CERTIFICATE

Certified that the work incorporated in the thesis entitled "**PLETHORA-autophagy axis in plant regeneration**" submitted by **Akansha Ganguly** was carried out by the candidate, under my supervision. The work presented here or any part of it has not been included in any other thesis submitted previously for the award of any degree or diploma from any other University or institution.

Prof. Kalika Prasad

(Supervisor)

Date: 27-02-2026

ACKNOWLEDGEMENTS

This thesis, as it stands today, is a culmination of labour, love, good juju, a whole lot of fried chicken, biryani, and chai. Maybe that is why it reads less like a scientific treatise and more a detective novel. Or maybe that's the fiction writer in my head peeking from her shell, as Kalika declared after the second draft of my manuscript landed on his desk (the first draft was summarily rejected because it was too dry and robotic, go figure).

I can claim as much credit for the questions, experiments, and findings written in this doctoral work, as a lump of batter can claim for becoming a well-made cake. For none of this would exist in its present form without my formidable mentor, Kalika. We met at an interesting junction of our careers, I think. He had newly joined the department and was busy shifting his research group from IISER TVM to IISER Pune, while I was looking for a new PhD supervisor amidst dealing with the sudden loss of my father and the resulting personal upheaval at home. What did he gather from two brief half-hour discussions behind COVID masks I do not know, but his ready acceptance to have me working with him changed my trajectory entirely. It was an entirely surreal experience working with him for many reasons. No person I have met balances ruthless scientific critique and boisterous cheerleading quite like Kalika can. His constant challenging of experiment design, analysis methods, and critical thinking were the whetstone that shaped every part of my journey up to this thesis. It is a privilege few can claim, to work with a mentor who has an intuitive understanding of what each person of their team needs to drive them towards the zenith of their potential, and tailors their approach accordingly. Anyone who has spent a few minutes with him is aware of the sheer depth of his scientific acumen, reasoning, and his infectious enthusiasm for being a researcher. Combined with his total detachment from expecting a comfortable outcome from any experiment, these attributes make him stand out among his peers by every metric one may judge. Working with Kalika means being honed in a crucible of relentless discipline, commitment to independent thought, and uncompromising efforts to achieve scientific excellence. Every person that graduates from his group, does so with heads held high and with tremendous satisfaction to have received such an incredible calibre of scientific mentorship. Now I am also one of them. All my thanks and gratitude to him.

Another one of Kalika's skills is the uncanny knack of picking those people who are generous, jovial, and as committed to joyfully exploring cool science as he is. That's why the lab functions much like the Fellowship of the Ring, except we're all carrying our own rings of power and our journey begins from the fires of Mt. Doom and ends at the Gray Havens. This fellowship has seen many stalwarts come and go, but the spirit of generosity and togetherness always binds us. I was warmly welcomed to this lab by the trinity – Anju, Vijina, and Mabel – along with Aiyaz our postdoc, who ensured I could quickly adapt to the ecosystem and access every resource possible to make my project work. Even though in the initial months after joining, they were at IISER TVM wrapping up their work and other sundry lab tasks, and I was here at Pune trying to figure out plant tissue culture and regeneration, they remained ever accessible through late night sessions to help me navigate through experiments and microscopy protocols. Their intellect, generosity, and warmth were the essence of this lab's ethos, and I gladly took

part in this endeavour. I entered this lab at Pune along with Srijan, who is this group's Batman, Samwise, and right-hand man for all intents and purposes – scientific, gastronomic, adventurous – or otherwise. Other members of the fellowship – Ankita, Yamini, Kreedika, Deepshikha, Ashmita, Sonal – joined after me and added more colour and oomph with their own traits and idiosyncrasies. In Ankita, I found a disciple willing to learn finance and assorted nefarious lab tricks, with Kreedika, a fellow tea addict, and with everyone together – a bonafide squad of regeneration, microscopy, and fun-loving zealots. My thanks to each and every one of them for ensuring a vibrant and joyful lab environment and being a team, I am most happy to call myself part of.

One of the many pros of being at IISER is the opportunity to work with incredibly talented undergraduates who make me aspire to become a colleague they can trust and learn from. Among them I count Yadhu, Saket, Komal, Atharva, Ameya, Parth, Anugraha, Gaurav, Souparnika, and countless more. The quest to become a good researcher and rational thinker cannot succeed if one is not challenged to revise their ideas and concepts, which is something these young students do with an alacrity that amazes me. I deeply thank them for being an essential part of my own growth as a researcher and an amateur mentor. Their daily shenanigans and antics would brighten my days and make the lab a workplace I always looked forward to going every day.

While working on my thesis paper, I had the privilege and opportunity to work with Aabha – our new PhD joinee, and Komal – an undergrad student. Their dedication, enthusiasm, and commitment to work with seamless sync and help me reach the final goal made them my dream team, and colleagues I am proud to work with. They have shown incredible potential at such an early stage of their careers, I cannot wait to see what comes next!

Many many thanks to our wonderful collaborators – Viola Willemsen, Lin Xu, and Yasin Dagdas – for generously sharing their reagents and feedback with us to keep my project going smoothly. Their feedback and advice were crucial to finetune my experiments and enhance my own understanding and appreciation of this work.

My PhD batchmates have been my backbone and true companions on this ride. They saw me at my lowest, and were the best, most boisterous supporters one could ask for. Our late-night tea and biryani sessions were the best and every 'baithak' was memorable. Benchamin, Akash, Rushik, and Nikki – your friendship was my lifeboat in every way possible. Benchamin, Ashwin, Arnab, Sanjana (with her cats) were people that shamelessly entered my life on campus, and have now become extended family. My best fooding, outing, and general hangout people. Along with them, I include the chambers of my heart, my close friends – Souja, Ruchicka, and Aish, who kept me going even from hundreds of miles away. I thank you all.

The microscopy facility here at IISER Pune is the best technical arm of the department, with some world-class scopes and facilities, meticulously maintained by Santosh and Vijay, our facility specialists. They were indispensable for all microscopy and related analyses, which are the experimental backbone of my thesis. Many thanks to them.

The biology dept functions like a well-oiled engine entirely because of Piyush, Kalpesh, Hariprasad, Mahesh, Mrinalini, Sandeep, Sachin, and Rupali, our bio-office team members. They work tirelessly behind the scenes to keep the department running well, from procuring reagents, maintaining the bio-store, repairing our overworked lab instruments, to organizing any department event with maximum efficiency, and accommodating all our working needs. Many thanks for making this department a good workplace.

Having mentioned tea several times until now, I would be remiss to not thank the people at MDP and Shivsagar for constantly providing good tea, food and fuel. They nurtured my 'badi-chai' addiction faithfully at all times. Thank you so much! Special thanks to hostel food suppliers, Kaka's Kitchen and Khaidai, for tasty meals all these years.

No research can be done with peace of mind if not sustained financially. I acknowledge DBT for providing my research stipend, along with funding our lab grants. For the latter I also thank DST-SERB, and the ANRF. Thank you for funding our science.

I end my acknowledgements by categorically stating that none of this would have manifested without the ferocious support, love, and encouragement of Ma, Baba, Mamu, Dada, Bhaiyya, Didibhai, Onida, Mou, Jeju, Amma, and Haha. When I say I grew up with 3 sets of parents and 3 siblings, I mean it. Ganguly and associates are a family I am beyond fortunate to be part of. You are the village that raised me, and watched from near, far and now the heavens above, as I took this journey. It will require another thesis to explain what each of you means to me, so I end with only this. THANK YOU.

- Akansha Ganguly

"Home is now behind you, the world is ahead!"
— J.R.R. Tolkien

Copyright Statement

Parts of the data and the text presented in this thesis have been adapted from the publications given below. The representation is in compliance with the copyright policy and with prior permission from the publishers.

1. A. Ganguly, A. Humnabadkar, K. Gautam, V. Willemsen, L. Xu, Y. Dagdas, & K. Prasad, PLETHORA–autophagy axis activates organ regeneration through ROS modulation, *Proc. Natl. Acad. Sci. U.S.A.* 123 (6) e2513954123, https://doi.org/10.1073/pnas.2513954123 (2026). (*Featured on Cover, highlighted in Commentary: More than a blueprint: Developmental regulators secure the cellular environment for regeneration*, *https://doi.org/10.1073/pnas.2600463123 (2026)*)

PUBLICATIONS

1. A. Ganguly, A. Humnabadkar, K. Gautam, V. Willemsen, L. Xu, Y. Dagdas, & K. Prasad, PLETHORA–autophagy axis activates organ regeneration through ROS modulation, *Proc. Natl. Acad. Sci. U.S.A.* 123 (6) e2513954123, https://doi.org/10.1073/pnas.2513954123 (2026). (*Featured on Cover, highlighted in Commentary: More than a blueprint: Developmental regulators secure the cellular environment for regeneration*, *https://doi.org/10.1073/pnas.2600463123 (2026)*)

2. Mathew, M. M., Ganguly, A., & Prasad, K. (2024). Multiple feedbacks on self-organized morphogenesis during plant regeneration. *New Phytologist*, *241*(2), 553-559.

THESIS SYNOPSIS

Every organism is susceptible to environmental pressures during their life-cycle, that include predation, pathogens, and environmental pressure. Among higher-order organisms, both the plant and animal kingdoms have complex eukaryotes with specialized organ systems and stem cell niches. While in animals, physical or chemical stress is mitigated by specific cell lineages that can migrate towards or away from the site of injury, plants are constrained by their rigid cell walls and thus rely on the transmission of signals through cell-cell contacts or through the vascular system (1, 2). Despite these limitations, plants possess an extraordinary capacity for wound repair and regeneration across diverse tissues that allows for the age-old practices of plant propagation. Irrespective of the organism, any cellular injury will disrupt homeostasis and trigger stress signals in the vicinity of the wound. How do plants mitigate these stress signals, initiate cellular reprogramming, and regenerate lost tissue, is a Pandora's Box that has long fascinated plant biologists. Furthermore, regeneration covers a spectrum of cell-fates ranging from wound-healing, cell proliferation, stem cell reprogramming, up to *de novo* organogenesis to replace lost or damaged tissue (3). These cell-fates are the outcome of complex genetic and biochemical networks activated at the site of injury. Depending on the injury context, wound induced signals are translated into different modes of survival and rejuvenation such as apoptosis, autophagy, and programmed cell-death (PCD) (4–8). Among aerial plant organs, detached leaves can either undergo local cell proliferation to form a wound-induced callus, or create *de novo* adventitious roots (9). This diversity invites exploration into an essential question – what pathways determine regenerative cell-fate post injury?

Objectives of this thesis:

Using the binary regenerative response of excised leaves, this thesis aims to answer the following objectives-

1. How do cell stress-response pathways like autophagy impact cell-fate post injury?
2. What are the key genetic regulators of autophagy during plant regeneration?
3. How do these genetic modules influence cellular behaviour post injury?
4. How does autophagy-mediated stress management influence cell-fate transitions during organ regeneration?

Chapter 1

This chapter provides an introduction to the principles of wound induced regeneration in plants. This chapter explores the core components of the plant regeneration response post wounding in roots and aerial organs. In aerial organs, the mechanisms regulating callus proliferation, *de novo* organ regeneration, as well as vascular regeneration are discussed. Following this, the chapter introduces the spectrum of cellular stress signals experienced by plants during the process of wound perception and repair. Here it touches on how universal processes such as autophagy and PCD, that are activated post injury, impact cellular homeostasis and reprogramming in plants. The chapter uses extant literature to discuss the interesting, unanswered open questions in these areas, of which some were investigated and worked on for this thesis.

Chapter 2

This chapter contains the experimental design and step-by-step protocols used to investigate the role of autophagy and its key regulators during wound healing and organ regeneration from excised leaves in *Arabidopsis thaliana*. Experimental procedures include confocal microscopy of live and fixed samples, qPCR for gene transcript levels and promoter occupancy, regeneration assays with relevant pharmacological treatments, with the relevant statistical tests. All reagents, culture media and buffer recipes, plant materials, and plasmid constructs used in this thesis are detailed here. Reagents from other research groups are duly mentioned along with citations.

Chapter 3

The role of plant autophagy in chemical stress, nutrient starvation, herbivory, and pathogen immune response has been previously studied. However, its role in plant regeneration has been confined to studying autophagy-related gene (*ATG*) mutant phenotypes during tissue culture and grafting (10–12). Chapter 3 of this thesis shows how autophagy is activated during *de novo* organ regeneration from excised plant leaves with contact, but not during wound-induced callus formation. Genetic and molecular experiments reveal that among the known *ATG8* genes in *A. thaliana*, specific members of the *ATG8* gene family, *ATG8B-ATG8C-ATG8F-ATG8H*, are essential for *de novo* root regeneration. *De novo* root regeneration in excised leaves is a multistep process that includes the formation of an endogenous healing callus at the cut end where root founder cell expressing WOX11, a known regeneration factor, are formed, from where root primordium stem cells eventually differentiate and emerge (13).

This chapter shows that WOX11^{+} founder cell fate is not unique to the root regeneration response and is formed during wound-callus formation too. Furthermore, inhibition of autophagy either by genetic or pharmacological means does not interfere with founder cell formation post injury. Taken together, the results show how autophagic response coordinated by specific *ATG8* genes is essential to *de novo* organ regeneration and not wound-callus formation, and is likely to operate downstream of founder cell differentiation.

Chapter 4

While autophagy in plants is largely studied by the biochemistry of ATG protein interactions, the upstream genetic modules necessary to sustain their transcriptional output remain relatively less explored (14, 15). Previous studies have shown that the PLETHORA (PLT) family of transcription factors (TFs) are plant specific regulators essential for several developmental and regenerative processes (9, 16, 17). The known downstream targets of PLTs include other TFs such as PLT1/2 and CUC2, but other effectors are yet unknown (17, 18). Here using genetic and molecular approaches, this chapter shows that PLT7 transcriptionally activates *ATG8* genes, specifically *ATG8F*, during *de novo* root regeneration. Imaging the PLT7-vYFP translational reporter in excised leaves both with and without contact reveals an expression pattern that closely resembles the *ATG8F* promoter domain, and mutant analyses reveal that the loss of PLT7 significantly affects *de novo* root regeneration and *ATG8* gene expression during the process. *In toto*, this chapter discovers that PLT7 transcriptionally upregulates autophagy by *ATG8F* gene activation during *de novo* root regeneration.

The PLT factors mainly PLT3, PLT5, and PLT7, are known to function redundantly during development and regeneration, and their triple loss-of-function mutant is deficient in *de novo* root regeneration (9, 18). Since PLT7 transcriptionally regulates *ATG8* genes for *de novo* root regeneration, and loss of PLT7 alone significantly affects the phenotype, the regeneration frequencies of other *plt* mutants was analysed. Strikingly, PLT3 is both necessary and sufficient to activate *de novo* organ regeneration from excised leaves. Using different transgenic backgrounds, this chapter illustrates how the PLTs, thought to be redundant in expression and function, have evolved unique non-overlapping roles during this specific regeneration process. PLT3 functions upstream of the PLT7-*ATG8* module during *de novo* root regeneration, and is activated early post-injury. Interestingly, while loss of PLT3 significantly downregulates PLT7, PLT7 overexpression or loss does not affect PLT3 levels during *de novo* root regeneration. The loss of root regeneration in a PLT3 genetic mutant could be partially rescued by *ATG8F*

overexpression, highlighting the importance of autophagy as a pivotal downstream mechanism by which PLT3 regulates *de novo* root regeneration. Strikingly, expressing PLT3 in the PLT7 promoter domain completely rescues root regeneration like the full-length PLT3 translational fusion, whereas PLT7 in the PLT3 promoter domain partially rescues the process. The results of this chapter reveal a hitherto unknown layer of complexity among the PLT family that emerges during *de novo* root regeneration, and provide interesting insights into finer aspects of the PLT-*ATG8* regulatory axis discovered in this study.

Chapter 5

Chapters 4 entailed thorough molecular and genetic analyses of how the PLT-*ATG8* axis activates *de novo* organ regeneration. However, autophagy is an intracellular, cytoplasmic process involving the recycling and removal of cellular parts within the plant lytic vacuole to restore homeostasis (19). It becomes imperative to understand the cellular consequences of this axis in the cells surrounding the site of injury, and how does this impact cellular reprogramming. Chapter 5 utilizes extensive live-imaging of mesophyll cells near the site of injury to observe "cellular behaviour" post injury. Tracking the real-time dynamics of the lytic vacuole and surrounding chloroplasts in the cytosol, this chapter's findings unveil how in cells with contact, chloroplasts actively migrate into the vacuole lumen in mesophyll cells, a hallmark feature of organelle turnover during autophagy (20–22). Interestingly, these chloroplast dynamics are severely compromised in cells without contact, and also upon perturbing the PLT-*ATG8* axis. The findings from this chapter paint an emerging picture of the consequences of disrupting the PLT-*ATG8* axis on the cells undergoing active reprogramming post injury, that evidently affect the regeneration phenotype.

Loss of organelle turnover and recycling in cells post injury would undoubtedly lead to buildup of intracellular stress and prevent restoration of cellular homeostasis (23–25). With this in mind, the levels of reactive oxygen species (ROS) in cells near the site of injury were assessed using H2-DCFDA, an ROS responsive fluorescent probe. In the wildtype, while ROS levels surge early post injury irrespective of the regeneration response, leaves with contact show a spatiotemporal modulation of ROS, whereas those without contact show accumulation of ROS over time. ROS levels are also dramatically increased in *PLT* and *ATG8* mutants, supporting the notion that loss of the PLT-*ATG8* axis affects ROS regulation and cellular redox balance. However, a brief pulse of ROS scavenger treatment is sufficient to activate *de novo* root regeneration across all *plt* and *atg8* mutants, irrespective of the leaf 'contact' pose. Taken

together, the findings of this chapter illuminate how the precise spatio-temporal regulation of wound-induced ROS by the PLT-*ATG8* axis is an essential pre-requisite of *de novo* root regeneration. The controlled regulation of ROS by PLT-*ATG8* is essential to create the correct cellular redox environment for the differentiation of root founder cells into root primordium stem cells, marked by the root stem cell regulator WOX5. This chapter brings to the fore how the control of ROS by a finely-tuned autophagy response presents a physiological threshold between cell proliferation and differentiation, that promotes diverse regenerative fates in plants.

Chapter 6

This chapter summarizes the key findings of Chapters 3-5 and discusses the fundamental insights into the role of cellular homeostasis mechanisms in cell-fate transitions discovered in this work. Through a variety of genetic, molecular, and cellular approaches, this study illustrates how plants use their developmental regulators to deploy a universal, kingdom-wide cellular process like autophagy to enable organ regeneration. Moreover, key plant factors like PLTs have evolved novel regulatory interactions in tandem with cellular survival mechanisms, that work synergistically to alleviate cell-stress and activate stem cell regulator expression. This study's findings reveal how plants harness kingdom-specific developmental regulators to activate ancient cell survival pathways, alleviating wound-induced stress and promoting organ regeneration.

REFERENCES

1. K. D. Birnbaum, A. S. Alvarado, Slicing across kingdoms: regeneration in plants and animals. *Cell* **132**, 697–710 (2008).
2. K. Sugimoto, S. P. Gordon, E. M. Meyerowitz, Regeneration in plants and animals: Dedifferentiation, transdifferentiation, or just differentiation? *Trends Cell Biol.* **21**, 212–218 (2011).
3. M. M. Mathew, K. Prasad, Model systems for regeneration: Arabidopsis. *Development (Cambridge)* **148** (2021).
4. C. Gordy, Y. W. He, The crosstalk between autophagy and apoptosis: Where does this lead? *Protein Cell* **3**, 17–27 (2012).
5. M. Dickman, B. Williams, Y. Li, P. Figueiredo, T. Wolpert, Reassessing apoptosis in plants. *Nature Plants 2017 3:10* **3**, 773–779 (2017).
6. D. V. Savatin, G. Gramegna, V. Modesti, F. Cervone, Wounding in the plant tissue: The defense of a dangerous passage. *Front. Plant Sci.* **5**, 111139 (2014).

7. R. K. Monson, A. M. Trowbridge, R. L. Lindroth, M. T. Lerdau, Coordinated resource allocation to plant growth–defense tradeoffs. *New Phytologist* **233**, 1051–1066 (2022).

8. S. A. Eming, P. Martin, M. Tomic-Canic, Wound repair and regeneration: Mechanisms, signaling, and translation. *Sci. Transl. Med.* **6**, 265sr6 (2014).

9. A. P. Shanmukhan, *et al.*, Regulation of touch-stimulated de novo root regeneration from Arabidopsis leaves. *Plant Physiol.* (2021). https://doi.org/10.1093/PLPHYS/KIAB286.

10. J. V. Kanne, *et al.*, Overexpression of ATG8/LC3 enhances wound-induced somatic reprogramming in Physcomitrium patens. *Autophagy* **18**, 1463–1466 (2022).

11. E. Rodriguez, *et al.*, Autophagy mediates temporary reprogramming and dedifferentiation in plant somatic cells. *EMBO J.* **39**, e103315 (2020).

12. K. I. Kurotani, *et al.*, Autophagy is induced during plant grafting to promote wound healing. *Nature Communications 2025 16:1* **16**, 3483- (2025).

13. L. Xu, De novo root regeneration from leaf explants: wounding, auxin, and cell fate transition. *Curr. Opin. Plant Biol.* **41**, 39–45 (2018).

14. C. Yang, M. Luo, X. Zhuang, F. Li, C. Gao, Transcriptional and Epigenetic Regulation of Autophagy in Plants. *Trends in Genetics* **36**, 676–688 (2020).

15. W. Agbemafle, M. M. Wong, D. C. Bassham, Transcriptional and post-translational regulation of plant autophagy. *J. Exp. Bot.* **74**, 6006–6022 (2023).

16. A. Kareem, *et al.*, PLETHORA genes control regeneration by a two-step mechanism. *Current Biology* **25**, 1017–1030 (2015).

17. D. Radhakrishnan, *et al.*, A coherent feed-forward loop drives vascular regeneration in damaged aerial organs of plants growing in a normal developmental context. *Development (Cambridge)* **147** (2020).

18. W. Liu, *et al.*, Transcriptional landscapes of de novo root regeneration from detached Arabidopsis leaves revealed by time-lapse and single-cell RNA sequencing analyses. *Plant Commun.* **3**, 100306 (2022).

19. K. Yoshimoto, Y. Ohsumi, Unveiling the Molecular Mechanisms of Plant Autophagy—From Autophagosomes to Vacuoles in Plants. *Plant Cell Physiol.* **59**, 1337–1344 (2018).

20. M. Izumi, H. Ishida, S. Nakamura, J. Hidema, Entire Photodamaged Chloroplasts Are Transported to the Central Vacuole by Autophagy. *Plant Cell* **29**, 377–394 (2017).

21. C. Wan, *et al.*, Selective autophagy regulates chloroplast protein import and promotes plant stress tolerance. *EMBO J.* **42** (2023).

22. H. Ishida, K. Yoshimoto, Chloroplasts are partially mobilized to the vacuole by autophagy. *Autophagy* **4**, 961–962 (2008).

23. S. Michaeli, G. Galili, Degradation of Organelles or Specific Organelle Components via Selective Autophagy in Plant Cells. *International Journal of Molecular Sciences 2014, Vol. 15, Pages 7624-7638* **15**, 7624–7638 (2014).

24. A. L. Anding, E. H. Baehrecke, Cleaning House: Selective Autophagy of Organelles. *Dev. Cell* **41**, 10–22 (2017).

25. J. Wang, Q. Zhang, Y. Bao, D. C. Bassham, Autophagic degradation of membrane-bound organelles in plants. *Biosci. Rep.* **43** (2023).

LIST OF CONTENTS

CERTIFICATE....5
ACKNOWLEDGEMENTS....6
PUBLICATIONS....10
THESIS SYNOPSIS....11
LIST OF CONTENTS....18
LIST OF FIGURES....21
ABBREVIATIONS....23
ABSTRACT....25
CHAPTER 1 Introduction....26
1.1 Introduction....27
1.2 Wound-induced regeneration responses in roots....28
1.3 Wound-induced regeneration responses in aerial organs....31
1.3.1 Wound-induced callus formation....32
1.3.2 *De novo* root regeneration....34
1.3.3 *De novo* shoot regeneration....36
1.4 Vascular regeneration....37
1.5 Wound signalling – hedging between survival and regeneration....40
1.5.1 How is a wound perceived?....42
1.5.2 Wound signalling cascades instruct both cell survival and cell death....43
CHAPTER 2 Materials and Methods....45
2.1 MATERIALS....46
Table 1. Plant lines used in this study....46
Table S2. List of recombinant plasmids used in this study....47
Table 3. List of primers used in this study....49
2.2 METHODS....57
2.2.1 Plant materials and growth conditions....57
2.2.2 Contact-mediated regeneration assay....57
2.2.3 Molecular cloning and plant transformation....59
2.2.4 Sample fixation, clearing, and confocal microscopy....60
2.2.5 Live sample confocal microscopy....61
2.2.6 H_2DCFDA staining and live microscopy....62
2.2.7 RNA extraction and RT-qPCR....62

2.2.8 Chromatin immunoprecipitation (ChIP) 62
2.2.9 Image analysis 64
CHAPTER 3 Autophagy activation is essential for de novo root regeneration, and dispensable for wound healing 66
3.1 INTRODUCTION 67
3.2 RESULTS 68
3.2.1 Cellular events that instruct organ regeneration are initiated rapidly post wounding 68
3.2.2 Autophagy is activated during *de novo* root regeneration, but not during wound-induced callus formation 69
3.2.3 Autophagy response for *de novo* root regeneration is coordinated by specific members of the *ATG8* gene family 72
3.2.4 Activation of autophagy is essential to promote procambium reprogramming during *de novo* root regeneration, but not founder cell identity 77
3.3 DISCUSSION 80
CHAPTER 4 PLETHORA factors non-redundantly activate ATG8 genes during de novo root regeneration 82
4.1 INTRODUCTION 83
4.2 RESULTS 84
4.2.1 PLT7 transcriptionally activates *ATG8* genes during *de novo* root regeneration 84
4.2.2 PLT7 expression pattern recapitulates *ATG8F* during *de novo* root regeneration, and remains unchanged by loss of *ATG8F* 87
4.2.3 PLT3 and PLT7 have novel, non-redundant functions during *de novo* root regeneration 89
4.2.5 PLT3 both directly and indirectly activates *ATG8* genes during *de novo* root regeneration 97
4.3 DISCUSSION 100
CHAPTER 5 The PLT-ATG8 axis is essential to coordinate organelle turnover and modulate ROS levels during de novo root regeneration 103
5.1 INTRODUCTION 104
5.2 RESULTS 105
5.2.1 Autophagy activation leads to coordinated organelle turnover during *de novo* root regeneration 105
5.2.2 Disrupting the PLT-*ATG8* axis severely compromises organelle turnover and impairs *de novo* root regeneration 108
5.2.3 Wound-induced ROS is spatiotemporally stabilized during *de novo* root regeneration and not during wound-induced callus formation 111

5.2.4 PLT-*ATG8* axis mediated modulation of ROS levels is essential for *de novo* root regeneration....112
5.2.5 PLT-autophagy-ROS module promotes stem cell activation during *de novo* root regeneration....117
5.3 DISCUSSION....119
CHAPTER 6 Conclusions and broader perspectives of this thesis....121
6.1 Thesis Summary....122
6.2 Autophagy is dispensable for wound healing in plants, and activated specifically during organ regeneration....122
6.3 Plant-specific PLETHORA factors transcriptionally regulate autophagy genes in a non-redundant manner during *de novo* root regeneration....124
6.4 The PLT-autophagy axis stabilizes wound-induced ROS and restores cellular homeostasis to the optimal levels necessary for *de novo* root regeneration....126
6.5 Summary....128
CHAPTER 7 References....129

LIST OF FIGURES

Figure 1.1 Schematic showing regeneration response in roots in diverse contexts. 30
Figure 1.2 Comparison of different callus types. 33
Figure 1.3 De novo root regeneration post wounding in aerial organs. 35
Figure 1.4 Vascular regeneration in plants. 39
Figure 1.5 Interplay of wound signals and cellular reprogramming post wounding. 42
Figure 3.1 Early events post wounding are sufficient to determine organ regeneration fate. .69
Figure 3.2 Autophagy is activated during *de novo* root regeneration but not during wound-induced callus formation. 72
Figure 3.3 *ATG8* genes are differentially activated between de novo root regeneration and wound induced callus formation. 73
Figure 3.4 *ATG8F* promoter activity gradually increases during de novo root regeneration. .74
Figure 3.5 Functional depletion of *ATG8* genes impairs *de novo* root regeneration only. 75
Figure 3.6 Severe genetic or pharmacological inhibition of autophagy impairs de novo root regeneration. 76
Figure 3.7 Autophagy activation promotes procambial stem cell activity during *de novo* root regeneration. 78
Figure 3.8 Founder cell specification and endogenous callus formation remains unaffected by the loss of autophagy either by pharmacological or genetic means. 79
Figure 4.1 PLT7 DAP-seq analyses indicate possible binding of PLT7 to *ATG8* gene loci 85
Figure 4.2 PLT7 transcriptionally activates *ATG8F* during *de novo* root regeneration. 86
Figure 4.3 PLT7 reporter expression resembles the *ATG8F* promoter pattern during *de novo* root regeneration. 88
Figure 4.4 PLT3 is both necessary and sufficient for *de novo* root regeneration. 90
Figure 4.5 Loss of PLT3 does not affect founder cell identity, but interferes with procambium activity during de novo root regeneration. 91
Figure 4.6 PLT3 expression domain is restricted to the procambium and the endogenous callus during de novo root regeneration. 93
Figure 4.7 PLT3 transcriptionally activates PLT7 during de novo root regeneration, but not vice-versa. 94
Figure 4.8 PLT3 and PLT7 retain their wound-induced expression patterns with high fidelity even under heterologous PLT promoters. 96
Figure 4.9 PLT3 directly upregulates *ATG8H* and indirectly activates *ATG8F* during *de novo* root regeneration. 98

Figure 4.10 Constitutive ATG8F can partially rescue *de novo* root regeneration in *plt3* loss-of-function mutant 99
Figure 5.1 *De novo* root regeneration necessitates autophagy for coordinated organelle turnover in cells post wounding. 106
Figure 5.2 Genetic disruption of the PLT-*ATG8* axis severely compromises organelle turnover in cells post wounding. 109
Figure 5.3 Analysis of intravacuolar chloroplast localization and turnover during *de novo* root regeneration..... 110
Figure 5.4 Wound-induced ROS accumulates in cells at the cut end of excised leaves and is spatiotemporally regulated during *de novo* root regeneration. 111
Figure 5.5 Disrupting the PLT-*ATG8* regulatory axis leads to ectopic accumulation of ROS. 113
Figure 5.6 Excessive ROS impairs *de novo* root regeneration, while optimal ROS levels boost *de novo* root regeneration..... 114
Figure 5.7 ROS quenching by external means successfully boosts *de novo* root regeneration across *PLT* and *ATG8* mutants irrespective of contact. 115
Figure 5.8 Regulation of ROS levels by the PLT-autophagy module activates root stem regulator expression and drives *de novo* root regeneration. 117
Figure 6.1 Restoration of cellular homeostasis instructs regenerative fate post wounding... 127

ABBREVIATIONS

AP2 – APETALA2

At – Arabidopsis thaliana

CBF3 – C-REPEAT BINDING FACTOR 3

Ca^{2+} - calcium ions

ChIP – Chromatin Immuno-precipitation

CHX – cycloheximide

CIM – Callus Inducing Medium

Col – Columbia ecotype

CUC – CUP-SHAPED COTYLEDON

DPC – Days post cut

DAMP – Damage Associated Molecular Patterns

H_2-DCFDA – 2′,7′-Dichlorodihydrofluorescein diacetate

DEX – Dexamethasone

DNRR – *de novo* root regeneration

DPG – Days post germination

ESR – ENHANCER OF SHOOT REGENERATION

ERF – ETHYLENE RESPONSE FACTOR

EST – Estradiol

g – gram

GFP – Green Fluorescent Protein

GLR – Glutamate Receptor-Like

GR – Glucocorticoid Receptor

H – Hour

JA – jasmonic acid

LBD – LATERAL ORGAN BOUNDARIES DOMAIN

mg – milligram

ml – milliliter

mm – millimeter

MS – Murashige and Skoog medium

3-MA – 3-methyladenine

NAC – N-acetyl cysteine

PAMP – Pathogen Associated Molecular Patterns

PFD – perfluorodecalin

PI – Propidium Iodide

PLT – PLETHORA

PXY – PHLOEM INTERCALATED WITH XYLEM

QC – quiescent center

qRT-PCR – Quantitative Real-Time Polymerase Chain Reaction

RAM – Root Apical Meristem

RBR – RETINOBLASTOMA-RELATED

RNS – Reactive nitrogen species

ROS – Reactive oxygen species

rpm – rotations per minute

rcf – relative centrifugal force

ROI – Region of Interest

s.e.m –standard error of mean

SAM – Shoot Apical Meristem

SCR – SCARECROW

SHR – SHORTROOT

SIM – Shoot Induction Medium

UTR – Untranslated region

UV – Ultra Violet

WIND – WOUND INDUCED DEDIFFERENTIATION

WHR – wound healing response

WOX – WUSCHEL-RELATED HOMEOBOX

WT – WT

WUS – WUSCHEL

vYFP – Venus-Yellow Fluorescent Protein

YUC – YUCCA

µg – microgram

µL – microliter

µm – micrometer

ABSTRACT

All life-forms in the world exhibit growth and respond to stimuli, where this response plays an extrinsic role in shaping organismal longevity beyond the default genetic blueprint. Both plants and animals are higher-order eukaryotes with complex organ systems and specialized stem cell niches. However, plants are especially vulnerable to injury and cellular stress due to their non-motile physiology and continual dependence on external developmental cues. Despite these limitations, the plant kingdom displays remarkable cellular and organ-level regenerative capacities, ranging from simple wound healing to local cell proliferation and even *de novo* organogenesis. This raises an essential question–what pathways determine these different cell-fates in damaged plant tissue?

In this thesis, I leveraged the regenerative plasticity of detached plant leaves to explore the mechanisms regulating wound healing and organ regeneration in *Arabidopsis thaliana*. Here I discovered that autophagy, an ancient cellular recycling process, is essential for *de novo* root regeneration but completely dispensable for wound-callus formation at the cut end of an excised leaf. Interestingly, this phenotype hinges on the transcriptional upregulation of specific genes in the *ATG8* (autophagy-related gene 8) family, specifically *ATG8F* and *ATG8H*. Using a suite of molecular and genetic tools, I established that the plant-specific developmental regulators PLETHORAs (PLT) activate these *ATG8* genes during *de novo* root regeneration. A striking observation from this work is that the PLTs operate in distinct, non-overlapping roles during this particular regeneration process, which was not seen across developmental or regenerative phases in previous studies. Herein, PLT3 transcriptionally upregulates PLT7, and both PLT3 and PLT7 directly activate *ATG8H* and *ATG8F* during *de novo* root regeneration. Perturbing the PLT-*ATG8* genetic axis severely compromises organelle turnover in cells post injury, and this compromised cellular homeostasis leads to the ectopic accumulation of ROS in cells undergoing active reprogramming during *de novo* root regeneration. However, external ROS quenching successfully boosts rooting, and restoring this redox balance is essential for the activation of stem cell regulators for *de novo* root regeneration. Taken together, my findings reveal the role of plant-specific developmental regulators in the focused activation of a cellular quality-control mechanism conserved across kingdoms to manage cellular stress and facilitate *de novo* root regeneration in plants. This thesis provides genetic, molecular, and cellular insights into how plants selectively channel autophagy and ROS to facilitate the specific cell-fate transitions required for *de novo* root regeneration.

CHAPTER 1

Introduction

"Set your course by the stars, not by the lights of every passing ship."

– Omar Bradley

1.1 Introduction

The ability to grow, and respond to external stimuli, are intrinsic properties of all lifeforms, whether simple or complex. Among multicellular organisms, plants are especially vulnerable to frequent injury and external stress due to their sessile nature and dependence on abiotic factors as development cues (26, 27). To overcome these challenges, plants have evolved an arsenal of stress-response pathways, which are similar as well as different from animals. Both kingdoms deploy wound signalling cascades that activate cell rejuvenation, wound healing and tissue repair, culminating into varied regeneration responses (1, 2, 28–32). Regeneration and wound healing in higher-order animal models remain confined to specific stem cell lineages, wherein differentiated cells must migrate long distances in response to chemokines (33, 34). Plant cells are encased in rigid cell walls that prevent any cell migration, and the stem cell niches are confined to the apical meristems and the vascular procambium. Despite this, plants exhibit ubiquitous regenerative fates and can repair wounds through rapid local cell reprogramming to close off the injury site by cell proliferation, as well as regenerate adventitious roots or shoots *de novo*. In the laboratory context for ease of experimentation, these regenerative responses can be broadly categorized as tissue-culture mediated regeneration, and mechanical injury-induced regeneration (3, 35). The tissue-culture method of *de novo* organogenesis follows the age-old facile technique of vegetative propagation using any explant, where calibrated ratios of auxin and cytokinin in culture media instruct the formation of roots and shoots either directly or via an intermediate pluripotent callus stage (3, 36, 37). Conversely, in response to mechanical injury, plants deploy rapid wound repair pathways that culminate in either local cell proliferation to prevent pathogen exposure, or the complete regeneration of *de novo* organs to replace lost parts, an ability vital to asexual (clonal) propagation in horticulture (1, 35, 38).

However, whether from biotic or abiotic stressors, wounding is a constant environmental pressure for all complex lifeforms. It damages tissue integrity, exposes cells to shear stress and pathogens, and also causes loss of vital metabolites. As a result, both plants and animals have evolved rapid, conserved strategies to perceive damage, activate defense signaling, and restore homeostasis, even if the molecular regulators differ (39). These wound signalling pathways majorly affect the trade-off between regeneration and defensive cell survival. This chapter

provides a comprehensive review of the cellular and molecular events that influence wound-induced regeneration responses in plants. The role of cell-fate determinants and regulatory networks in these processes are also discussed. Lastly, the open questions arising from gaps in current literature are noted, of which some will be explored in detail in the following chapters of this thesis.

1.2 Wound-induced regeneration responses in roots

Roots are crucial organs performing a multitude of functions. They are physical anchors that support the plant body, absorb water and essential nutrients from their surroundings for systemic transport, provide a barrier to pathogens and abiotic stressors, and act as both source and sink for plant metabolites (40). Roots therefore routinely cope with environmental damage by calibrating existing endogenous pathways between wound repair and defense. In the laboratory context, the response of roots to wounding is studied through multiple approaches – laser ablation or targeted cell death of the quiescent center (QC) and surrounding stem cell niche (SCN) (41–43), DNA damage treatment (44, 45), periderm incision (46), and resection of the root tip (47, 48) (Figure 1.1A). All of these experiments collectively reveal that the regeneration capacity of roots does not mandate a functional stem cell niche, i.e. the root apical meristem (RAM). Rather, in response to wounding, the adjacent cells undergo rapid changes in morphology and exude wound signals that activate long-range systemic pathways, that further builds back on localized cell morphology, cell-cycle progression and reprogramming to repair the wound and restore lost tissue (49).

Among the most extensively studied systemic signals in response to wounding is auxin. Aside from being a crucial regulator of normal plant development programs, auxin signaling is essential to initiate cellular reprogramming at the site of injury. Both local auxin biosynthesis and polar auxin transport are necessary for root regeneration. Wounding in roots triggers changes in turgor pressure and cell wall integrity of the wound-adjacent cells, which leads to local auxin accumulation that promotes stress response factors such as ETHYLENE-RESPONSIVE 115 (ERF115) (42, 50) (Figure 1.1B). These early cellular responses boost local auxin biosynthesis in the wound-adjacent cells and cause the cells to re-enter the cell cycle, undergo repeated divisions, and also activate stem-cell gene programs to form daughter cells that are capable of restoring cells lost to ablation or DNA damage, up to reforming the QC post ablation and the regenerating the entire root tip post resection (42, 50–53) (Figure 1.1 C, D). Post QC ablation, root developmental regulators such as PLETHORA (PLT), SHORTROOT

(SHR), and SCARECROW (SCR), regulate the expression and dynamics of (PIN-FORMED) PIN proteins to restore polar auxin transport in renewed root tips (43) (Figure 1.1D). Root specific developmental regulators such as PLT2 not only regulate auxin biosynthesis through genes like YUCCA3 (YUC3) during normal root development, but are rapidly upregulated in response to injury, and its auto-feedback regulatory network also determine the spatial limits of regeneration in the root, beyond which the organ loses its regenerative potential (48) (Figure 1.1 E, F). While PIN-mediated auxin transport is not typically essential during root tip restoration, a recent report reveals that maintaining auxin transport is vital to position and restore stem cells during cambium regeneration post ablation (41, 51). These findings highlight the multifaceted roles of auxin and stem cell regulators in orchestrating regeneration response in roots under diverse injury conditions (Figure 1.1F).

Auxin signalling however, does not work alone to restore cells in their original pattern and function in the root. During root tip regeneration, the proliferating cells at the site of injury gain transient embryonic identity, and require cytokinin signaling along with auxin to pattern the proximo-distal axes of the regenerating root cell files (52). Among the early signals that activate auxin are stress hormones like jasmonic acid (JA), salicylic acid (SA), and ethylene (54). While these hormone paths converge at activating auxin production, they diverge depending on the injury context, creating additional upstream controls of wound response. Ethylene signalling is activated during single cell ablations in the epidermis, whereas JA activation occurs post QC ablation (55, 56). JA in synergy with auxin activates an RBR (RETINOBLASTOMA-RELATED) - SCR (SCARECROW) - SHR (SHORTROOT) network through ERF109 (ETHYLENE RESPONSE FACTOR 109), ERF115 and CYCD6;1 (CYCLIND6;1) enabling restoration of lost tissue by concerted feedback between stem cell and cell cycle regulators (55) (Figure 1.1F).

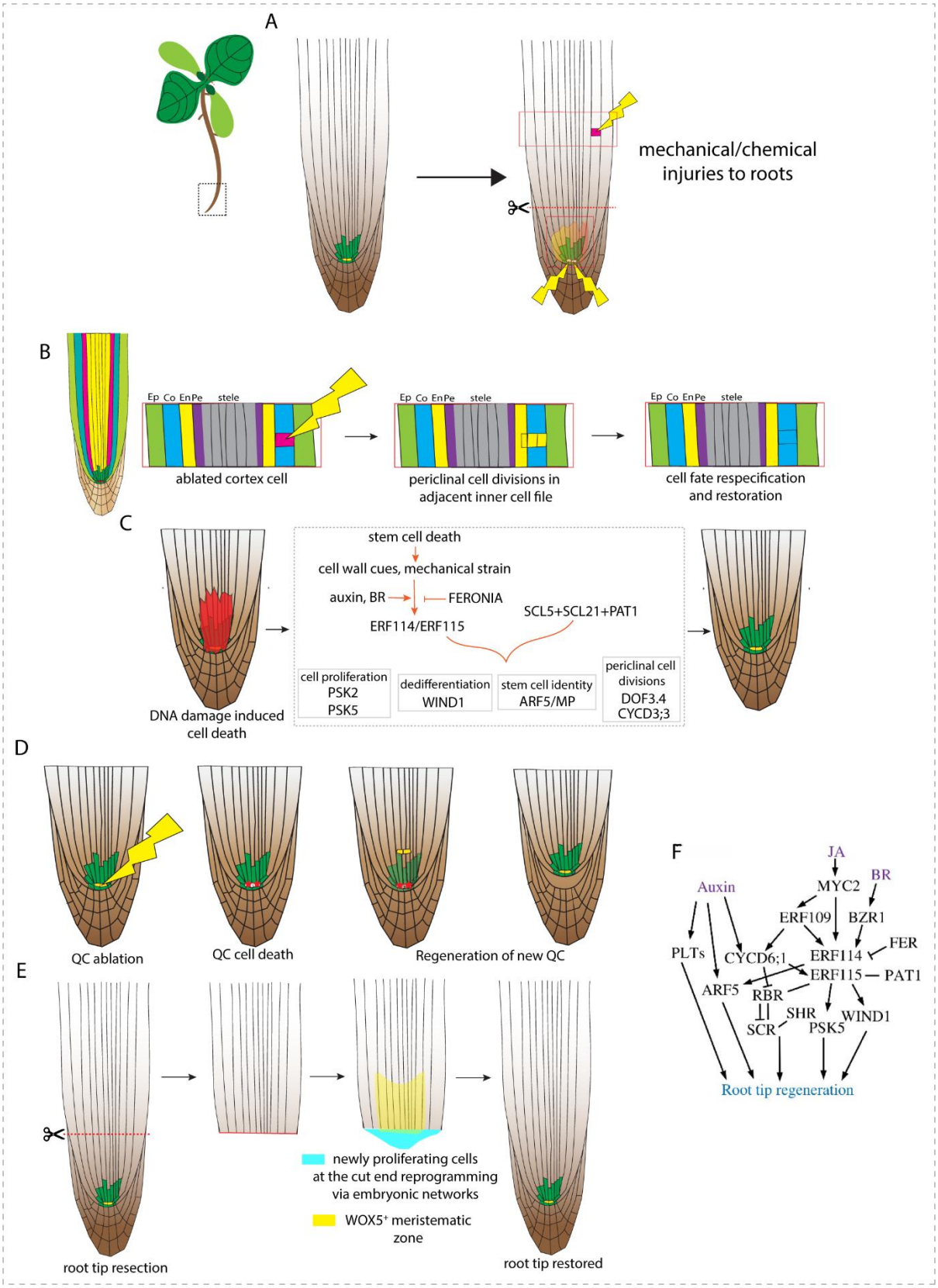

Figure 1.1 Schematic showing regeneration response in roots in diverse contexts. (A) Root regeneration response has been studied in response to single cell ablations in inner cell files, laser or chemical induced QC ablation, SCN cell death due to DNA damage drugs, and complete resection of the root tip. (B) Root schematic depicting individual cell files – epidermis (Ep), cortex (Co), endodermis (En), pericycle (Pe), and the stele.

When a cortical (Co) or endodermal (En) cell is laser ablated, the adjacent cells of the inner cell file lose cell wall integrity. Cell damage leads to local auxin accumulation that rewires the inner cells into cell cycle reentry and periclinal cell divisions towards the affected layer. Cell fate is respecified and ablated cells are restored. (C) When the SCN is damaged and stem cell death occurs, restorative reprogramming in the neighboring endodermal cells replenishes lost vascular initials. (D) Targeted ablation of the QC triggers new QC regeneration above the original site, and cells at the previous niche differentiate into columella cells. (E) When a root tip is removed, the wound-adjacent endodermal/stelar cells proliferate and transiently activate embryonic signaling pathways to restore the root tip. The cells near the cut end undergo rapid morphological and molecular changes (depicted as the meristematic zone) to support restoration of the original root tip shape and function. (F) Schematic of signalling networks activated during root tip regeneration (reprinted from (57)).

While the known regenerative networks consist of genetic regulators, emerging work provides evidence of how local cell behavior influences cellular patterning during root regeneration. The conserved root-specific microRNA miR396 and its targets, the GROWTH-REGULATING FACTORs (GRFs), uncouple root growth from meristem reconstruction after excision by controlling the transition from stem cells to proliferative cells, independent of the PLT2-demarcated regeneration zone (58). Another study shows how post excision, the regenerating cells undergo transient symplastic restriction mediated by lateral organ boundary domain (LBD) genes, that is necessary for root tip cell patterning during the later stages of regeneration (59). This shape restoration is also mediated by transient growth conflicts between the existing root cell files post excision, that allows cells adjacent to the excision site to deform into rhomboids and undergo diagonal cell divisions to create deflector cells that reshape newly emerging cells to restore the tapering root tip (60). Taken together, it becomes clear that roots activate diverse regulatory networks in response to injury, that allow the neighboring cells to undergo spatially restricted cell division and reprogramming to repattern lost or damaged tissue. Where do universal wound signals converge with these specific regenerative programs, is uncharted territory that awaits investigation.

1.3 Wound-induced regeneration responses in aerial organs

Extensive research exists on the regenerative responses of underground organs to injuries, partly enabled by ease of observation and analysis under controlled laboratory conditions. In contrast, while aerial plant organs are extensively used for tissue-culture mediated vegetative propagation since ages, the molecular and cellular behaviours that enable these organs to survive constant environmental shear stress and herbivory have been analysed carefully only in the last few decades. Aerial organs utilised for vegetative propagation include inflorescence, stem, cotyledons, leaves, and the shoot apical meristem (SAM), each with their specific regulatory networks. Post wounding, regenerative responses range from local cell proliferation to make a wound-induced callus, to *de novo* organ regeneration such as adventitious roots. The

following section covers what is known about the molecular and cellular mechanisms promoting wound induced regeneration in aerial organs of plants.

1.3.1 Wound-induced callus formation

Wound callus develops at sites of mechanical injury, such as cuts, graft junctions, or pathogen invasion. Unlike the tissue-culture callus that functions as an intermediate for *in vitro* organ regeneration, callus formed in response to wounding is an unorganized, proliferating cluster of cells arising from cell layers exposed at the wound site (61, 62). This makes the wound callus highly versatile in composition, with a molecular signature that is different from the tissue-culture derived callus (62). While both are products of cell dedifferentiation, one occurs in response to wounding alone, while the latter is created from wounded explants on auxin-rich callus induction media (CIM), that is amenable for further *in vitro* root or shoot propagation (61). The wound induced callus does not typically function as a pluripotent cell mass for organogenesis, rather, it has a more defensive purpose. It acts as an adhesive that seals surface wounds, provides a barrier against pathogens, providing immediate protection in response to environmental pressures. For example, targeted abrasion of the leaf epidermis activates expression of epidermal regulator ATML1 in the mesophyll cells below the wound site post, that allows these cells to transition to an epidermal identity to seal the wound site with a cork like barrier (63). Typically, calli that are unable to regenerate organs are considered “friable”, i.e. they do not gain *de novo* organ regeneration competence. Despite this, the wound induced callus shares some similarities with CIM derived callus with regards to the initial regulators that drive cellular dedifferentiation and promote cell survival (64).

Mechanical injury has long been recognized as a major stimulus of callus induction, but the molecular regulators activated by this stimulus are poorly understood. The AP2/ERF factor WOUND INDUCED DEDIFFERENTIATION1 (WIND1), and its homologs WIND2, WIND3, and WIND4, are consistently upregulated post wounding, and are central regulators of plant callus formation (65) (Figure 1.2). WIND1 is activated in response to injury, and is essential for cellular dedifferentiation during both wound and CIM-callus induction. Similar to WIND1, the PLT factors PLT3, PLT5, and PLT7, are also essential for cellular dedifferentiation during callus formation across different origins (16). It is evident that regulators such as WINDs and PLTs are activated early post injury, and initiate molecular networks for cell reprogramming, which is common to both conditions. So where does a wound callus and CIM-callus differ?

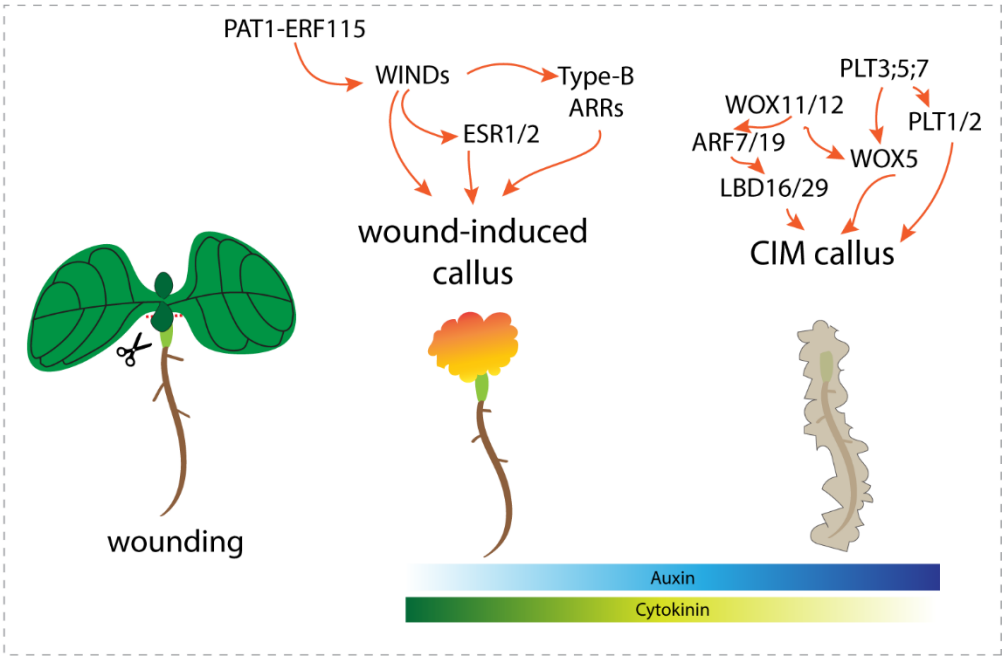

Figure 1.2 Comparison of different callus types. While wounding is the primary stimulus in all conditions, the wound-induced callus is created by random cell proliferation at the wound site due to endogenous cytokinin signalling with negligible auxin involvement. Meanwhile, wounding followed by exposure to an auxin rich CIM induces reprogramming networks to create a more pluripotent CIM callus, whose cells gain a uniform root primordium like state, allowing for planned de novo organ regeneration.

Tissue culture induced calli exhibit a root primordium-like molecular signature, which is a result of dedifferentiation and proliferation induced by the combination of mechanical wounding and auxin-rich CIM, irrespective of the explant used (Figure 1.2). Along with auxin, JA signalling pathway works to induce this pluripotent state that makes the CIM callus competent for organogenesis. On the other hand, the wound induced callus activates cytokinin signalling to promote dedifferentiation. These cells undergo dramatic shape deformation, and expand their vacuolar volume and cell turgor, due to transcriptional activation of cell wall modifying enzymes by the wound induced WUSCHEL-RELATED HOMEOBOX 13 (WOX13), which is also a key regulator of cell adhesion for grafting, along with wound callus formation (66, 67). Another interesting difference between these callus types originates from their epigenetic landscape. Histone acetylation mediated by the GNAT-MYST-family histone acetyltransferases is essential for wound induced callus formation, but severely inhibits the CIM callus (68). CIM induced callus occurs from dedifferentiation of the pericycle and pericycle-like cells through a root developmental pathway, across all explants. Therefore, CIM calli possess cells with a root primordium identity, expressing root promoting factors such as PLT1/PLT2, WOX5, SCR, LBD16, and more (69). This synchronization ensures uniform competence for *de novo* organogenesis. Wound induced callus cells originate from multiple

tissue types and are a heterogenous cell mass composed of dedifferentiated cells from the vasculature, pith, cortex, and the epidermis, where expression of root regulators PLT2, LBD16 are noticeably absent (70). While the WIND and PLT3,5,7 factors are found across both callus types, indicating their global role in the initiation of cell dedifferentiation, how do their downstream targets differ and influence different callus identities remains an open question. Another interesting avenue to explore is how the morphological and molecular heterogeneity in wound callus cells impacts regeneration competence, and whether these friable cells are capable of organogenesis under controlled conditions. Insights from such studies would bear important implications for manipulating organ regrowth post injury not just in plants, but other complex eukaryotes too.

1.3.2 *De novo* root regeneration

Adventitious or *de novo* roots are formed from non-root tissues and specific aerial organs post wounding, or in response to environmental stresses like flooding, and circadian stress. This ability of plants to perform d*e novo* root regeneration (DNRR) is extensively exploited in horticulture and forestry for asexual propagation, including everyday practices like air layering (71). *De novo* root regeneration is seen in root-excised hypocotyls, inflorescence stem, and strikingly, even in detached leaves and cotyledons that are entirely disconnected from the parent plant (Figure 1.3). Although phenotypically these are broadly categorized as *de novo* roots, their initiating stimuli vastly differ depending on tissue type and stress context. Detached leaves and cotyledons can initiate DNRR after simple physical contact with a media or substrate at the cut end, similar to roots borne from air layering of wounded stems, whereas crown roots or brace roots are a result of flooding or nutrient stress. Interestingly, the regenerative outcome of excised leaves appears to be initiated mainly by physical substrate contact – contact of the cut end with any substrate (plain agar, soil, water, simple plant growth media) can induce *de novo* root regeneration, while without contact condition leads to wound-induced callus formation. This highlights the need for investigating the regulatory networks that determine regenerative outcomes post injury, and which pathways actually instruct the cell-fate transitions that promote *de novo* organ regeneration post wounding.

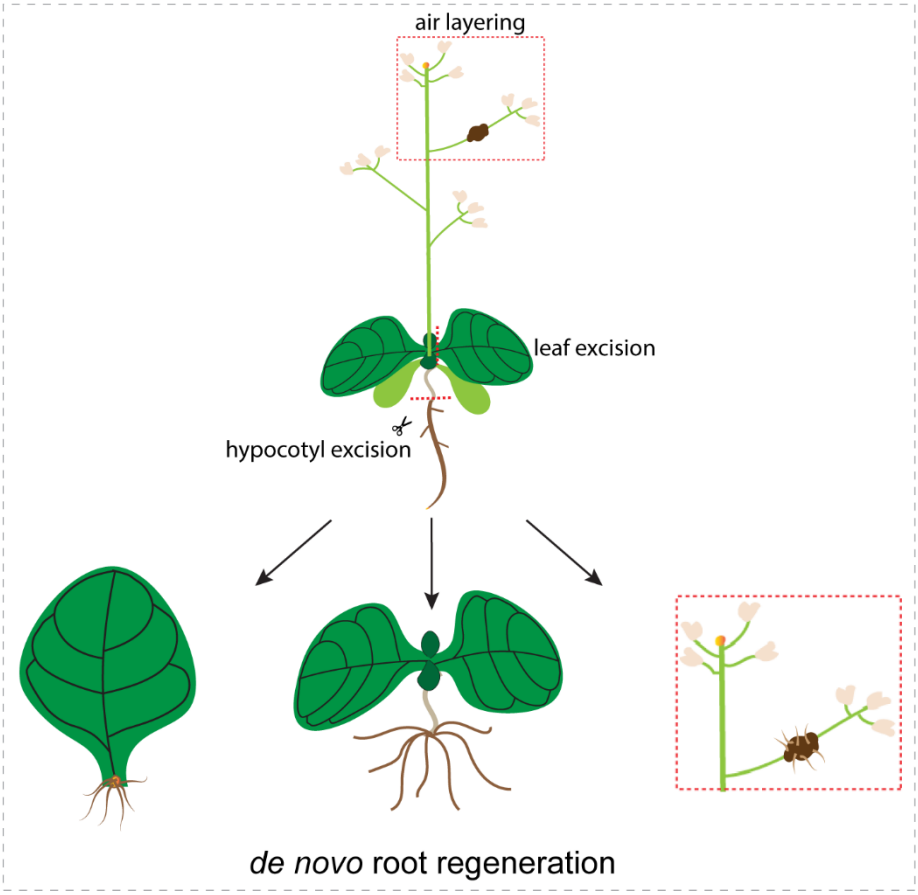

Figure 1.3 *De novo* root regeneration post wounding in aerial organs. Aerial organs are capable of regenerating adventitious roots in response to mechanical injury. De novo root regeneration is observed from the cut ends of excised leaf, cotyledon, hypocotyl, and even in stem cuttings.

Due to ease of handling and analysis, *de novo* root regeneration from leaf explants has been studied extensively (Figure 1.3). Previous studies have elucidated the role of different plant specific transcription actors (TFs) and hormone pathways to create a molecular timeline of the leaf to root DNRR process. Ca^{2+} flux, reactive oxygen species (ROS) signals and abscisic acid (ABA) induced factors, coupled with stress response signalling pathways such as ethylene, jasmonate and salicylate are activated early in response to wounding, that synergistically initiate local auxin biosynthesis (72–76). These stress signals are also regulated by small peptides like CLAVATA3/EMBRYO SURROUNDING REGION-RELATED26 (CLE26) that attenuates wound signaling during DNRR. (77) These signals impact multiple cell types exposed at the wound site – vascular, mesophyll, and epidermal cells – that undergo hormonal flux induced reprogramming, and become regeneration competent “converter cells” (13). Activation of local auxin production and polar transport through factors like YUCCA4 and ASA1, along with cytokinin signaling in the wound vicinity initiates rapid reprogramming of the wound-adjacent vascular procambium cells to root founder cells at the site of injury (78,

79). These root founder cells express specific TFs like WUSCHEL-RELATED HOMEOBOX 11/12 (WOX11/12) that establish regeneration competence by forming an endogenous healing callus at the site of injury (80–82). This further leads to the transition of specific root founder cells to root primordium cells that differentiate further to regenerate an adventitious root. Aside from these, wound-induced TFs such as PLT3/5/7, ENHANCER OF SHOOT REGENERATION1 (ESR1), NAC1, ERF109, EIN3, are upregulated post excision, that are essential to initiate and maintain regeneration competence, and also activate the root primordium specific factors such as WOX5, PLT1/2, and LATERAL ORGAN BOUNDARIES DOMAIN16 (LBD16) (18, 83–87). In summary, an intricate regulatory network is activated in excised leaves after wounding to facilitate *de novo* root regeneration, with the intersection of wound signals, auxin biosynthesis, and wound induced regulators to facilitate the reprogramming pipeline of converter – founder – primordium cell-fates (88).

1.3.3 *De novo* shoot regeneration

Tissue-culture induced shoot regeneration is a fundamental tool of plant biotechnology. However, plant species exhibit variable affinity for this *in vitro* process, requiring extensive effort of standardizing cytokinin: auxin ratios, culture protocols, and time required for successful organ regeneration. This is also due to the fact that *in vitro* shoot morphogenesis is an energy intensive process incorporating multiple regulatory nodes, ranging from phytohormone signalling and regeneration-specific transcriptional programs, to local cell-cell mechanics and metabolic shifts (89). Key shoot promoting factors essential for meristem initiation include WUSCHEL (WUS), SHOOT MERISTEMLESS (STM), CUP SHAPED COTYLEDON1 (CUC1) and CUC2, ESR1 and ESR2 (48). Aside from these factors, the PLT factors confer a global regeneration competence by promoting pluripotency acquisition through PLT1/PLT2, and shoot regeneration competence through CUC2 (16). Loss-of-function mutants of any of these factors severely impairs tissue-culture shoot regeneration, making them potential candidates for enhancing shoot regeneration efficiency by ectopic gene manipulation.

During tissue culture, shoot regeneration is initiated from an intermediate pluripotent callus. Though the callus is composed of asynchronous cells, they possess a uniform root primordium like identity. Irrespective of the parent explant, the CIM derived auxin-rich callus is a population of cells with a relatively homogenous molecular profile (61). But whether shoot regeneration can be initiated from a wound-callus made of heterogenous cell types is an unanswered question. Wounding is the primary trigger for all cellular reprogramming, as

uninjured plants cultured on callus or shoot induction media do not regenerate ectopic shoots (90). This evokes an essential question – does wounding promote any shoot regeneration competence? Is it dependent on the parent explant? An interesting study showed wound induced WIND1 directly activates ESR1 for shoot initiation, and ectopic expression of ESR1 is sufficient to drive *de novo* shoot regeneration even from wound-induced calli across multiple aerial organs (91). Furthermore, external injection of WIND1-ESR1 transgenes to injured aerial organs on growing plants induced ectopic shoots from the wound sites, indicating that WIND1-ESR1 network is an important regulator for *de novo* shoot morphogenesis across multiple wounding contexts (92). Taken together, it is evident that wound-induced *de novo* shoot regeneration requires complex interactions through key shoot promoting factors that provide competence to the heterogenous wound-callus cells to promote meristem initiation and shoot development. Uncovering these networks would provide brilliant insights into the fundamental processes that enable asynchronous and amorphous cells to morph into the complex biochemical and biophysical framework necessary for *de novo* organogenesis.

1.4 Vascular regeneration

Mechanical injury as well as pathogen invasion also damage existing vasculature, which triggers local cell reprogramming in order to seal the injury site as well as reconnect the severed vascular strands by *de novo* vascular regeneration (Figure 1.4). Restoration of vascular continuity is essential for the regulated transport of water, nutrients, phytohormones, and other metabolites across the body axis, which also makes vascular regeneration the cornerstone of horticultural practices like grafting (Figure 1.4 B-D). Vascular regeneration is broadly a three-part process – establishment of an auxin source-sink gradient, reprogramming of local ground tissue, and cell-cell interactions to ensure accurate reconnection of new vessels to the existing layers (93). Landmark studies by Tsvi Sachs led to the auxin canalization hypothesis, which proposes that the directional flow of auxin from a source (site of normal growth or externally applied auxin) to a sink (site of wounding) determines the orientation of newly forming vascular tissue (94). The reunion of severed vasculature occurs by the differentiation and reprogramming of the local parenchymatous cells, making new vessels in response to the realigned auxin flux, that bypass the wound site and “loop” around the damaged cells (95, 96). This transdifferentiation process would likely necessitate activation of cell-wall modifiers to facilitate cell shape deformations, which in turn is known to activate DNA BINDING WITH ONE FINGER (DOF) transcription factors during grafting-mediated regeneration (97) (Figure

1.4D). Polar auxin canalization also impacts the extent of vascular differentiation, which may have a direct effect on the regeneration efficiency of vasculature with respect to the site and extent of injury, as seen during mid-vein incisions in the *Arabidopsis* leaf (98) (Figure 1.4E). Along with reestablishment of polar auxin transport, *de novo* vein regeneration also necessitates YUCCA4-mediated local auxin biosynthesis at the wound site, which is regulated by a coherent feedforward loop of the PLT factors and CUC2, that is activated post vein incision (17) (Figure 1.4F). This local auxin production likely facilitates the rejoining of new vasculature to the existing vein, creating a new path to resume systemic transport. Such regenerative programs are not activated ubiquitously post wounding; when *Arabidopsis* leaf tip is excised, or the leaf is cut into parts, the excised tissue is not replaced and the exposed area is sealed by local callus/cuticle growth (85, 99). This also suggests that only physiologically relevant tissues within growing leaves are regenerated post wounding.

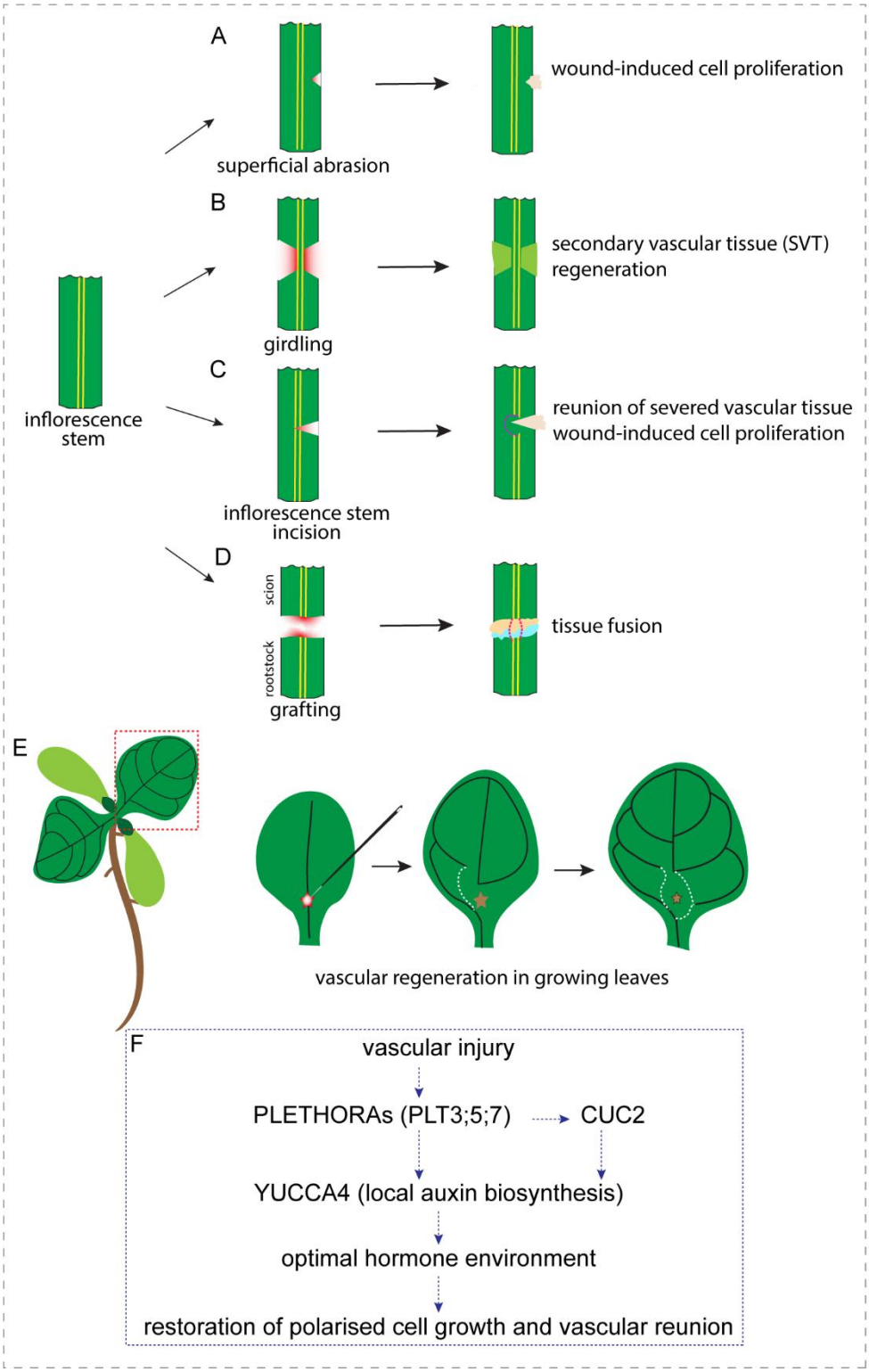

Figure 1.4 Vascular regeneration in plants. (A-D) The inflorescence stem displays a spectrum of wound response proportional to the extent of wounding within the inner cell layers. Superficial or local abrasions on the surface elicit proliferation from the exposed parenchyma at the wound site to seal off the site and heal the wound (A) (63). Meanwhile, the technique of girdling removes protective bark and exposes the inner vascular bundle (B), that activates secondary vascular tissue (SVT) regeneration programs from the xylem and phloem channels to restore the lost tissue. However, when the vasculature itself is severed through incision (C), the local parenchymatous cells undergo polarized cell divisions to generate new vascular channels to reunite the severed parental strands around the site of injury, while sealing the external wound through cell proliferation. (D) Grafting

involves complete severing of the inflorescence axes of the rootstock and scion, followed by reunion of both parts through activation of cell wall modifying genes among others, that mold local proliferating cells to seal the graft site, along with regenerating de novo vascular channels to fuse the two separate plant vasculatures and restore nutrient/hormone/metabolite transport. (E-F) When the midvein of a young leaf is excised, the PLT-CUC2 module activates YUCCA4 mediated local auxin biosynthesis, to create the optimal local environment that permits new vascular strands to loop around the wound site and reestablish vascular connectivity.

Besides auxin flux, recent evidence also shows that after girdling, DELLA-gene mediated gibberellic acid (GA) signaling determines the spread and gradient of auxin flux through the polar auxin transporter PIN1 during cambium regeneration in *Populus* (100). Interestingly, while cytokinin signaling is essential for cambium development, it is inhibitory for cambium regeneration, and specifically promotes phloem regeneration in response to girdling (101). It is important to note here that vascular tissue specification may occur from different sources depending on the wounding context. While local ground tissue maybe the source of *de novo* vessels for the reunion of completely severed strands, partial abrasion due to girdling causes the existing xylem vessels to differentiate and form secondary phloem, cambium, and cork tissue (Figure 1.4 B, C). While the specification of different vascular cells in the early stages of initiation may come from similar stimuli, these would gradually transform into cell specific cues as the regenerating vessels gain functional continuity. One such common cue that activates vascular repair is warm temperature, which enhances auxin signaling to accelerate xylem bridge reformation during grafting based vascular regeneration (102). Furthermore, these regeneration specific cues maybe transient in nature and gradually recede once the vascular network is fully restored in the host organ to prevent uncontrolled tissue outgrowth. Taken together, vascular regeneration arises from the synergistic feedback of both differentiation and polarity-oriented growth of new strands in response to injury; but what are the informative cellular cues that guide these processes? Subcellular events that spatiotemporally reorient local cell polarity and activate gene programs in response to wound signals may be where these events converge (96).

1.5 Wound signalling – hedging between survival and regeneration

Post wounding, plants allocate resources between two immediate demands – defending damaged tissue from environmental stress or pathogens, and repairing the lost tissue by sealing the wound, or by regenerating *de novo* organs. Therefore, plants have evolved elaborate mechanisms to rapidly activate and coordinate both processes through extensive crosstalk, mostly involving wound-responsive phytohormones that are accumulated rapidly after injury. These stress hormones – JA, ethylene, ABA, and SA – are not only essential to initiate auxin-

cytokinin signaling gradients vis-à-vis the wound site, but also to confer pathogen resistance and boost local immune response. Among these, evidence suggests that JA and ethylene pathways are involved in wound repair and regeneration, along with electrical signals (73, 103–106). But the exact nature of their role in translating local/systemic wound signals into cellular reprogramming cues remains unclear. Wound signals like Ca2+ ions, ROS, RNS, damage and pathogen-associated molecular patterns (DAMPs), and MAP-kinases (MAPK) rapidly emerge at the site of injury, that are transmitted through specific biochemical networks to elicit stress hormone activation (107–109). Furthermore, signals such as ROS, Ca2+, and glutamate are also propagated at sites distal from the injury, eliciting a systemic wound response. Although plant regeneration and wound repair comprise a rapidly growing body of knowledge, the nature of crosstalk between wound signals and diverse regenerative outcomes remains a mystery. Nevertheless, some common principles can guide exploration on how wound signals induce cellular reprogramming. Damaged or stressed cells release a repertoire of wound signals that are picked up by the cells in the vicinity. These wound signals are translated into reprogramming cues that initiate cell proliferation to create a cohort of regeneration competent cells, and also to seal the wound. Under regeneration competent conditions, the newly emerged daughter cells undergo differentiation to create new tissue to replace the damaged one, or even create stem cells capable of *de novo* organogenesis (Figure 1.5).

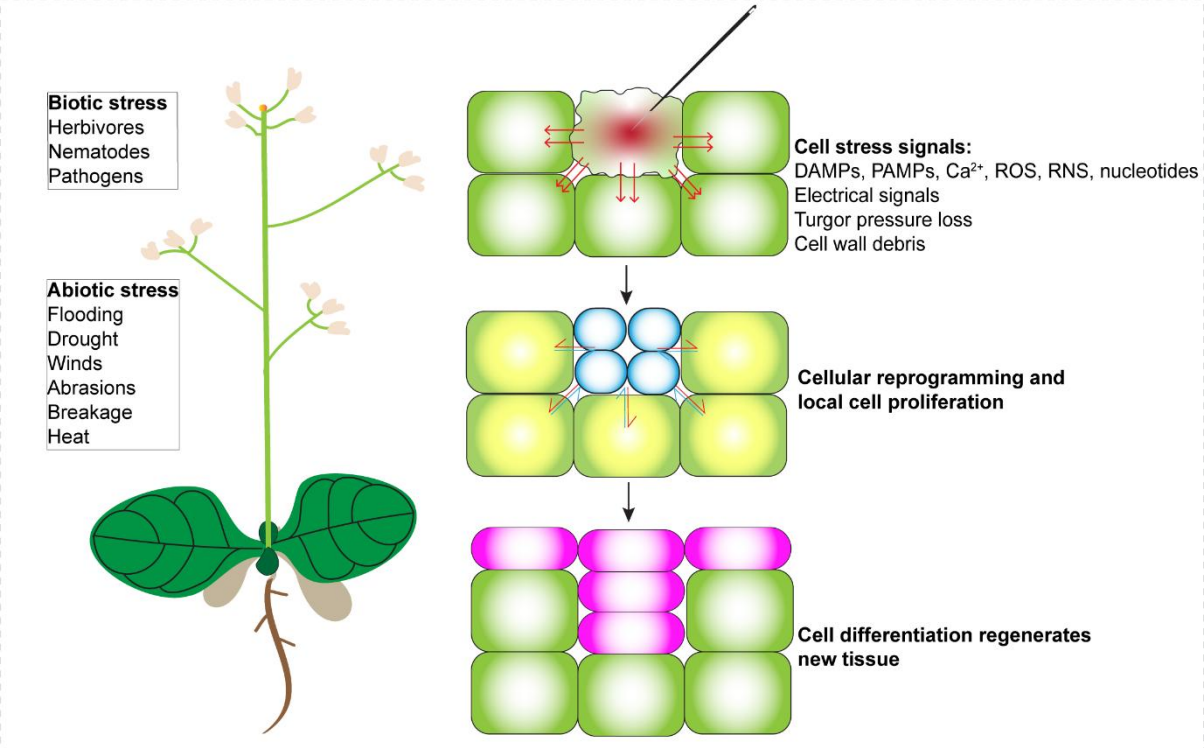

Figure 1.5 Interplay of wound signals and cellular reprogramming post wounding. Plants are vulnerable to both biotic and abiotic stressors on a daily basis. Stress signals from damaged cells are received by cells in the vicinity, which triggers cell-cycle reentry, cell proliferation, and recalibration of cellular homeostasis. Under optimal conditions, the neighboring cells further confer fate determining signals to the newly proliferating cells for differentiation (110).

1.5.1 How is a wound perceived?

When cells are wounded, there is rapid release of damage/pathogen -associated molecular patterns (DAMPs and PAMPs), such as extracellular ATP, calcium ions, and fragmented cell wall or extracellular matrix components. DAMPs have been extensively characterized in mammals, such as oligonucleotides, ATP, DNA/RNA fragments, uric acid, heat shock proteins; plants additionally incorporate cell wall fragments in this repertoire (107). The accumulation of these molecules is interpreted as stress signals to the adjacent cells in the vicinity, which catalyzes the initiation and propagation of wound induced signals from the wound site to the surrounding tissue and beyond. While the speed of signal propagation varies between plant and animal cells, some conserved universal wound signals include Ca2+, ROS, and RNS. Typically post wounding, the dead and ruptured cells at the wound site activate calcium ion signalling due to ion leakage (111). In this case, plants have evolved an additional upstream responder – glutamate. While glutamate is an excitatory neurotransmitter in vertebrates, interestingly, plants utilize glutamate for long-range electrical signaling and systemic activation of wound repair (108). Apoplastic glutamate accumulates at wound sites, thereby triggering rapid cytosolic Ca^{2+} flux in the adjacent cells through GLUTAMATE RECEPTOR-LIKE (GLR) ion channels, which is further propagated to cells away from the vicinity. GLR-mediated Ca^{2+} propagates systemically though the vascular bundle, even priming organs distal from the wound site to orchestrate cellular defense mechanisms in response to local stimuli (112, 113). The role of glutamate signalling appears biphasic, where GLR signaling can activate immune response and defense-related gene networks, and also dampen regenerative events such as cell cycle reprogramming, and meristem recovery post wounding (114). Meanwhile, calcium signals appear largely necessary to rapidly rewire the local auxin environment as well as activate long-range signaling in response to injury. In the context of wound response, Ca^{2+} signaling is essential to activate auxin biosynthesis and transport during wound induced *de novo* rooting, two-step tissue culture regeneration, and even shoot meristem restoration, through different interactors (115–117). Moreover, this signal cascades activates hormone-dependent reprogramming locally at the wound site, and at the systemic level, elicits an immune response, thus having dual regulatory roles at scale (118). It is likely that changes in

this ionic flux are instrumental for rewiring the existing auxin gradient into repair mode, that can be reversed to normal development guided gradients once the wound is healed and the Ca^{2+} waves are abrogated.

Another essential wound signal is ROS, that propagates systemically in response to wounding. The term encompasses a group of doublet oxygen (O_2) derived molecules - hydrogen peroxide (H_2O_2), superoxide ($O_2^{\cdot -}$), singlet oxygen ($^1O_2$), the hydroxyl radical ($HO^{\cdot}$) and various forms of organic and inorganic peroxides, including RNS (119). These species are highly reactive, and produced by many cell organelles including mitochondria, peroxisomes, and chloroplasts in plants during the normal course of cellular homeostasis, as byproducts of catabolic reactions. Therefore, ROS are kept under tight control to prevent cytosolic accumulation and cellular oxidation. Several gene families encode enzymes that regulate ROS metabolism and transport at both intra- and inter- cellular levels. Chief among these are the RESPIRATORY BURST OXIDASE HOMOLOGUES (RBOHs), which are the functional equivalents of mammalian NADPH oxidases. RBOHD, a key member of this group, rapidly produces H_2O_2 in wound-adjacent cells triggered by calcium flux, which eventually builds up to an "ROS wave" that propagates at the systemic scale through plasmodesmata (120). In response to specific stimuli such as high light stress however, this signal propagation is channeled through GLRs in the vascular bundle (121). From this it seems probable that ROS generation and propagation are mutually separate events that are dependent on the exact stress context. This is understandable given that ROS function not only as universal stress signals, but also actively impact the cellular redox state. ROS-mediated redox state of cells is a crucial signal for stem cell maintenance or differentiation, and also determines the transition threshold of different compartments in organs (122, 123). This makes ROS signalling a very crucial fulcrum between wound repair and defense, and also a deterministic factor of any local cell reprogramming essential for generating new cells in the wound area. How does ROS regulation coordinate these diverse events to ensure the correct regenerative outcome post wounding remains unclear.

1.5.2 Wound signalling cascades instruct both cell survival and cell death

Wound induced signals work in tandem to generate a spectrum of different cellular responses, including cell reprogramming, and cell death, which is tightly interlinked with the pathways of apoptosis and autophagy (124). In a nutshell, apoptosis results in cellular fragmentation and death via catabolic enzymes, whereas autophagy ('self-eating') involves the recycling and catabolic turnover of damaged cytosolic components (125). Autophagy serves the dual function

of both promoting cellular homeostasis or cell death, depending on the developmental context or stress condition (126, 127). In plants, autophagy has been extensively studied in pathogen defense, herbivory, viral infection, and senescence (19, 128, 129). Its role in regeneration however, remains largely unexplored, and limited to studies on wound healing during grafting, and delayed regenerative responses in tissue culture. Functional insights have come from loss-of-function mutants in autophagy-related genes (ATG), such as *ATG2* and *ATG5* (11, 12). It remains unclear whether autophagy directly regulates wound-induced tissue replacement or organ regeneration, or how it influences cell fate decisions during these processes (130).

In summary, during the process of wound healing, local cellular changes are contingent upon the spectrum of wound signals that plant cells can emit. These signals can be both local and systemic in scale, which primes the larger organism towards cellular defense, while simultaneously regulating cell fate changes and coordinated reprogramming at the wound site for regeneration. Moreover, these wound signals are coordinated by diverse gene families that function under their individual regulatory networks. How do these wound signals intersect with plant transcription factor networks and influence the ultimate regenerative outcome, is a fascinating question that invites exploration.

CHAPTER 2

Materials and Methods

"Create with the heart; build with the mind."

– Criss Jami

2.1 MATERIALS

The following section details all the materials and resources used in this thesis. All reagents obtained from commercial sources have been mentioned with relevant catalog details. Reagents provided by other research groups have been duly cited.

Table 1. Plant lines used in this study

Sr. no.	Plant background	Source
1.	Arabidopsis thaliana, *Columbia (Col-0)* ecotype	(16)
2.	*plt3-1*	(131)
3.	*plt5-2*	(132)
4.	*plt7-1*	(132)
5.	*plt3;plt5*	(132)
6.	*plt5;plt7*	(132)
7.	*plt3;plt7*	(132)
8.	*plt3;plt5;plt7*	(132)
9.	*atg2*	Yasin Dagdas
10.	*atg5*	Yasin Dagdas
11.	*Δatg8a-i*	Yasin Dagdas
12.	*Δatg8a-I; pUBQ10::GFP-ATG8H*	Yasin Dagdas
13.	*atg8b*	ABRC
14.	*atg8c*	ABRC
15.	*atg8f*	ABRC
16.	*atg8h*	ABRC
17.	*atg8f;atg8h*	This study
18.	*plt3-cr*	(133)
19.	*plt7-cr*	(133)
20.	*Col-0; pPLT7::gPLT7:vYFP*	(132)
21.	*Col-0; pPLT3::gPLT3:vFP*	(132)
22.	*Col-0; pWOX11::H2B-GFP*	(134)
23.	*Col-0; pUBQ10::NG-ATG8F*	This study
24.	*Col-0; pATG8F::erNeonGreen*	This study
25.	*atg8f; pWOX11::H2B-GFP*	This study
26.	*plt3-1; pWOX11::H2B-GFP*	This study
27.	*Col-0: pPXY::erYFP*	(135)
28.	*atg8f: pPXY::erYFP*	This study
29.	*plt3-1: pPXY::erYFP*	This study
30.	*atg8f; pPLT7::gPLT7:vYFP*	This study
31.	*plt3-1; pPLT7::gPLT7:vYFP*	This study
32.	*plt3-1; pPLT3::gPLT3:vYFP*	This study
33.	*plt3-1; pPLT3::gPLT7:vYFP*	This study

34.	*plt3-1; pPLT7::gPLT3:vYFP*	This study
35.	*plt3-1; pATG8F::erNeonGreen*	This study
36.	*plt3-1;p UBQ10::GTIP1:TagRFP*	This study
37.	*Col-0;p UBQ10::GTIP1:TagRFP*	This study
38.	*atg8f; pUBQ10::GTIP1:TagRFP*	This study
39.	*plt3-1; pUBQ10::NG-ATG8F*	This study
40.	*atg8f; pUBQ10::NG-ATG8F*	This study
41.	*Col-0; pWOX5::gWOX5:mRFP*	This study
42.	*plt3-cr; pWOX5::gWOX5:mRFP*	This study
43.	*plt7-cr; pWOX5::gWOX5:mRFP*	This study
44.	*plt3-1; pG1090.XVE::gATG8F:3AT*	This study
45.	*Col-0; pG1090.XVE::gATG8F:3AT*	This study

Table S2. List of recombinant plasmids used in this study

Plasmid	**Purpose**	**Source**
pCam-hyg pPLT3::gPLT3:4xgly-vYFP-3AT	PLT3 translational reporter	(132)
pCam-hyg pPLT7::gPLT7:4xgly-vYFP-3AT	PLT7 translational reporter	(132)
pBI101 pWOX11::H2B-GFP:NosT	WOX11 transcriptional reporter	(134)
pCam-kan pUBQ10::NG-gATG8F:3AT	constitutive NG-ATG8F reporter	This study
pCam-kan pATG8F::erNeonGreen:3AT	ATG8F transcriptional reporter	This study
pCam-kan pG1090.XVE::gATG8F:3AT	estradiol inducible ATG8F construct under G1090 constitutive promoter	This study
pFRm43GW pPLT3::gPLT7:4xgly-vYFP-3AT	PLT7-vYFP fusion protein expressed under PLT3 promoter	This study
pFRm43GW pPLT7::gPLT3:4xgly-vYFP-3AT	PLT3-vYFP fusion protein expressed under PLT7 promoter	This study
pFG7m34GW pUBQ10::GTIP1:TagRFP-OcsT	constitutive GTIP1-tonoplast reporter	This study
pH7m34GW pWOX5::gWOX5:mRFP	WOX5 translational reporter	This study
pH7m34GW pPXY::erYFP:3AT	PXY transcriptional reporter	(135)

p1R4a-UBQ10	5' element	This study
p1R4a-ATG8F	5' element	This study
p1R4a-PLT3 (7.7 kb)	5' element	(132)
p1R4a-PLT7 (5 kb)	5' element	(132)
p1R4a-WOX5	5' element	This study
p1R4a-G1090.XVE	5'element	(136)
p221a-gATG8F	central element	This study
p221a-mNG-gATG8F	central element	This study
p221a-erNeonGreen	central element	This study
p221a-gGTIP1	central element	This study
p221a-gWOX5	central element	This study
p221a-gPLT7	central element	(132)
p221a-gPLT3	central element	(132)
2R3-3AT	3' element	Addgene #71273
2R3-mRFP	3' element	(137)
2R3-4xgly-vYFP-3AT	3' element	Addgene #71269
2R3-TagRFP-OcsT	3' element	Addgene #71270
pGEMTeasy P2R-P3 mNeonGreen	3' element	(137)

pCam-kan-R4R3	Gateway destination vector	Addgene #71275
pFG7m34GW	Gateway destination vector	Addgene #133747
pFRm43GW	Gateway destination vector	Addgene #133748
pH7m34GW	Gateway destination vector	(137)

Table 3. List of primers used in this study

Genotyping primers	
Primer name	**Primer Sequence 5'-3'**
SALK_LBb1.3	ATTTTGCCGATTTCGGAAC
SAIL_LB1	GCCTTTTCAGAAATGGATAAATAGCCTTGCTTCC
PLT3-1_SALK_F	CACTACCACCCATCTCTGAAAAC
PLT3-1_SALK_R	GCTGATACGTTTGGTCAAAGG
PLT5-2_SALK_F	TGAAATGATTACCCAACCGTG
PLT5-2_SALK_R	TAGGCATTAGTCCACCCACAG
PLT7_SAIL_F	GCCTTGACCCTAATCAAATCC
PLT7_SAIL_R	AGCAACTGTTGTTGTTGGAGG
ATG8B_SALK_023952.44.05.x_LP	TTCGGTTATCCATTCGGTTTC
ATG8B_SALK_023952.44.05.x_RP	GCCCAAAAGATCGAAGAAAAC
ATG8C_SALK_003706.44.25.x_LP	GTTAATGCGTTTTGGTGCATC
ATG8C_SALK_003706.44.25.x_RP	GAAAGAGTGTGCCTTGCTTTG
ATG8F_SALK_057021.55.25.x_LP	ACTTCAATGGTCCAAAATCCC
ATG8F_SALK_057021.55.25.x_RP	TTTTCATTCGGACCTGACTTG

ATG8H_SALK_119920.15.95.n_LP	GCAGACACAAAGACCTTTTGC
ATG8H_SALK_119920.15.95.n_RP	GAAGTCGTCTCCGACATTGAC
qPCR primers	
Primer name	**Primer Sequence 5'-3'**
qRT PLT3 FP	CGGTTCAGAGGTCGATGACT
qRT PLT3 RP	AGATCCACCGTGAAACCCTA
qRT PLT7 FP	TTTCCTCGGTGATTCCTTTG
qRT PLT7 RP	TGACGTGGATCGTAGAATGG
qRT ATG8A_A_F	CAGTTCCGTGTAGGCAACCA
qRT ATG8A_A_R	TGCGATTCGATTAGTCTCCGA
qRT ATG8B_A_F	GTTTCGTCTTTTGGTTTCGAGT
qRT ATG8B_A_R	TCACGGGAACTCTTTCAGGG
qRT ATG8C_A_F	TCGTGCATAGATTAGGAATCTCG
qRT ATG8C_A_R	AGCCATGGCGATTAAAGAATCAAA
qRT ATG8D_A_F	GTTGCCAAGCGTACCCTTTTT
qRT ATG8D_A_R	TGCTTCAGCTTGTCTCTTTTCAAG
qRT ATG8E_A_F	CCATCAAATTCTCTCTCTAAGCAAA
qRT ATG8E_A_R	GGTCTGATGGCACAAGGTACT
qRT ATG8F_A_F	GAGAATCTCTGACCTTATCGCAT
qRT ATG8F_A_R	TTCCTTCCACGCCTGTAGAC
qRT ATG8G_A_F	TCACACAAAGTCGAATCCAAAGT
qRT ATG8G_A_R	CTCCACAATCACCGGGACTC
qRT ATG8H_A_F	TTCCTCAAACCGCTAGTCGC
qRT ATG8H_A_R	ACAAGAGCTGACGTTATTCACA
qRT ATG8I_A_F	GCCGCTTGCTTTTGAGAGAC
qRT ATG8I_A_R	CGAGCCTTTCATCCAACGTG
ACT2_qPCR_F	CGCTCTTTCTTTCCAAGCTCA

ACT2_qPCR_R	GCCTACCAACAACACTGGGA
ATG8B_ChIP_0-200_FP	TAAAGGCCCAATAAATAGTTCACAA
ATG8B_ChIP_0-200_RP	CAAAAAAATGAAAAAAGGAGAGAATATAT
ATG8C_ChIP_0-200_FP	GTATAAATTTTTTGTTTTGTATCTTGTA
ATG8C_ChIP_0-200_RP	TATTGAAGTCTGAAACTTTCGA
ATG8F_ChIP_0-200_FP	TGAGATTCCTATTTCAGTAAATAGCTAATA
ATG8F_ChIP_0-200_RP	TAACGAAAAAATATGAAAGAAAAAGCAA
ATG8H_ChIP_0-200_FP	AGAATAAAAGAGTTTGTAATACACTTG
ATG8H_ChIP_0-200_RP	CGAGAAGAAACGGTAAAAGATGAG
ATG8H_ChIP_400-600_FP	ATAAACGGATATGCCAATGCCGGT
ATG8H_ChIP_400-600_RP	AAACGTTCTTGAATCGCATACGCATTG
ATG8H_ChIP_800-1000_FP	AAGGTTTGATCAGATGGAGAAAGTT
ATG8H_ChIP_800-1000_RP	TAAGAACCAATCAAAATATTGAAAGTCCG
ChIP-TA3_FP	CTGCGTGGAAGTCTGTCAAA
ChIP-TA3_RP	CTATGCCACAGGGCAGTTTT
Cloning primers	
Primer name	**Primer Sequence 5'-3'**
pATG8F_5kb_1R4_FP	GGGGACAACTTTGTATAGAAAAGTTGTTgactcctctctccacaatgac
pATG8F_5kb_1R4_RP	GGGGACTGCTTTTTTGTACAAACTTGTtccttccacgcctacacaca
mNG_gATG8F_overlap_RP	TGCTTGAACGAGCTTTTTGCCATcgcgccaccaccaccCTTGTACAGCTCGTC
mNG_gATG8F_overlap_FP	GACGAGCTGTACAAGggtggtggtggcgcgATGGCAAAAAGCTCGTTCAAGCA
p221_gATG8F-stop_RP	GGGGACCACTTTGTACAAGAAAGCTGGGTTTTATGGAGATCCAAATCCAAATG
gATG8F_221_FP	GGGGACAAGTTTGTACAAAAAAGCAGGCTGTATGGCAAAAAGCTCGTTCAAG

gATG8F_221_RP	GGGGACCACTTTGTACAAGAAAGCTGGGTTTGGAGATCCAAATCCAAATGTG
pUBQ10_2kb_1R4_FP	GGGGACAACTTTGTATAGAAAAGTTGTTatttatggatacacagtcta
pUBQ10_2kb_1R4_RP	GGGGACTGCTTTTTTGTACAAACTTGTctgttaatcagaaaaactca
p221a_mNeonGreen_FP	GGGGACAAGTTTGTACAAAAAAGCAGGCTGTATGGTGAGCAAGGGCGAGGA
p221a_NG-HDEL-stop_RP	GGGGACCACTTTGTACAAGAAAGCTGGGTTTTACAATTCGTCGTGCTTGTACAGCTCGTC
GTIP1_p221_FP	GGGGACAAGTTTGTACAAAAAAGCAGGCTGTATGCCGATCAGAAACATCGC
GTIP1_p221_RP	GGGGACCACTTTGTACAAGAAAGCTGGGTGTAGTCTGTGGTTGGGAGC
gWOX5 FP	GGGGACAAGTTTGTACAAAAAAGCAGGCTGTATGTCTTTCTCCGTGAAAGGTCGAAGCTTAC
gWOX5 RP	GGGGACCACTTTGTACAAGAAAGCTGGGTTAAGAAAGCTTAATCGAAGATCTAATGGC
1R4a-pWOX5-FP	GGGGACAACTTTGTATAGAAAAGTTGTTtttgtctataaggttttacc
1R4a-pWOX5-RP	GGGGACTGCTTTTTTGTACAAACTTGTgttcagatgtaaagtcctca

Table 4. Resources used in this study

Reagent / Resource	**Source**	**Identifier**
Recombinant Antibodies		
Rabbit polyclonal α-GFP antibody	Abcam	Cat# ab290
Goat Anti-Rabbit IgG H&L (HRP)	Abcam	Cat# ab6721
Bacteria and Plant Strains		
Escherichia coli (DH5a)	N/A	N/A
Agrobacterium tumefaciens (C58)	N/A	N/A
Arabidopsis thaliana (Columbia ecotype)	(16)	Col-0

Plant and Bacterial Culture Reagents		
Murashige & Skoog basal salts Medium	Sigma	Cat# M5524
Agar PT	Himedia	Cat# RM7691-1KG
Sucrose	Sigma	Cat# S0389
Potassium hydrochloride (KOH)	Himedia	Cat# MB262
β-Estradiol	Sigma	Cat# 250155
Dexamethasone	Sigma	Cat# D2915
3-Methyladenine	TCI	Cat# M2518-1G
N-Acetyl-L-cysteine	TCI	Cat# A0905
Kanamycin sulfate from *Streptomyces kanamyceticus*	Sigma	Cat# K1377
Rifampicin, Plant Culture Tested	Himedia	Cat# PCT1119-25G
Spectinomycin dihydrochloride pentahydrate	Himedia	Cat# TC034
Hygromycin B from *Streptomyces hygroscopicus*	Sigma	Cat# H9773-250MG
Ampicillin sodium salt, Plant Culture Tested	Himedia	Cat# PCT1101-25G
Luria Bertani broth	Himedia	Cat# M1245
Luria Bertani agar	Himedia	Cat# M1151
Molecular Biology Reagents		
Gateway™ BP Clonase™ II Enzyme mix 100 reactions	Invitrogen	Cat# 11789100
LR Clonase™ II Plus enzyme	Invitrogen	Cat# 12538200
Nuclease Free Water	Himedia	Cat# TCL016
PrimeSTAR GXL DNA Polymerase	Takara	Cat# R050A

Taq Polymerase	Takara	Cat# R500A
LEO PRIME 2X MASTERMIX	DXBIDT	Cat# R8220
Agarose for Molecular Biology	Himedia	Cat# MB080
Dimethyl-sulfoxide	Sigma	Cat# D8418
Glycerol	Sigma	Cat# G5516
Complete Protease Inhibitor Cocktail (PIC)	Roche	Cat# 16829800
Phenylmethylsulfonyl fluoride (PMSF)	Sigma	Cat# P7626
NaCl	Himedia	Cat# GRM031
Na_2HPO_4	Himedia	Cat# RM1417
NaH_2PO_4	Himedia	Cat# RM3964
Glycine for molecular biology, 99.5%	SRL	Cat# 64072
Sodium dodecyl sulfate (SDS)	Sigma	Cat# L4390
Triton X-100	Sigma	Cat# X100
Glycerol	Sigma	Cat# G5516
IGEPAL	Sigma	Cat# I3021
LiCl	Sigma	Cat# L9650
Tris base	Himedia	Cat# TC072
β-Mercaptoetanol	Sigma	Cat# M3148
EDTA disodium dihydrate	Sigma	Cat# GRM1195
Tris-Cl	Himedia	Cat# MB030
DYNABEADS PROTEIN A, 1 ML	Invitrogen	Cat# 10001D

Sodium acetate	Himedia	Cat# GRM1012
Ethanol, molecular biology grade	Himedia	Cat# MB228-500ML
General Apparatus		
Plasticware (pipette tips, microcentrifuge tubes, tube-stands, boxes)	Tarsons	N/A
Glassware – glass test tubes, tissue culture plates	Duran	N/A
Square petriplates (tissue culture treated)	Himedia	Cat# PW050
Circular tissue culture petriplates (100mm, 60mm, 35mm)	Himedia	N/A
40µM cell strainer	BD Falcon	Cat# 352340
Commercial Molecular Biology Kits		
PrimeScript™ RT Reagent Kit (Perfect Real Time)	Takara	Cat# RR037A
TB Green™ Premix Ex Taq™ II (Tli RNaseH Plus)	Takara	Cat# RR820A
NucleoSpin Gel and PCR Clean-up (50)	Macherey-Nagel	Cat# 740609.50
NucleoSpin Plasmid (50)	Macherey-Nagel	Cat# 740588.50
NucleoSpin RNA Plant (250)	Macherey-Nagel	Cat# 740949.250
Reagents for Microscopy		
Paraformaldehyde	TCI	Cat# P0018-500G
Xylitol	Sigma	Cat# X3375-500G
UREA POWDER BIOREAGENT FOR MOLECULAR &	Sigma	Cat# U5378-500G
SODIUM DEOXYCHOLATE BIOXTRA, >= 98.&	Sigma	Cat# 30970-500G
Calcofluor White M2R, Plant Culture Tested	Himedia	Cat# PCT1551
Glass slides	Himedia	N/A

Coverslips (24x60, 22x40, 18x18)	Himedia	N/A
Octadecafluorodecahydronaphthalene-25g (perfluorodecalin)	TCI	Cat# P0837-25G
Propidium iodide	Sigma	Cat# P4170
Instruments		
AR100 plant growth chamber	Percival	N/A
AR66 plant growth chamber	Percival	N/A
Leica TCS SP8 Multiphoton microscope	Leica	N/A
Zeiss LSM 780 Multiphoton microscope	Zeiss	N/A
Evident FV4000 microscope	Olympus	N/A
Nikon AX microscope	Nikon	N/A
Leica S8 APO stereozoom microscope	Leica	N/A
Olympus MVX10 stereozoom microscope	Olympus	N/A
CFX Opus 96 Real-Time PCR System	BioRad	N/A
Software		
FIJI	Open source	https://fiji.sc/
Adobe Photoshop 2023	Adobe Acrobat	N/A
Adobe Illustrator 2022	Adobe Acrobat	N/A
Graphpad Prism 10	Graphpad	N/A

2.2 METHODS

2.2.1 Plant materials and growth conditions

All transgenic and mutant lines used in this study are in the *Arabidopsis thaliana* Columbia (Col-0) wildtype background. Seeds were surface sterilized using 70% ethanol and 20% bleach, followed by seven washes with sterile distilled water, and vernalized for 3-4 days at 4°C in the dark before plating. Seeds were plated on half-strength Murashige and Skoog (1/2 MS, Sigma # M5524) medium with 1% sucrose (Sigma #S0389), 0.7% plant agar (Himedia # RM7691), pH 5.7-5.75, and grown vertically under a 16H light – 8H dark photoperiod (45 µmol/m^2/s white light) at 22°C and 70% relative humidity.

The T-DNA mutants *plt3-1, plt5-2, plt7-1, plt3;plt5, plt5;plt7, plt3;plt7, plt3;plt5;plt7* have been described previously (132, 138). ATG8 family T-DNA mutants *atg8b* (SALK_023952C), *atg8c* (SALK_003706C), *atg8f* (SALK_057021C), *atg8h* (SALK_119920C) were procured from the Arabidopsis Biological Resource Center (ABRC). The *atg8f;atg8h* double mutant was generated by genetic crossing. All T-DNA mutants were confirmed homozygous by genotyping PCRs (primers listed in Table S3). CRISPR-Cas engineered *PLT* mutants for *plt3-cr* and *plt7-cr* have been described previously (139, 140). Translational reporter lines *pWOX11::H2B-eGFP*, *pPLT3::gPLT3:vYFP*, *pPLT7::gPLT7:vYFP*, *p35S::PLT7:GR*, and *p35S::PLT3:GR* have been described previously (16, 134, 141). All mutant and transgenic plant lines used in this study are listed in Table S1.

2.2.2 Contact-mediated regeneration assay

Contact-dependent regeneration assay was adapted from Shanmukhan *et al,* 2021 with minor modifications (9) (Figure 2.1). Briefly, the 1st pair of leaves from 10–11-day old seedlings were excised at the petiole ~0.5mm from the petiole-lamina junction with angled Vannas microscissors. Excised leaves were transferred to freshly prepared hormone-free 1/2MS media (1% sucrose, 0.7% agar). Leaves were kept abaxial side down with the cut end of the petiole in contact with the media to induce *de novo* root regeneration, or with the adaxial leaf lamina in contact and cut end protruding upward for wound induced callus formation. The leaves were assayed either vertically on square 150mm petri-plates with 50ml media in two rows of 10 leaves each, or horizontally on 100mm circular petri-plates with 30ml media, 18-20 leaves arranged radially at the periphery. Regeneration plates were incubated in continuous light at 22°C and 70% relative humidity, and *de novo* root or wound callus formation was scored

between 10 - 15 days post cut. All scoring experiments were replicated between two independent T2 or T3 lines. For autophagy inhibition, 10-11 DPG leaves were excised and transferred to ½ MS media supplemented with 2 mM 3-MA (TCI #M2518 or Sigma #M9281) for sustained autophagy inhibition post excision. For ROS induction, 10-11 DPG leaves were excised and transferred to 1/2MS media supplemented with different concentrations of hydrogen peroxide to facilitate ROS accumulation (0.1 mM, 0.5 mM, 1 mM) for regeneration scoring.

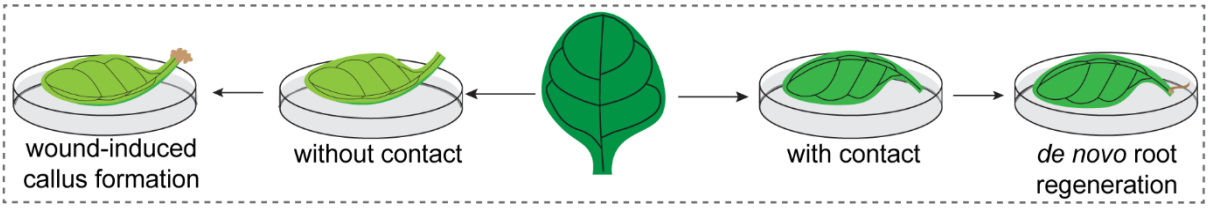

Figure 2.1 Schematic of contact-mediated regeneration assay

Estradiol treatment for ATG8F inducible overexpression

WT and *plt3-1* rosette leaves with the *pG1090.XVE::ATG8F* construct were excised and incubated on 1/2MS media supplemented with 5µM estradiol (in DMSO) for ATG8F ectopic overexpression (OE). WT ATG8F-OE in leaves with contact was done by long term incubation on estradiol media. ATG8F-OE in *plt3-1* was done by a 2-step method. The excised leaves were initially kept in with contact pose on estradiol for 12H post cut. After 12H the leaves were carefully cleaned using kim-wipes to remove media at the cut end and were kept back on the estradiol plate in without contact pose. Proliferating wound-calli seen while scoring at 15DPC confirmed that the cut end of the petiole was free of residual media after changing the contact condition of all samples tested.

N-acetylcysteine (NAC) treatment

Suboptimal concentration of NAC for ROS quenching during *de novo* root regeneration was selected after scoring phenotypes in WT and *plt3* leaves incubated in a variety of NAC treatment regimens as shown –

Sr. no.	**N-acetylcysteine concentration**	**Pulse duration**	***De novo* root regeneration**
1	50 µM	24H or continuous	×
2	75 µM	24H or continuous	×

3	100 µM	24H or continuous	×
4	0.25 mM	12H, 48H, or continuous	12H pulse with contact
5	0.5 mM	12H, 48H, or continuous	×
6	0.75 mM	48H	×
7	1 mM	6H, 12H, or continuous	12H pulse with and without contact
8	1.5 mM	6H, 12H, or continuous	×
9	2 mM	6H, 12H, or continuous	×

Two concentrations of NAC were selected based on consistent rescue of *plt3-1* mutant phenotype, 0.25 mM NAC with contact, and 1 mM NAC without contact. WT, *plt3-1*, *plt3-cr*, *plt7-cr*, *atg8f*, *atg8f;atg8h* and WT; WOX5-RFP, *plt3-cr*; WOX5-RFP, *plt7-cr*; WOX5-RFP leaves were excised and pulsed for 12H on 1/2MS media supplemented with 0.25 mM or 1mM NAC for chemical quenching of ROS. On 0.25 mM NAC, leaves were kept with contact for 12H, then transferred to normal 1/2MS media with contact until scoring. On 1 mM NAC, leaves were kept with or without contact for 12H, then carefully cleaned and transferred to normal 1/2MS plates in the opposite pose (with contact switched to without contact pose and *vice versa*) where they were kept until scoring. Leaves pulsed with 1mM NAC and switched in position were scored as per their contact pose at the time of scoring for regeneration phenotypes.

Dexamethasone and cycloheximide treatment

10-11 DPG leaves of the relevant PLT-overexpression background were excised and transferred to 1/2MS media for 12 hours with contact before any treatment. Following this, for dexamethasone treatment, leaves were incubated in liquid 1/2MS supplemented with 20 µM dexamethasone or DMSO for 4 hours (to induce PLT7 overexpression) or 8 hours (to induce PLT3 overexpression) (141). For cycloheximide treatment, the leaves were incubated for 4 hours in liquid 1/2MS supplemented with 40 µM cycloheximide, or 40 µM cycloheximide and 20 µM dexamethasone. Post incubation, leaves were dried on sterile kim-wipes and flash frozen in liquid nitrogen before RNA extraction.

2.2.3 Molecular cloning and plant transformation

All the plasmid constructs used in this study are listed in Table 2. All the primers used for cloning are listed in Table 3. Relevant genomic sequences were amplified from *Arabidopsis*

thaliana Col-0 genomic DNA. The promoter and gene sequences were individually amplified via PCR using Takara PrimeSTAR GXL DNA Polymerase (#R050A) and 100nM primers (Table S3) containing 5' att-sequences for Multisite Gateway Cloning. *UBQ10, WOX5,* and *ATG8F* promoters were cloned into the pGEM-TP4P1R entry vector via BP recombination. mNeonGreen-*ATG8F* reporter-gene template was amplified by overlap PCRs between mNeonGreen (gift from Ikram Blilou) and the *ATG8F* genomic sequence with a linker sequence between them. Both *NG-ATG8F* and *GTIP1* genomic templates were cloned into the pGEMteasy221 vector via BP recombination. mNeonGreen was amplified from pGEMTeasy P2R-P3 mNeonGreen (gift from Ikram Blilou) with a 3'-HDEL sequence for ER-localization and cloned into pGEMteasy221 via BP recombination. P1R4-UBQ10, P221-NG-ATG8F, P2R3-3AT were recombined into the pCam-kan-R4R3 destination vector to generate *pUBQ10::NG-ATG8F:3AT* by LR recombination. P1R4-G1090.XVE (136), P221-ATG8F, P2R3-3AT were recombined into pCam-kan-R4-R3 to generate *pG1090.XVE::ATG8F* by LR recombination. P1R4-ATG8F, P221-erNeonGreen, P2R3-3AT were recombined into pCam-kan-R4-R3 to generate *pATG8F::erNeonGreen:3AT* by LR recombination. P1R4-UBQ10, P221-GTIP1, P2R3-TagRFP-OcsT were recombined into pFG7m34GW destination vector to generate *pUBQ10::GTIP1:TagRFP-OcsT* by LR recombination. P1R4-PLT3, P221-PLT7, P2R3-4xgly-vYFP-3AT were recombined into the pFRm43GW destination vector to generate *pPLT3::gPLT7:vYFP-3AT* by LR recombination. All entry clones were recombined in their respective destination vectors using the Gateway™ LR Clonase™ II enzyme (Invitrogen). Constructs generated were introduced into *Agrobacterium tumifaciens* strain C58 by freeze-thaw or electroporation and further transformed into WT or mutant *Arabidopsis* plants by floral-dip method (142). Transgenic seeds were screened either by antibiotic selection plating or by seed-coat fluorescence using an Olympus MVX10 stereozoom microscope.

2.2.4 Sample fixation, clearing, and confocal microscopy

WOX11-GFP, PLT3-YFP, PLT7-YFP, WOX5-RFP reporter lines were imaged post sample fixation and clearing by ClearSee protocol (143). Briefly, leaves were fixed in freshly prepared 4% formaldehyde (in 1X PBS) under vacuum infiltration for 1 hour with intermittent breaks. Samples were washed twice with 1X PBS, 10 mins per wash to remove all fixative. The leaves were then incubated with ClearSee solution (10% xylitol, 15% sodium deoxycholate, 25% urea) for one week, with fresh ClearSee changed every 2 days. Before imaging, the leaves were stained with 0.1% Calcofluor White (Sigma) made in ClearSee for 1 hour, followed by destaining in fresh ClearSee for 1 hour. Cleared leaves were mounted on glass slides with

ClearSee and fixed under 24x60 coverslips for imaging. Confocal micrographs were captured using an upright Leica TCS SP8 confocal laser-scanning microscope with a HyD detector and a 20X/0.75 DRY PL APO CS2 objective. Image acquisition parameters were set to 1 airy unit, 1024x1024 pixel frame size, line average 2, scan-speed 200-400 Hz, digital zoom 0.75, with bidirectional scanning. YFP fluorescence was excited with an OPSL 514nm laser at 10% power and detected between 525-545nm with gain 100 using the HyD detector. Confocal z-stacks were taken in 2µm slices. WOX11-GFP samples were imaged using an inverted Nikon Ti2 Eclipse confocal laser-scanning microscope equipped with two GaAsP detectors and a 20X/0.8 OFN 25 PLAN APO objective. GFP fluorescence was excited with an OPSL 488nm laser at 5% power and detected between 495-520nm with gain range 20-30, other image acquisition parameters were kept identical as for the Leica TCS SP8. WOX5-RFP was imaged with an OPSL 561nm laser at 8% on an Olympus Evident FV4000 microscope equipped with SILVIR detectors and a 20X/0.8 UPLXAPO20X objective. Calcofluor white was excited with a 405nm UV laser at 1-2% and detected between 420-485nm. Gain and emission range was adjusted to avoid signal saturation and bleaching.

2.2.5 Live sample confocal microscopy

NG-ATG8F and GTIP1-RFP reporters were imaged in live leaves to investigate real-time cytoplasmic dynamics. Leaves were perfused with perfluorodecalin (PFD, TCI Chemicals #P0837) for 2-3 mins, then washed in sterile milli-Q water (MQ) for 5 mins. The leaves were mounted with the adaxial side towards the objective for imaging adaxial mesophyll cells adjacent to the cut end. Confocal micrographs were captured using an upright Leica TCS SP8 microscope with a HyD and two PMT detectors, and a HCX APO L U-V-I 40x/0.80 WATER objective. Image acquisition parameters were set to 1 airy unit, 1024x1024 pixel frame size, line average 2, scan-speed 200-400 Hz, with bidirectional scanning and 1µm z-width. NG-ATG8F fluorescence was excited using OPSL 488nm laser at 15% and captured with HyD gain 100 and emission range 495-525nm. GTIP1-TagRFP fluorescence was excited with OPSL 561nm laser at 8% with HyD gain 100 and emission range 575-600nm. Chlorophyll autofluorescence was captured in simultaneous acquisition with either fluorophore with a PMT detector at gain 850, -2 digital offset, and detection range set to 700-750nm. WT; *pATG8F::erNeonGreen* leaves were imaged abaxially for NeonGreen fluorescence with the 20x/0.75 DRY objective.

2.2.6 H_2DCFDA staining and live microscopy

DCFDA stained ROS were imaged in live leaves to observe real-time ROS levels in excised leaves. Leaves were incubated in 10 µM H_2DCFDA (or v/v DMSO in MQ as vehicle control) for 10-15 mins in the dark, room temperature. Leaves were washed in sterile MQ under the same conditions to wash off excess stain before imaging. Samples were mounted using sterile MQ and imaged on the abaxial side. Image acquisition was done at the Leica SP8 multiphoton microscope using the 20X dry objective. Images were acquired at 1024x1024 pixel frame size, line average 2, scan-speed 400 Hz, digital zoom 0.75, with bidirectional scanning. DCFDA fluorescence was excited with the OPSL 488nm laser at 5% power and detected between 515-545nm with gain 100 using the HyD detector. Confocal z-stacks were taken in 2µm slices.

2.2.7 RNA extraction and RT-qPCR

Assayed leaves were collected at the required experimental timepoints (4H post steroid treatment for dexamethasone and cycloheximide induced expression, 48HPC for *plt3* and *plt7* mutants, along with the experimental controls) and flash frozen in liquid nitrogen. Total RNA was extracted using Nucleospin RNA plant extraction kit (Macherey-Nagel #740949.250) and given on-column DNase treatment as per kit guideline. 1µg of pure RNA was used for cDNA synthesis using the PrimeScript RT Reagent Kit (Takara #RR037). All cDNA were diluted to 1:10 using nuclease free water before qPCR. Exon-spanning RT-qPCR primers were designed with NCBI Primer-BLAST. RT-qPCR was carried out in 96-well qPCR plates (Biorad) in 10ul reactions containing TB Green (Takara #RR820), 400nM qPCR primers (Supplementary Table 3), 5ng diluted cDNA, and nuclease free water in the Biorad CFX Opus 96 cycler. All reactions were performed in three biological replicates with three technical replicates each (N=3, n=9). Fold change of gene expression was calculated using the $-\Delta\Delta C^T$ method and *ACT2* was used as the internal housekeeping control in all reactions. Data were normalized using the dCt values of the biological replicates.

2.2.8 Chromatin immunoprecipitation (ChIP)

To confirm direct binding of PLT7-YFP to the *ATG8* gene loci, chromatin immunoprecipitation was carried out on WT; *pPLT7::gPLT7:vYFP* leaves post 5DPC with contact with Col-0 WT as untransformed control. Leaves were pooled and dried on sterile kim-wipes to remove any residual media stuck to the samples. The samples were then fixed in freshly prepared 1% formaldehyde (in 1X PBS) and subjected to intermittent vacuum infiltration for 60 minutes at room temperature for chromatin cross-linking. The volume of formaldehyde used was 5x the

total sample dry weight. When most of the leaves sank within the solution (indicating successful infiltration), the formaldehyde solution was decanted and fixation was neutralized with 0.125 M glycine (in 1X PBS) of equal volume. Neutralization was done under vacuum infiltration for at least 15-20 minutes to quench the reaction. Following this, the leaves were washed in ice-cold sterile 1X PBS twice, 10 minutes each to rinse off all fixative. Leaves were pat-dried carefully and flash frozen in liquid nitrogen. The frozen tissue was ground to a powder using micro-pestles under liquid nitrogen, and resuspended in 1mL ice-cold Nuclei Extraction Buffer (50 mM Tris-HCl pH 7.5, 150 mM NaCl, 1% Triton X-100, 0.1% Na-deoxycholate, 2.5 mM EDTA, 10% glycerol, supplemented with 1X protease inhibitor cocktail (Roche) and 1 mM PMSF (Sigma)). Solution was then filtered through a 40 µm cell strainer (BD Falcon), twice. The strained solution was centrifuged at 1000g, 4°C for 10 min to pellet the nuclei. Nuclei pellet was then resuspended in 1mL ice-cold Nuclei Lysis Buffer (25 mM Tris-HCl, 5 mM EDTA pH 8, 0.5% SDS) with gentle pipette mixing. Chromatin sonication was done for a total of 35 cycles of 10s ON/15s OFF at 35% amplitude (Sonics VCX 130) until the chromatin was sheared to 200-500bp (5 µL chromatin checked on a 1% agarose gel). Triton X-100 was added to the sonicated chromatin up to 1.1% and the solution was centrifuged at 13000rpm, 4°C for 5 min to extract clear supernatant into fresh tubes. Preclearing was done using 20 µL of 1mg/mL Protein A Dynabeads (Invitrogen, #10001D) and samples were incubated for 2H at 4°C with gentle shaking. Cleared chromatin was transferred to fresh tubes by using a DynaMag™ to separate the Dynabeads. 10% of each chromatin sample was processed as input DNA with ethanol (3x input volume) and 40 µL 3M sodium acetate for overnight DNA precipitation at -20°C. The remaining sample was split 1:1 and treated with 2µL of anti-GFP antibody (Abcam #ab290) or anti-rabbit IgG (Invitrogen) and chromatin was immunoprecipitated overnight at 4°C on a rotor. 50 µL of 1mg/mL Protein A Dynabeads was added to each fraction and further incubated at 4°C for 5H on a rotor. The IP'ed protein-DNA complex was sequentially washed with ice-cold low salt buffer (150 mM NaCl, 0.2% SDS, 0.5% Triton X-100, 2 mM EDTA, 20 mM Tris-HCl), high salt buffer (500 mM NaCl, 0.2% SDS, 0.5% Triton X-100, 2 mM EDTA, 20 mM Tris-HCl), LiCl wash buffer (0.25M LiCl, 0.5% IGEPAL, 0.5% sodium deoxycholate, 1 mM EDTA, 10 mM Tris-HCl), and TE buffer (10mM Tris-HCl, 1mM EDTA). Each buffer wash was done twice for 5 mins each. Finally, the beads were resuspended in 200 µL TE buffer with 4 µL Proteinase K (20mg/mL) and reverse cross-linking was carried out at 65°C for 1 hour. DNA was then purified using 1:1 phenyl:chloroform:isoamyl alcohol (Himedia #MB078) followed by overnight precipitation with ice-cold isopropanol and 40 µL 3M Na-acetate. DNA was pelleted down and washed with

70% ethanol (molecular biology grade), then air-dried and resuspended in 30 nuclease free water (Himedia #ML024). Equal volumes of both ChIP and IgG fractions were used for qPCRs.

ChIP-qPCR primers were designed against the first 200bp region upstream of the transcription start site of each gene using NCBI Primer-BLAST. qPCR was carried out in 10µL reactions of TB Green (Takara #RR820), 400nM qPCR primers (Supplementary materials), 1µL ChIP/IgG DNA, and nuclease free water in the BioRad CFX Opus 96 cycler. Reactions were performed in two biological replicates and three technical replicates each (N=2, n=6). PLT7 enrichment on *ATG8* promoters was calculated using $-\Delta\Delta C^T$ method and *TA3* was used as the housekeeping control for all reactions.

2.2.9 Image analysis

2.2.9.1 Autophagic puncta analysis

NG-ATG8F puncta numbers were counted using Fiji. Maximum intensity projections were prepared of single mesophyll cells. Background fluorescence was subtracted with rolling ball size <10 pixels to remove any diffuse signal. Cell outline was mapped with the 'Polygon' selection tool and NG-ATG8F puncta were counted using the 'Find Maxima' function with 'Prominence>80.0' and excluding edge maxima.

2.2.9.2 ATG8F promoter intensity analysis

pATG8F::erNeonGreen intensity was analyzed using Fiji. Maximum intensity projections were prepared of leaves imaged at 20X magnification. A rectangular ROI was drawn across the central width of the petiole spanning the entire length till the cut end and marked as signal ROI. A smaller rectangular ROI was made at the bottom right corner of the projection image and marked as background ROI. Mean grey values of each ROI were recorded and signal intensity was calculated as difference between signal and background ROI mean grey value.

2.2.9.3 Vacuole-chloroplast dynamics analysis

Multichannel line-scan graphs of WT, *atg8f*, *plt3* GTIP1-RFP 2DPC cells were prepared using the 'Plot_Multicolor' macro on Fiji (Macro_plot_lineprofile_multicolor; https://github.com/KeesStraatman/Multi-color-line-profile-plot). A line ROI of 1 pixel width was drawn longitudinally through the center slice of the full cell-stack and the macro was run

with the ROI to plot line intensity for both GTIP1-RFP and chlorophyll autofluorescence channels.

Kymographs were generated on Fiji using the 'KymoResliceWide' v.0.5 plugin for Fiji (https://github.com/ekatrukha/KymoResliceWide). A line ROI of 50 pixels width was drawn across the sagittal section of the z-stack with both GTIP1-RFP and chlorophyll autofluorescence channels and the plugin was used to generate a kymograph across the z-stack with maximum transverse intensity.

2.2.9.4 DCFDA intensity analysis

DCFDA intensity was analyzed using Fiji. Maximum intensity projections were generated for each z-stack. Three rectangular ROIs of the same dimensions were made across the petiole and designated as ROI 1 (farthest from cut end), ROI 2 (middle ROI), and ROI 3 (adjacent to cut end) (Figure 6*F*). Mean grey values of each ROI were measured across different samples and analyzed for differences across timepoints.

2.2.10 Statistical quantification and figure preparation

Statistical analysis and quantification were done for all regeneration assays, qPCR, and live cell imaging experiments. Regeneration assays and qPCRs were done with minimum three biological replicates and all imaging was done with at least two iterations. The levels of statistical significance for each graph are included in the respective figure legends (SEM, standard error of mean, N = no. of biological iterations, n= no. of samples). Experiment sample size is mentioned in the respective figure legend. Welch's two-tailed t-test was used for all RT-qPCR quantification, ROI quantification for DCFDA imaging, and for regeneration assay scoring. One-way ANOVA was used for regeneration assay analysis of multiple mutants assayed simultaneously. Kruskal-Wallis test was used for autophagic puncta analysis and Mann-Whitney test for ATG8F promoter intensity analysis respectively. Pearsons's χ^2 test was used for the 3-MA autophagy inhibitor assay and ROS induction assay. Data on all graphs are shown as mean ± standard error of mean (s.e.m.). Confocal micrographs were prepared using LasX software or Fiji and brightness-contrast for each image was adjusted accordingly. Graphs and images were compiled on Adobe Illustrator for figure assembly.

CHAPTER 3

Autophagy activation is essential for de novo root regeneration, and dispensable for wound healing

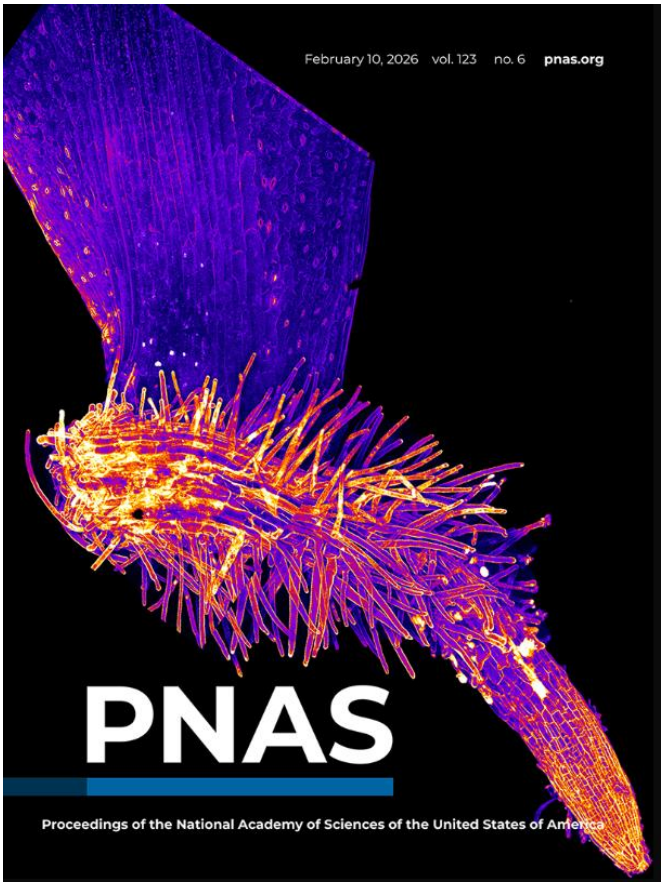

Results from this chapter have been published in:

Ganguly, A., Humnabadkar, A., Gautam, K., Willemsen, V., Xu, L., Dagdas, Y., & Prasad, K. (2026). PLETHORA–autophagy axis activates organ regeneration through ROS modulation. *Proceedings of the National Academy of Sciences*, *123*(6), e2513954123. (Featured on Cover)

"There is nothing like looking, if you want to find something. You certainly usually find something, if you look, but it is not always quite the something you were after."

– J.R.R. Tolkien

3.1 INTRODUCTION

In their natural environment, plants are exposed to constant physical and chemical threats across their body axis. To recover from the damage caused by these threats, the plant must initiate localised events in the cells at the wound site for wound closure, local cell proliferation, and propagating wound-induced signals, along with global activation of bioelectrical signals, hormone gradients and genetic regulatory networks to promote restorative cellular reprogramming (118, 144). Towards this cause, plants have evolved a robust system of hormone networks exclusively to manage wound induced stress metabolism, that includes jasmonate, salicylic acid, and ethylene signalling. These pathways act in concert to both mount an immune response at the wound site, and to activate auxin biosynthesis for further downstream cell reprogramming. Across different wounding contexts, these hormone signals first condition the cells in immediate vicinity of the wound to provide regeneration "competence" (17, 52, 81, 110, 145). These competent cells further differentiate to create *de novo* organs. However, wounding induced cell repair induces a spectrum of cell-fates, where organ regeneration is one of the possible outcomes. Often the cells at the wound site are reprogrammed to proliferate and form an unorganized wound-callus as seen in aerial organ cuttings of hypocotyl, cotyledon, and leaf (17, 64, 87, 146). Similar wound-induced cell proliferation is seen in ground tissue when resected distal from the regeneration competence zone near the root tip (48). The wound-induced callus has a distinct molecular signature from the tissue-culture induced pluripotent callus and is generally unable to undergo further differentiation to regenerate *de novo* organs (64, 65). Its function therefore appears limited to healing the wound and sealing it off to prevent pathogen infection and further damage.

Is there a difference in hormone activation post wounding that coordinates callus proliferation over organ regeneration and vice-versa? Establishing auxin and cytokinin gradients, appear to be necessary post-wounding responses for both wound callus formation and *de novo* root regeneration in excised leaves (13, 65, 70, 147). Stress-induced hormonal gradients are established early during the wound response and are necessary to condition the cells at the wound site for rapid changes in biochemical and genetic regulation (72, 105, 148–153), and appear to mostly facilitate the eventual downstream cell-fate transitions. The latter therefore must be coordinated by other unexplored cellular mechanisms that provide distinct signals for

cell proliferation post injury, and for cell differentiation to *de novo* stem cells capable of adventitious organ growth.

To investigate the mechanistic differences between wound healing and organ regeneration, I used the contact-mediated regeneration assay in excised *Arabidopsis* leaves (9). Previous work by Anju P. Shanmukhan in our research group determined that *de novo* root regeneration from an excised leaf occurs through physical media contact at the cut site, through pathways independent of nutrient availability and gravitropy, and occurs on minimal growth media, water, and even soil (9). Conversely, without media contact at the cut site, the cells undergo local wound healing and cell proliferation to make a wound-induced callus. This contact dependent leaf-to-root regeneration module thus provides a simple and elegant platform to investigate the pathways that distinguish wound-induced callus formation from *de novo* organ regeneration in plants. In this chapter, I investigated if autophagy, a universal cell survival and quality control mechanism, is equally essential for both cell-fates. Using several experimental approaches, I established that precise temporal activation of autophagy through specific members of the *ATG8* (autophagy-related gene 8) gene family is essential to activate *de novo* root regeneration, but completely dispensable for wound-induced callus formation. Further observation of procambial and regeneration-competent stem cell markers in excised leaves revealed that autophagy activation is essential for specific cell-fate transitions to orchestrate successful *de novo* root regeneration.

3.2 RESULTS

3.2.1 Cellular events that instruct organ regeneration are initiated rapidly post wounding

An excised leaf undergoes tremendous stress, firstly due to complete loss of contact and signalling cues from the parent body, and secondly from incubation on minimal growth media with no external hormone supplements. I surmised that in order to survive these extreme conditions and progress towards root regeneration or wound callus proliferation, the leaves must rapidly activate cell survival mechanisms post wounding. Here onwards the two scenarios will be referred to in text as “excised leaves with contact” and “excised leaves without contact”. To determine the early window of cell survival and regenerative reprogramming, I investigated the regeneration phenotype of excised leaves whose positions were switched after 48 hours, i.e., leaves cut and kept for 48H with contact on normal media were switched to the without contact pose, and *vice versa* (Figure 3.1A). Surprisingly, leaves kept for 48H with contact and switched to without contact pose for the remaining assay duration formed extensive *de novo*

roots along with wound-callus proliferation, at nearly the same frequency (~60%) as the control leaves kept with contact throughout the experiment (Figure 3.1B). Moreover, leaves that were switched to the 'with contact' pose after 48H without contact showed limited root regeneration of ~30%, with no visible wound-callus proliferation (Figure 3.1B). These results indicate that the cellular events occurring within the initial 48H time window post injury are crucial to determine the regeneration fate, and the pathways relevant for true organ regeneration may be uncoupled from simple wound healing and wound-induced callus formation. Importantly, these findings suggest that the fundamental processes to encourage organ regeneration fate are activated days before the actual differentiation of root founder cells into root primordium stem cells required for *de novo* root outgrowth, that occurs 4-5 days post leaf excision (70, 81, 83).

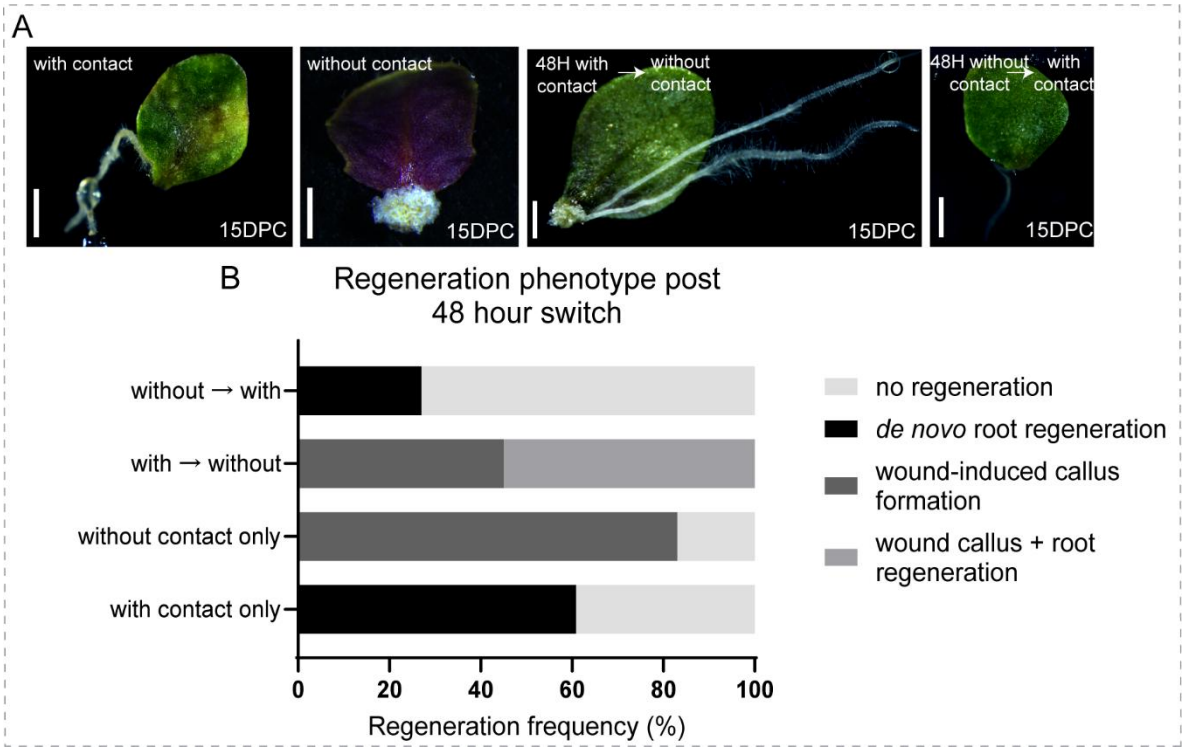

Figure 3.1 Early events post wounding are sufficient to determine organ regeneration fate. (A) Stereozoom images of excised leaves scored at 15 days post cut (DPC) with contact, without contact, 48H with contact → without contact, and 48H without contact → with contact (n=20-30 per group). (B) Graph showing regeneration phenotype and frequency of WT leaves kept in different contact poses (****P <0.0001, Pearson's $\chi 2$ test). Scale bar: 2 mm.

3.2.2 Autophagy is activated during *de novo* root regeneration, but not during wound-induced callus formation

In response to wounding, plants activate systemic cascades for reactive oxygen species (ROS), calcium levels, cell membrane potential, and hydraulic pressure, that originate from the cells at the wound site (111, 154). These signals increase intracellular stress within the cells that are damaged and exposed at the wound. Autophagy is an intracellular catabolic process essential

to remove damaged or cytotoxic components that are generated due to cell stress (155). However, as of this thesis, all known insights about the role of autophagy in plant wound repair have been inferred from *atg2*/*atg5* loss-of-function mutants or *ATG8* overexpression phenotypes during tissue culture shoot regeneration, graft wound healing, and wound-induced somatic reprogramming in *Physcomitrium patens* (10–12). How does autophagy influence cell-fate transitions during wound repair and regeneration in plants, remains unexplored. To investigate this, I first examined the autophagic response in excised leaves kept with or without contact. Among the vast family of autophagy proteins, the ubiquitin-like protein ATG8, undergoes ATG4 catalyzed- cleavage to act as a scaffold on the nascent phagophore complex surrounding the damaged cell component, and recruit core autophagy proteins to form the autophagosome (156). The ATG8-bound autophagosome is eventually transported to the lytic vacuole (in plants) or lysosome (in animals and fungi) for eventual degradation (157, 158). Thus, ATG8 is a core autophagy protein and a key marker for autophagy activation across eukaryotes.

To monitor autophagy response, I generated a constitutive translational fusion construct *pUBQ10::mNeonGreen-ATG8F* (NG-ATG8F) in wildtype (WT). Since root stem-cell reprogramming occurs in the deeply situated procambium layer (82, 83), imaging intracellular autophagy activation in these tissues was not feasible. Instead, I imaged mesophyll cells near the vasculature adjacent to the cut end. Post wounding, the mesophyll cells adjacent to the injury undergo reprogramming to become 'converter' cells that support rooting-competent cells in the vasculature during *de novo* root regeneration (81, 82). This is accomplished by rapid auxin biosynthesis and flux within the converter cells post wounding (13, 78, 82). Initially, I examined NG-ATG8F in excised leaves with contact. At 0 hours post cut (HPC), mesophyll cells displayed a diffuse ATG8F pattern with few NG-ATG8F-marked autophagic puncta, indicative of normal basal autophagy (Figure 3.2 A, A', G, G') (159). Over time (1–7 days post cut [DPC]), the number of ATG8F marked autophagic puncta significantly increased (Figure 3.2 B-F, B'-F', M). In contrast, the excised leaves without contact showed no significant increase in NG-ATG8F puncta compared to the initial levels observed at 0H (Figure 3.2 H-L, H'-L', M). These data suggest that in excised leaves, early activation and sustained autophagy is essential for *de novo* root regeneration, but dispensable for wound-induced callus formation.

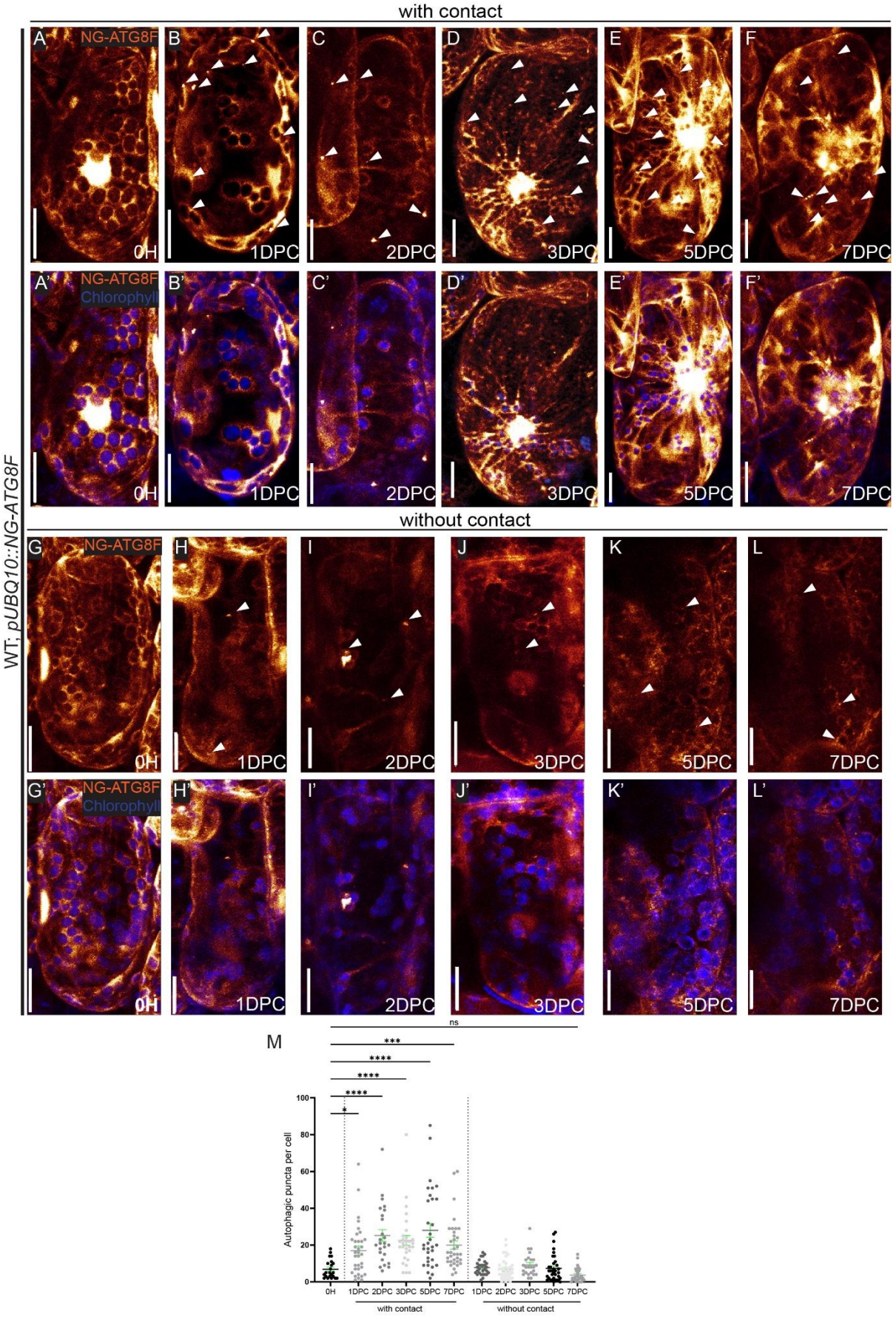
with contact
without contact
WT; pUBQ10::NG-ATG8F
NG-ATG8F
Chlorophyll
0H
1DPC
2DPC
3DPC
5DPC
7DPC
M
Autophagic puncta per cell
ns
***
****
****
****
*
with contact
without contact

Figure 3.2 Autophagy is activated during *de novo* root regeneration but not during wound-induced callus formation. *(*A-F, A'-F') Representative maximum projection images of WT mesophyll cells adjacent to the cut end of excised leaf expressing NG-ATG8F (WT; *UBQ10::NG-ATG8F*) at 0H, 1DPC, 2DPC, 3DPC, 5DPC, and 7DPC with contact. (A-F), NG-ATG8F channel (orange LUT); (A'-F'), NG-ATG8F merged with chlorophyll autofluorescence channel (blue). (G-L, G'-L') Representative maximum projection images of WT mesophyll cells adjacent to the cut end of excised leaf expressing NG-ATG8F (WT; *UBQ10::NG-ATG8F*) at 0H, 1DPC, 2DPC, 3DPC, 5DPC, and 7DPC without contact. (G-L), NG-ATG8F channel (orange LUT); G'-L', NG-ATG8F merged with chlorophyll autofluorescence channel (blue). (M) Graph representing quantification of NG-ATG8F autophagic puncta per mesophyll cell across each timepoint tested. Each point on the graph represents total number of NG-ATG8F puncta counted in one cell. n>20 cells were analyzed for each timepoint across both conditions. With contact, autophagic puncta significantly increase from 0H to 1DPC (*P=0.0179, Kruskal-Wallis test), 2DPC (****P<0.0001, Kruskal-Wallis test), 3DPC (****P<0.0001, Kruskal-Wallis test), 5DPC (****P<0.0001, Kruskal-Wallis test), and 7DPC (****P<0.0001, Kruskal-Wallis test). No change in autophagic puncta numbers seen in cells without contact across all timepoints tested (ns= not significant, Kruskal-Wallis test). Scale bars: 20µm. Data shown as mean ± s.e.m. White arrowheads: representative NG-ATG8F marked autophagic puncta. Note that puncta size shows variation across all conditions.

3.2.3 Autophagy response for *de novo* root regeneration is coordinated by specific members of the *ATG8* gene family

I next sought to identify the specific autophagy genes required for *de novo* root regeneration. The core genes encoding the autophagy machinery, initially identified in yeast, are highly conserved throughout eukaryotes, including plants (160–162). Autophagy is initiated upon activation of the ATG1 kinase complex, consisting of the ATG1 catalytic subunit with additional ATG13, ATG11 and ATG101 proteins, which phosphorylates and activates downstream autophagy components. An ATG6-ATG14-PI3K complex produces phosphatidylinositol 3-phosphate (PI3P) at the phagophore and recruits PI3P binding proteins like ATG2 and ATG18. Expansion and maturation of the phagophore requires delivery of lipids by the lipid scramblase ATG9 and lipid transfer protein ATG2, and two ubiquitin-like conjugation cascades – ATG5-ATG12-ATG16 and ATG8-phosphatidylethanolamine (through ATG7) – resulting in the conjugation of ATG8 on the autophagosome membrane. Most *ATG* genes have remained conserved in sequence and function across kingdoms. However, *ATG8* has evolved several orthologs in vascular plants like *Arabidopsis* compared to fungi and animals, whose individual functions are poorly understood (163, 164). In particular, the role of individual *ATG8* genes is not known in plant regeneration. I therefore focused on the *ATG8* family which contains nine genes (*ATG8A – ATG8I*) in *Arabidopsis thaliana*.

I first examined the transcript levels of all *ATG8* isoforms in excised leaves kept with contact and without contact. Since NG-ATG8F autophagic puncta formation increased at 1DPC itself (Figure 3.2 B, B'), I assessed the transcript levels of all endogenous *ATG8* isoforms at 12 hours post cut in leaves kept with or without contact. Among the nine isoforms, *ATG8B*, *ATG8C*,

ATG8F, and *ATG8H* were upregulated only in excised leaves with contact, with *ATG8F* showing the highest (~4-fold) increase (Figure 3.3A). Next, I checked the transcript levels of the four upregulated isoforms at different timepoints with contact. Here all four genes showed elevated transcript levels post 0H when leaves were kept with contact, among which *ATG8F* showed a steady pattern of increasing expression levels from 3H to 48H (Figure 3.3B). To further investigate *ATG8* activity, I examined the *ATG8F* expression domain using a transcriptional reporter construct (WT; *pATG8F::erNeonGreen)* driven by the 5kb *ATG8F* promoter. At 0H, ATG8F expression was widespread across the leaf (Figure 3.4 A, A'), consistent with previous reports on its expression in developing shoots (163, 165), indicating expected *ATG8F* expression in leaves during normal development. At the initial timepoints post excision, there was no discernible change in promoter activity between leaves with and without contact (Figure 3.4 B-C, B'-C'). However, with prolonged contact, promoter activity showed a significant increase by 7DPC (Figure 3.4 D-E, F), and without contact, the *ATG8F* promoter showed a significant decline in leaves without contact, falling below the original expression level observed at 0H (Figure 3.4 D'E', F). These results indicate that post-injury, specific *ATG8* isoforms, particularly *ATG8F*, are upregulated during *de novo* root regeneration and not wound-induced callus formation.

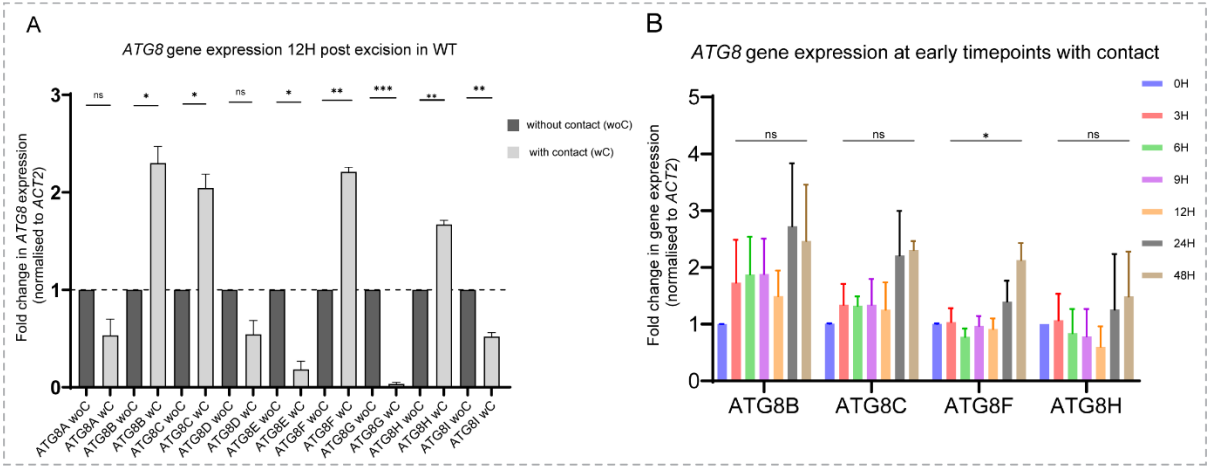

Figure 3.3 *ATG8* genes are differentially activated between *de novo* root regeneration and wound induced callus formation. (A) RT-qPCR graph of *ATG8* family gene expression levels in leaves kept for 12H without contact (woC) or with contact (wC) at the cut end (N=3, n= 9 technical replicates, 6-8 leaves per experiment). Out of 9 isoforms, *ATG8F* (**P= 0.0015, Welch's two-tailed t-test), *ATG8B* (*P= 0.0171, Welch's two-tailed t-test) *ATG8C* (*P= 0.0183, Welch's two-tailed t-test), and *ATG8H* (**P= 0.0042, Welch's two-tailed t-test) are significantly upregulated with contact. Gene expression levels in without contact group were normalized to 1 and used as control baseline to visualize differences in *ATG8* gene expression. (B) RT-qPCR graph of *ATG8* gene expression levels in leaves kept at different timepoints – 0H-3H-6H-9H-12H-24H-48H – with contact. While transcript levels of *ATG8B, ATG8C, and ATG8H* fluctuate within these timepoints, *ATG8F* levels show steady increase from 3H to 48H (*P= 0.035739, Welch's two-tailed t-test) indicating regulated transcriptional activation with contact. Data shown as mean ± s.e.m.

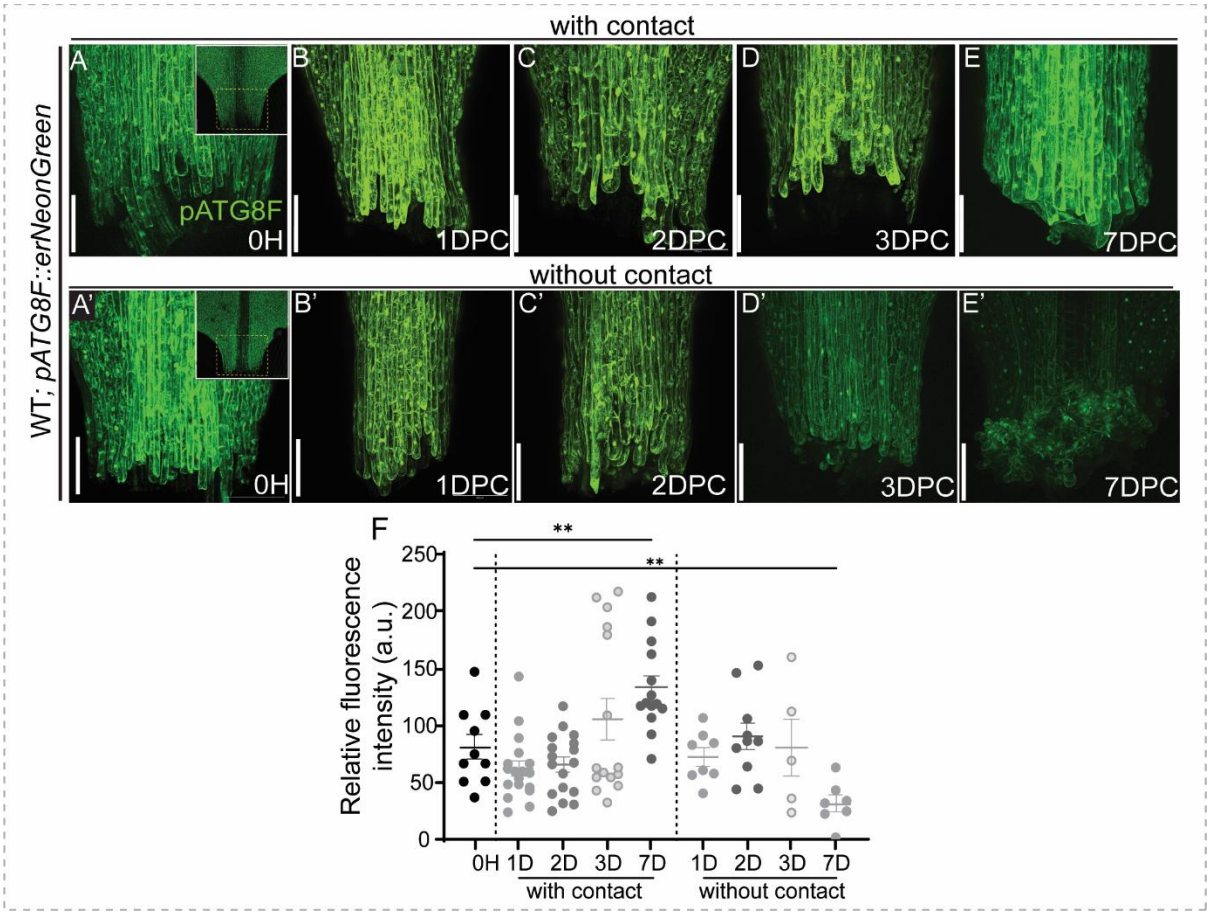

Figure 3.4 *ATG8F* promoter activity gradually increases during de novo root regeneration. (A-E) Representative maximum projection images of WT; *pATG8F::erNeonGreen* leaves post excision kept with contact. *ATG8F* promoter domain was widespread across the leaf even at 0H (A, A'). From 1DPC-7DPC, *ATG8F* reporter intensity increased significantly compared to 0H. (A'-E') Representative maximum projection images of WT; *pATG8F::erNeonGreen* leaves post excision kept without contact. From 1DPC-7DPC reporter intensity significantly reduced during wound-induced callus formation. (A-A') inset: 10x magnification of leaf at 0H. (F) Graph of relative fluorescence intensity of *pATG8F::erNeonGreen* in WT post excision. Each data point in the graph indicates the mean fluorescence readout from the petiole of one leaf. *ATG8F* promoter activity increased with contact (**P=0.0011, Mann-Whitney test) was seen. Without contact, reporter intensity significantly reduced by 7DPC (**P=0.0018, Mann-Whitney test).

I next tested if genetic depletion of these *ATG8* genes affects *de novo* root regeneration. To confirm the functional relevance of these genes, I analyzed T-DNA insertion mutants of five *atg8* mutants, i.e. four upregulated *ATG8* isoforms. Single mutants *atg8b* and *atg8c* exhibited a ~30% reduction in root regeneration, while *atg8f* and *atg8h* single mutants showed nearly a 50% reduction compared to WT (Figure 3.5 A, C). The *atg8f;atg8h* double mutant displayed a further 75% reduction in *de novo* root regeneration compared to WT (Figure 3.5A). Notably, none of these single or double mutants exhibited defects in wound-induced callus formation (Figure 3.5 B, D). Given the known redundancy among the *ATG8* genes, it was noteworthy that

atg8f and *atg8h* single mutants showed significant reduction in *de novo* root regeneration, and the double *atg8f;atg8h* mutant had a severe phenotype.

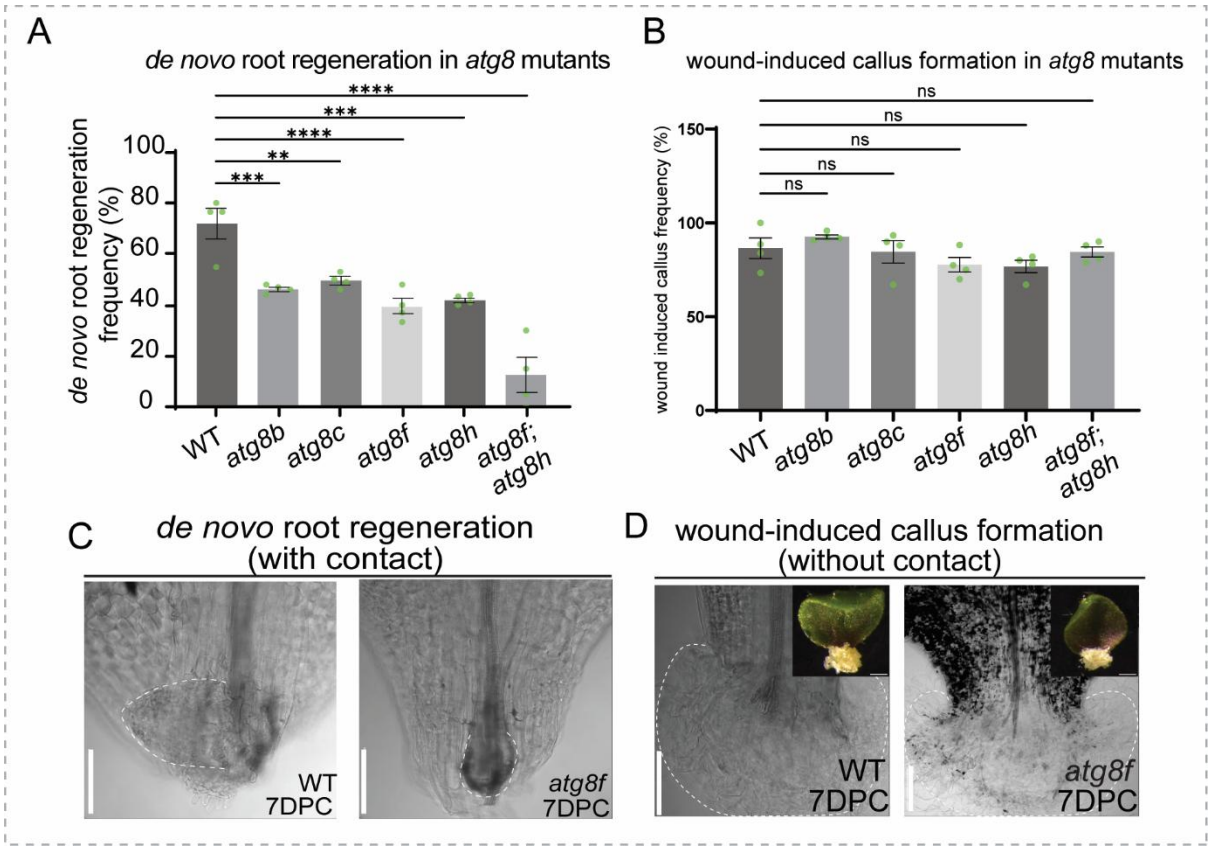

Figure 3.5 Functional depletion of *ATG8* genes impairs *de novo* root regeneration only. (A) Graph representing *de novo* root regeneration frequency (%) in WT, *atg8b* (***P=0.0001, ordinary one-way ANOVA), *atg8c* (***P=0.0004, ordinary one-way ANOVA), *atg8f* (****P<0.0001, ordinary one-way ANOVA), *atg8h (*****P<0.0001, ordinary one-way ANOVA), *atg8f;atg8h* (****P<0.0001, ordinary one-way ANOVA) (N=4, n=20-30 leaves per biological replicate). (B) Graph representing wound-induced callus frequency (%) in *atg8b* (ns, P=0.7406, Welch's two-tailed t-test) *atg8c* (ns, P=0.9973, Welch's two-tailed t-test), *atg8f* (ns, P=0.4373, Welch's two-tailed t-test), *atg8h* (ns, P=0.3485, Welch's two-tailed t-test), *atg8f;atg8h* (ns, P=0.9968, Welch's two-tailed t-test) mutants unchanged from wildtype (WT) (C) Representative brightfield images of cleared WT and *atg8f* mutant leaves kept with contact till 7DPC. Dashed white line: emerging root in WT, and endogenous callus in *atg8f* mutant. (D) Representative brightfield images of WT and *atg8f* mutant leaves kept without contact. Insets: stereozoom images of without contact wound-callus in WT and *atg8f* at 15DPC. Dashed white line: wound-induced callus outline. Scale bars: 2 mm.

I speculated that the functional redundancy between *ATG8* isoforms could partially compensate during wound repair and *de novo* root regeneration. Therefore, I next checked if the total inhibition of all autophagy responses would impact both root regeneration and wound callus formation. To test this, I first treated WT excised leaves with 2mM 3-methyladenine (3-MA), a phosphatidylinositol-3-kinase (PI3K) inhibitor that blocks all downstream autophagic responses (166). Strikingly, 3-MA treatment completely abrogated *de novo* root regeneration while leaving wound-induced callus formation unaffected (Figure 3.6 A, B). Next, I examined

the regeneration phenotype of the severe autophagy deficient *atg2* and *atg5* loss-of-function T-DNA insertion mutants (kind gift from Yasin Dagdas) compared to WT. *De novo* root regeneration was severely compromised in both *atg2-2* (~24%) and *atg5-1* (~5%) compared to the WT (~51%), whereas wound-induced callus formation was reduced only in *atg5-1* (Figure 3.6C). Taken together, these findings prove that the inhibition of autophagy either by pharmacological means or by genetic mutants results in the loss of root regeneration from excised leaves, with negligible effects on wound healing and wound-callus proliferation. These results further validate the functional relevance of spatiotemporal autophagy activation during *de novo* root regeneration.

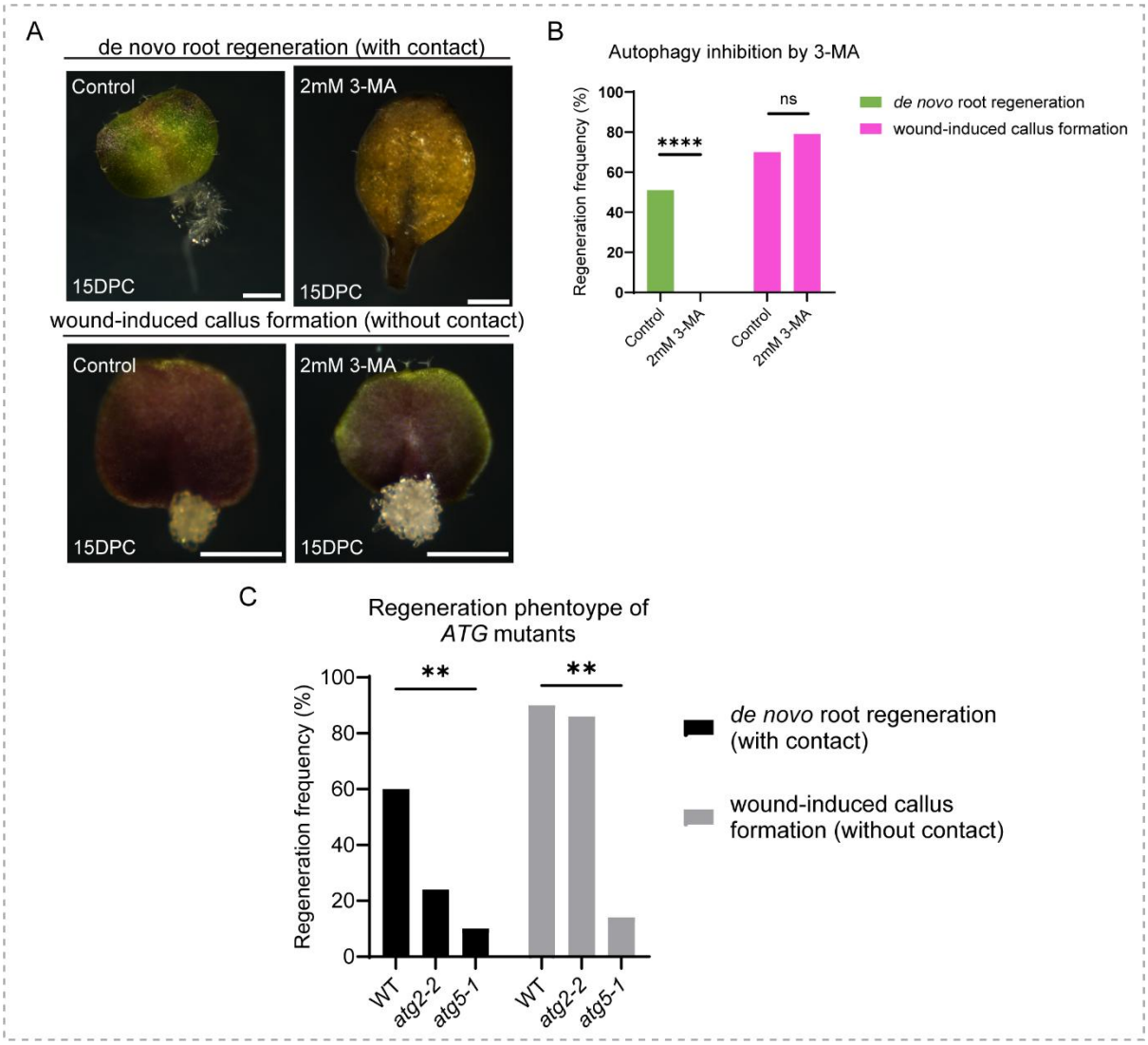

Figure 3.6 Severe genetic or pharmacological inhibition of autophagy impairs *de novo* root regeneration. (A) Representative stereomicroscope images of excised leaves kept with or without contact on 1/2MS control and 1/2MS + 2mM 3-MA. Phenotype was scored at 15 days post cut (15DPC). (B) Graph depicting *de novo* root regeneration frequency of untreated control (n=60, N=3) vs. 2mM 3-MA treated leaves (n=60, N=3) (****P<0.0001, Pearson's $\chi 2$ test) and wound-callus formation frequency of control (n=60, N=3) vs. 2mM 3-MA treated leaves (n=60, N=3) (ns = not significant, Pearson's $\chi 2$ test). (C) Graph depicting regeneration frequency

in severe autophagy deficient mutants *atg2-2* and *atg5-1* compared to WT. Both *atg2* and *atg5* were severely impaired in *de novo* root regeneration, while *atg5* alone showed a significant reduction of wound-induced callus formation (**P= 0.0057, Pearson's $\chi 2$ test). Scale bars: 2 mm. Data shown as mean ± s.e.m.

3.2.4 Activation of autophagy is essential to promote procambium reprogramming during *de novo* root regeneration, but not founder cell identity

The findings so far prove that autophagy is activated in the mesophyll converter cells early post wounding, and its sustained regulation by specific *ATG8* genes is essential for successful root regeneration. *De novo* root regeneration in excised leaves follows a 3-step reprogramming process – first, the rapid conditioning of cells adjacent to the site of injury into 'competent' and converter cells, second, differentiation of vascular stem cells into root founder cells that form an endogenous wound healing callus, and lastly, differentiation of a few root founder cells into root primordium stem cells capable of *de novo* root outgrowth (88). I next asked, which aspect of cellular reprogramming during *de novo* root regeneration requires autophagy activation?

To test this, I first monitored the expression of the procambium marker *PXY* (*PHLOEM INTERCALATED WITH XYLEM*) in leaves kept with or without contact. PXY is a receptor protein for regulating vascular development and differentiation (135). Using the transcriptional reporter line WT; *pPXY::erYFP* (kind gift from Ari Pekka Mahonen) I observed procambial activity in the vasculature of leaves post injury. At 0H, PXY expression was uniformly present across the leaf vasculature (Figure 3.7A). In leaves with contact, there was a localized increase in reporter intensity in the vascular network adjacent to the cut end between 2DPC-3DPC (Figure 3.7 A'-A''). This increased PXY expression in the leaf was visibly reduced at later timepoints during *de novo* root outgrowth at 6DPC (Figure 3.7 A'''). In contrast, prominent PXY expression was observed in the wound-induced callus cells formed in leaves without contact, which remained unchanged throughout the experiment (Figure 3.7 B-B'''). Interestingly, consistent PXY reporter activity was evident in 3-MA treated wildtype leaves and *atg8f* mutant leaves (Figure 3.7 C-C''', D-D''') even at later timepoints. These results suggest that post injury, there is specific spatiotemporal activity in the vascular stem cells at the site of endogenous callus formation and eventual root outgrowth that increases at the early timepoints post injury and gradually decreases during *de novo* root regeneration. Conversely, autophagy inhibition by 3-MA treatment or by genetic depletion interrupts the normal vascular reprogramming required for the root regeneration fate.

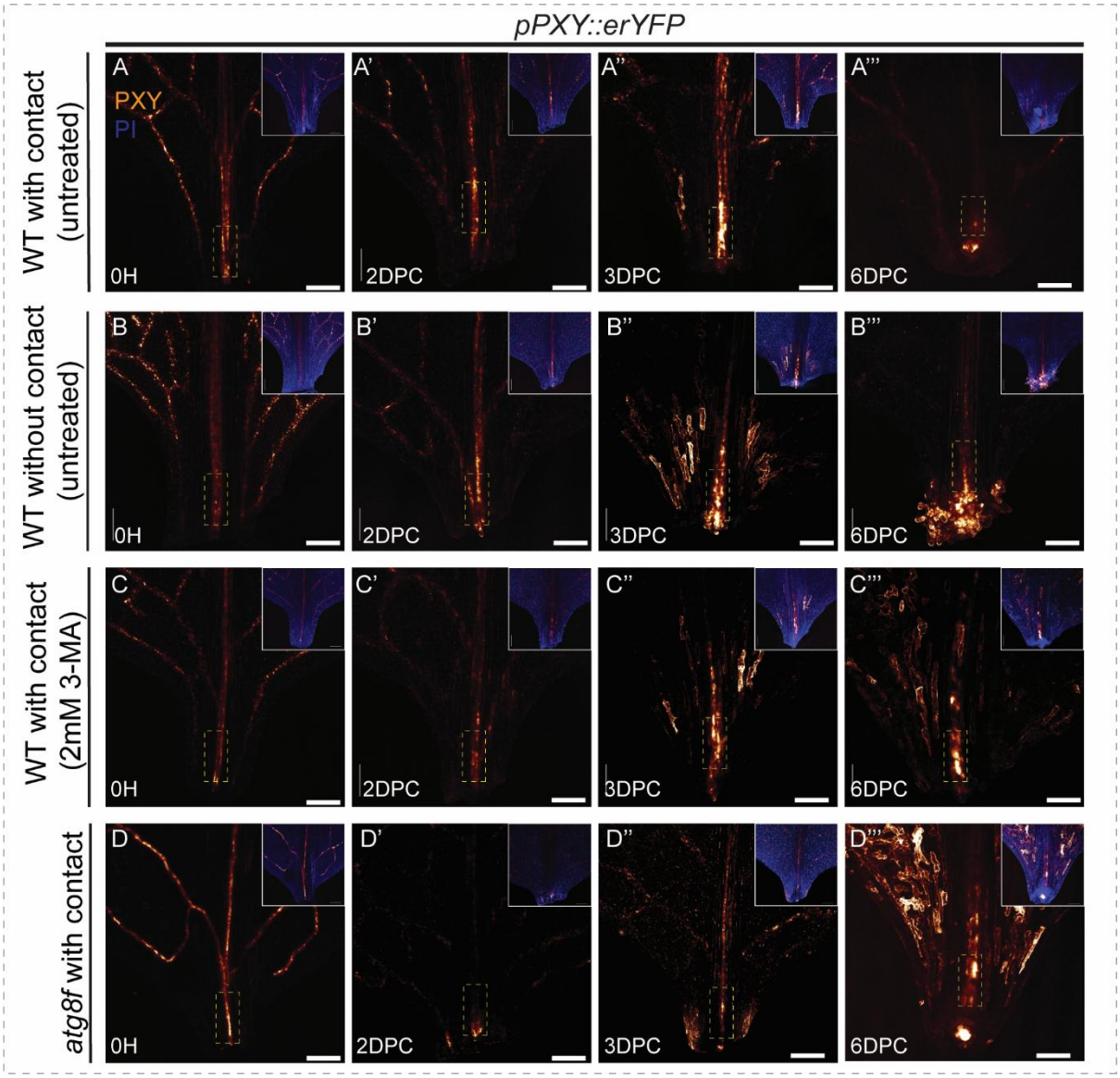

Figure 3.7 Autophagy activation promotes procambial stem cell activity during *de novo* root regeneration. (A-A''') Representative confocal micrographs of WT leaves expressing PXY-erYFP (orange LUT) at 0H-2DPC-3DPC-6DPC with contact. Insets: PXY-erYFP with propidium iodide (PI) stain (blue channel). The yellow dashed box indicates the region above the cut end with dynamic PXY promoter activity post excision. Between 0H (A) to 3DPC (A''), PXY activity visibly increased above the cut end, which reduced below detectable levels at 6DPC (A''') with the *de novo* root outgrowth. Unlike in WT leaves with contact, PXY-erYFP activity remained visibly increased even at 6DPC in WT leaves without contact (B-B'''), post 3-MA treatment (C-C'''), and in *atg8f* mutant with contact (D-D'''). (n>10 leaves per timepoint). Scale bars: 200 µm.

Among the reprogrammed 'regeneration-competent' cells, a few cells differentiate to form root founder cells within 48H post cut. These root founder cells are characterised by the expression of the transcription factor WUSCHEL RELATED HOMEOBOX 11 (WOX11) that further activates genes for endogenous callus formation and root primordium stem cell differentiation (83). I examined root founder cell identity using the *pWOX11::H2B-GFP* transcriptional reporter construct (kind gift from Lin Xu) in wildtype leaves with and without contact.

WOX11-GFP expression was visible in root founder cells at the site of injury within 1-2DPC with contact and was present in the endogenous callus even at later timepoints (Figure 3.8 A-A''). Interestingly, WOX11^{+} founder cells were also visible in leaves kept without contact, as well as in 3-MA treated and *atg8f* mutant leaves with contact (Figure 3.8 B-B'', C-C'', D-D''). This suggests that the inhibition of autophagy does not affect founder cell reprogramming during *de novo* root regeneration.

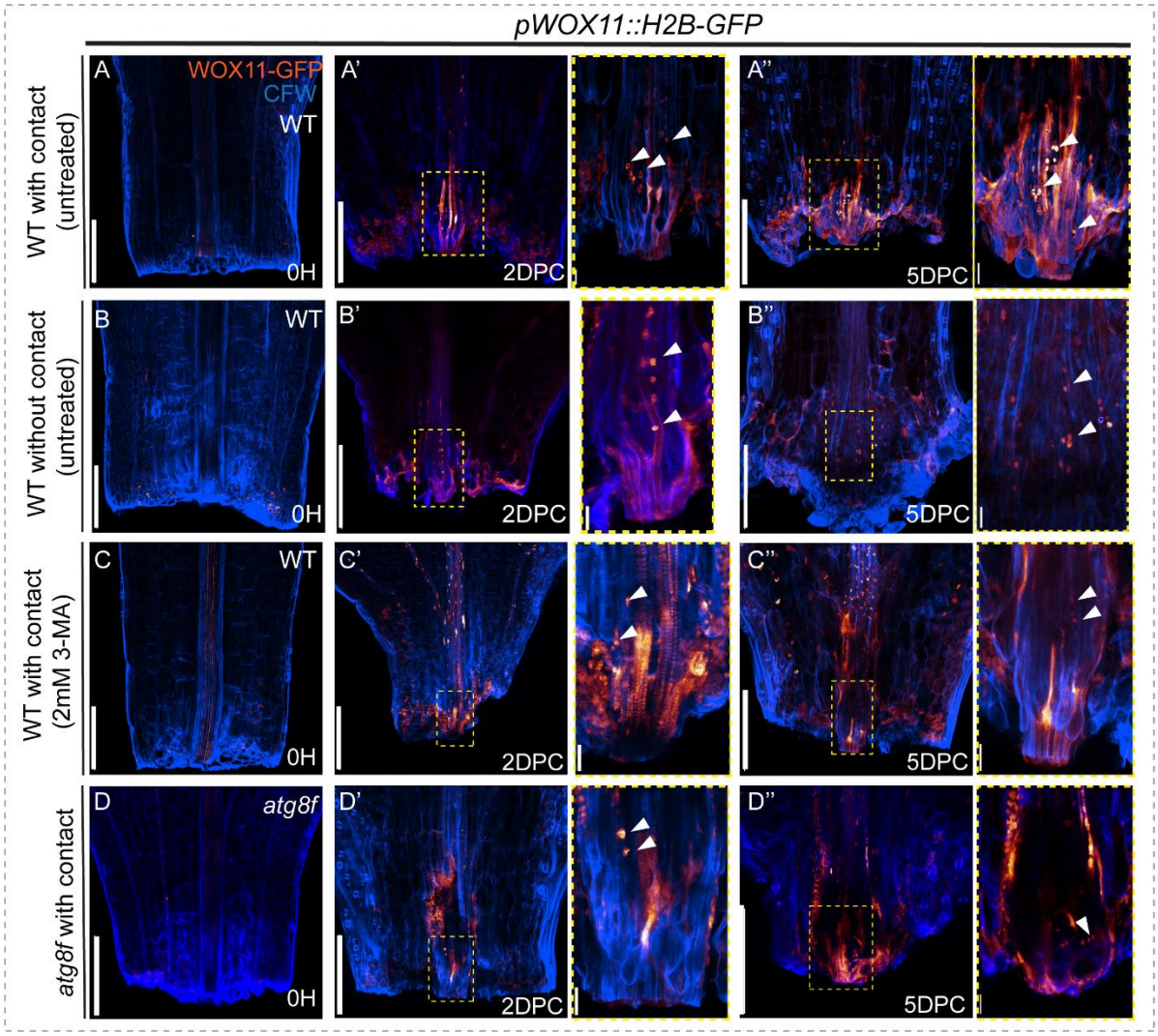

Figure 3.8 Founder cell specification and endogenous callus formation remains unaffected by the loss of autophagy either by pharmacological or genetic means. Representative maximum intensity projections of untreated WT with contact (*A-A''*), without contact (*B-B''*) WT with 2mM 3-MA (*C-C''*), and *atg8f* mutant (*D-D''*) lines expressing WOX11-GFP (orange LUT) with Calcofluor white (CFW, blue channel) cell boundary stain. At 0H post cut (*A, B, C, D*) no WOX11-GFP expression is seen near the cut end. At 2DPC (*A', B', C', D'*), WOX11-GFP expressing founder cells are visible at the cut end around the vascular bundle. White arrows indicate WOX11-GFP expressing nuclei. At 5DPC (*A'', B'', C'', D''*), the WOX11-GFP nuclei in 3MA treated leaves or in *atg8f* (yellow boxed insets are enlarged images of the cut end) do not show any difference in intensity or number compared to WT. Note that the orange striations and blotches are not true signal, but autofluorescence from cell damage at the cut end. Scale bars: 200 µm.

Taken together, these results indicate that spatiotemporal autophagy activation in excised leaves promotes vascular stem cell reprogramming, while leaving founder cell identity unchanged during *de novo* root regeneration.

3.3 DISCUSSION

Autophagy is a maintenance mechanism for most biochemical processes in living cells. It directs protein and organelle quality control, and recycles cell debris to meet the cells' metabolic demands. At the organismal level, overexpression of plant autophagy genes delays senescence, increases lifespan, enhances immunity against pathogens, and improves plant response to drought/salt/osmotic stress, oxidative stress, and nutrient starvation (155, 167–169). Conversely, autophagy deficient mutants show early senescence and are hypersensitive to abiotic stresses (169). Even so, not all autophagy genes in plants have the same phenotypes as seen in their fungal or animal homologs. *Atg9* mutants in yeast and animal models show defective autophagosome formation due to aberrant enzyme activity, while *Arabidopsis atg9* mutants show a slight reduction in macroautophagy flux (170, 171). This suggests that plants may have evolved specialized networks within the autophagy pathway for different purposes.

Despite the extensive volume of studies on autophagy response during nutrient stress, virus and other pathogen infections, abiotic (drought/salt/flooding) stress, the involvement of autophagy response in the plant wounding response has remained unexplored. Only recently some reports have shown that overexpression of ATG8/LC3 improves somatic cell reprogramming to protonema cells after wounding in *Physcomitrium patens* (10), and loss-of-function *ATG* mutants are unable to heal wounds and create protonema cells (11). Indeed, it would be a logical assumption that a quality control mechanism like autophagy may be essential universally across any injury context, but the current study shows otherwise. By analyzing autophagic activation across two distinct regenerative outcomes, my study shows that autophagy is essential for *de novo* root regeneration, but completely dispensable for wound healing and wound-induced callus proliferation. Using a combination of live cell imaging with genetic and molecular experiments, my findings reveal that autophagy activation in excised leaves occurs through a specific set of *ATG8* genes, among which *ATG8F* shows a clear upregulation during *de novo* root regeneration and not during wound-induced callus formation. While *ATG8C, ATG8E, ATG8F,* and *ATG8G* are all expressed in the *Arabidopsis* leaf during normal development (163), the single mutants *atg8f* and *atg8h* showed a more severe reduction in root regeneration compared to *atg8c*, whereas *ATG8E* and *ATG8G* transcripts did not show

any upregulation in leaves kept with contact. These findings suggest that within the *ATG8* gene family, individual functional isoforms are recruited for different cellular contexts. While autophagy response across different model systems including plants has been studied mainly in the context of the ATG protein interactors and their intracellular biochemical outputs, these proteins are subject to extensive turnover during active autophagy. Therefore, further study of the upstream transcriptional regulatory modules of the autophagy genes is a necessity to appreciate how their transcriptional output influences cellular homeostasis during organ regeneration.

Another long-standing question has been to understand the role of autophagy in cellular reprogramming. While several lines of evidence support autophagy mediated root and shoot meristem maintenance during development (172–174), whether it is essential for cell-fate transitions and reprogramming remains unclear. Herein my findings prove that autophagy activation is redundant for the differentiation of injury induced converter cells into root founder cells, that are common to both wound-induced callus formation and *de novo* root regeneration.

In summary, the findings of this study indicate that plants have adapted an ancient intracellular process like autophagy for orchestrating specific aspects of cellular reprogramming during wound repair to successfully promote organ regeneration post injury. Whether wounded cells can be conditioned towards a specific organ fate (e.g. root or shoot) by manipulating intrinsic cellular homeostasis pathways, is a fundamental and exciting question for plant biotechnology, and awaits further exploration.

CHAPTER 4

PLETHORA factors non-redundantly activate ATG8 genes during de novo root regeneration

Results from this chapter have been published in:

Ganguly, A., Humnabadkar, A., Gautam, K., Willemsen, V., Xu, L., Dagdas, Y., & Prasad, K. (2026). PLETHORA–autophagy axis activates organ regeneration through ROS modulation. *Proceedings of the National Academy of Sciences*, *123*(6), e2513954123. (Featured on Cover)

"See first, think later, then test. But always see first. Otherwise, you will only see what you were expecting. Most scientists forget that."

— Douglas Adams

4.1 INTRODUCTION

Given that autophagy is both a ubiquitous and selective intracellular pathway across development, stress response, and cell death, there must be tight control of autophagy activity in response to environmental or internal hormonal cues. While most of the autophagy proteome and its interactors are regulated by post-translational modifications, understanding the transcriptional regulation of autophagy related *ATG* genes during different physiological contexts has gained traction (15, 175). Since autophagy is a catabolic process where the protein complexes undergo rapid turnover, transcriptional control of *ATG* genes is essential to maintain a steady, sustained output during stress conditions or diverse developmental contexts. Stress-induced or adaptive autophagy is proposed to function as a biphasic mechanism in mammals (176, 177). The first phase utilizes the pre-existing cytosolic autophagy proteome with post-translational modifications to allow rapid activation of autophagy for cell repair. The second phase involves the activation of specific transcription factors (TF) that upregulate the necessary genes to sustain autophagy flux, allowing for an extended response to reestablish cellular homeostasis. Whether plant autophagy follows the same principle, especially during wound repair and regeneration, is not known.

Nevertheless, plant *ATG* gene regulators have been identified and characterized across limited stress contexts. HSFA1a and ERF5 upregulate core autophagy genes during drought and heat stress in *Solanum lycopersicum* (tomato), WRKY-family factors such as WRKY33 directly upregulate *ATG* genes during heat stress and against *Botrytis* infection in *Arabidopsis*, and BZR1, part of the brassinosteroid hormonal pathway, upregulates *ATG2* and *ATG6* in response to nitrogen starvation in tomato (169, 178). Another study identified several TF binding sites by a yeast one-hybrid screen on the *Arabidopsis ATG8* family gene promoters, and characterized TGA9 as an activator of specific *ATG8* genes during drought and osmotic stress (179). Transcriptional repressors of *ATG* genes include circadian clock related TFs such as TOC and LUX that control rhythmic plant autophagy, and SOC1 and HY5 that repress the expression of a subset of *ATG* genes to enhance tolerance during carbon and nitrogen starvation (175, 180).

In the context of *de novo* root regeneration from leaves, studies have revealed TF regulators from diverse developmental paths. Early signals such as ROS and abscisic acid (ABA)-induced factors, along with hormone pathways involving ethylene, jasmonate, and salicylic acid, are activated in response to injury, eventually triggering auxin biosynthesis (181). Local auxin biosynthesis and transport help establish root regeneration competence in the cells near the cut end. This further promotes the differentiation of founder cells into root primordium stem cells, which then develop into *de novo* adventitious roots. The PLETHORA family of factors are widely regarded as master regulators of plant regeneration and their triple loss-of-function mutant *plt3;plt5;plt7* is deficient across multiple regenerative and developmental contexts (9, 16–18, 132, 139, 182–184). Interestingly, among the PLTs, PLT7 overexpression activates *de novo* roots even in leaves kept without contact, thus identifying PLT7 as a candidate regulator of this process (9). However, the study also concluded that PLT-mediated *de novo* root regeneration does not occur via any of the known downstream targets (16–18, 139, 182), that opens up avenues for exploring novel PLT-regulated networks during this process.

In this chapter, using a suite of genetic and molecular tools, I examined the putative role of PLT factors as transcriptional regulators of autophagy mediated *de novo* root regeneration. Here my findings revealed that PLT7 both directly and indirectly activates *ATG8* genes during *de novo* root regeneration. While analyzing the necessity of PLT7, genetic analysis of *PLT* mutants revealed a surprising, non-redundant role for PLT3 in regulating PLT7 and *ATG8* genes for successful *de novo* root regeneration. *In toto*, the findings of this study illustrate how plant developmental regulators such as PLTs have evolved novel, non-redundant interactions among related members to spatiotemporally activate and sustain ancient cellular processes like autophagy during the process of *de novo* root regeneration.

4.2 RESULTS

4.2.1 PLT7 transcriptionally activates *ATG8* genes during *de novo* root regeneration

Having established the transcriptional upregulation of specific *ATG8* genes during *de novo* root regeneration, I next investigated the genetic regulators responsible for this surge. The *plt3;plt5;plt7* triple mutant phenocopies both chemical inhibition of autophagy and the genetic reduction of *ATG8* genes, suggesting potential molecular interactions between the PLT transcription factors and the sustained upregulation of *ATG8* genes during *de novo* root regeneration. To explore this hypothesis, I first analyzed the publicly available DAP-seq database that identifies in vitro interactions between transcription factors and genomic DNA

(Bartlett et al., 2017). This analysis revealed potential PLT7 binding loci at *ATG8* gene promoters (Figure 4.1). Since DAP-seq analysis provides an *in vitro* snapshot of protein-DNA interactions and does not reflect either tissue-specific or developmental contexts, I examined potential PLT7 binding at the *ATG8* promoter within 0-200 bp upstream of the transcription start site (TSS). CHIP and CHIP-qPCR analysis in 5-6 DPC leaves of a PLT7 translational reporter line (WT; *pPLT7::gPLT7:vYFP*) kept with contact showed nearly two-fold enrichment at the *ATG8F* promoter (Figure 4.2A), proving direct binding of PLT7 to *ATG8F* during *de novo* root regeneration.

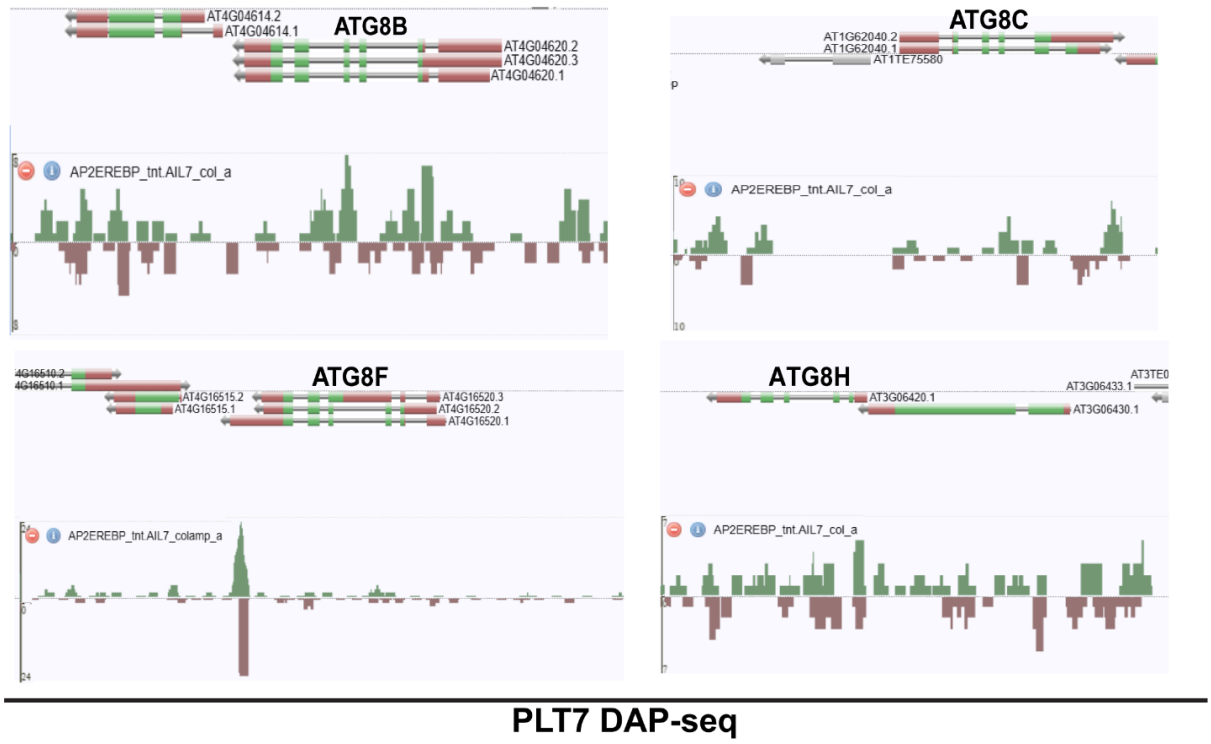

Figure 4.1 PLT7 DAP-seq analyses indicate possible binding of PLT7 to *ATG8* gene loci (Source: http://neomorph.salk.edu/dap_web/pages/). Screenshots of *ATG8B, ATG8C, ATG8F, ATG8H* gene loci with putative PLT7 DAP-seq DNA binding sites.

To validate the functional importance of PLT7-mediated *ATG8* expression during *de novo* root regeneration, I analyzed *ATG8* transcript levels across different *PLT7* genetic backgrounds in leaves with contact. First, I used a constitutive steroid inducible PLT7 overexpression line (WT; *p35S::PLT7:GR*) to induce PLT7 in leaves previously kept for 12H with contact so as to initiate the endogenous wound-induced molecular events before steroid treatment. In untreated cells, the GR (glucocorticoid receptor) peptide creates a complex of the fusion protein with chaperone proteins in the cytosol, preventing nuclear translocation. Addition of dexamethasone breaks this cytosolic complex and allows the GR-fused protein to enter the nucleus and execute its regulatory functions (186). Overexpression of PLT7 led to increased *ATG8F* transcript levels

within 4 hours, even with cycloheximide (CHX) treatment that inhibits protein synthesis (Figure 4.2B) (187). This further validates the result that *ATG8F* is rapidly and directly activated by PLT7 to promote autophagy during *de novo* root regeneration. Interestingly, only *ATG8F* showed direct transcriptional activation by PLT7 as transcript levels of the three other *ATG8* genes (*ATG8B, ATG8C, and ATG8H*) remained unchanged with CHX treatment during PLT7-GR induction (Figure 4.2C). However, these *ATG8* genes showed increased transcript levels with steroid induction alone, suggesting indirect regulation by PLT7 (Figure 4.2D).

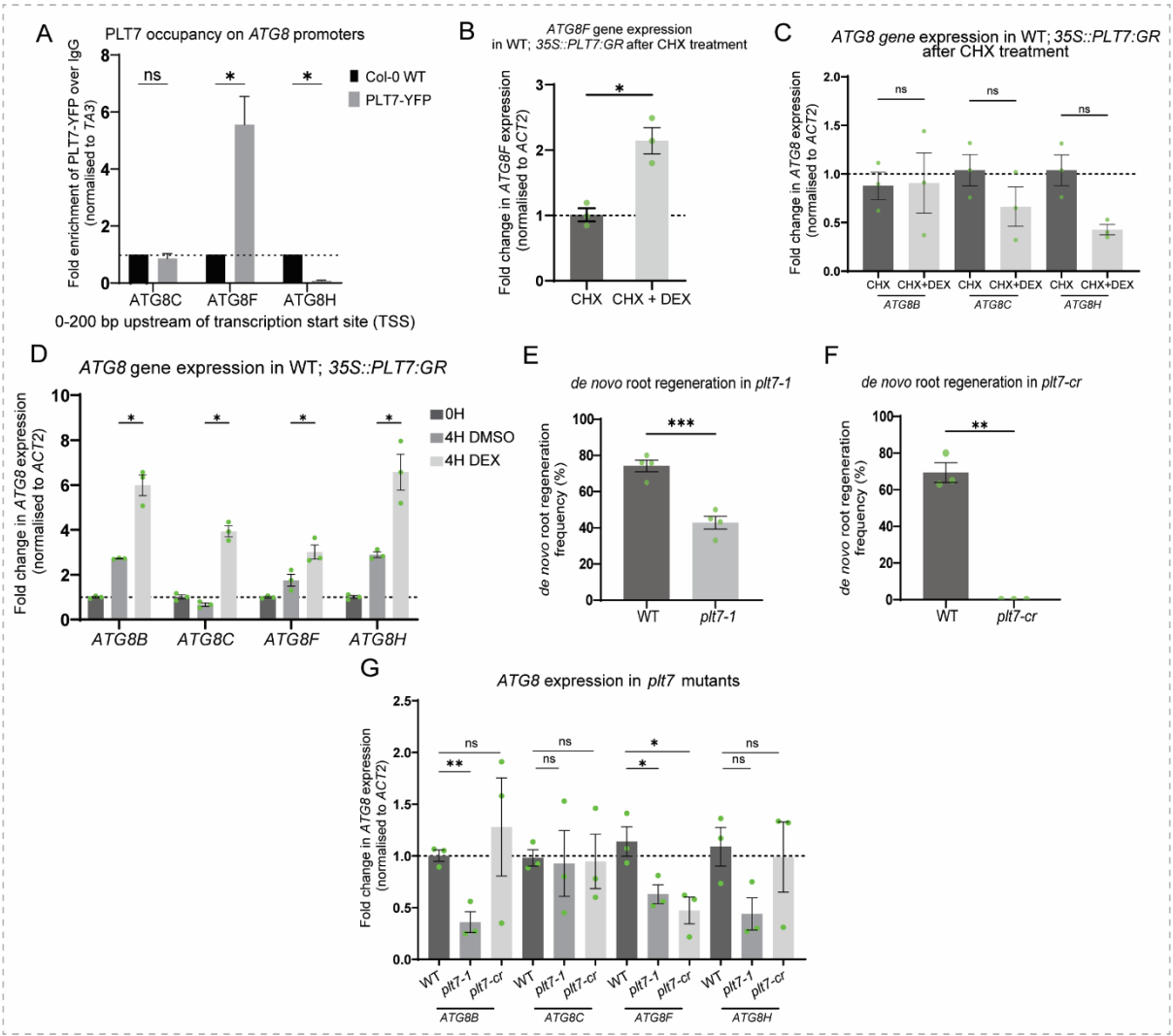

Figure 4.2 PLT7 transcriptionally activates *ATG8F* during *de novo* root regeneration. (A) Graph of ChIP-qPCR showing PLT7-YFP fold enrichment in the 0-200 bp promoter region upstream of transcription start site (TSS) for *ATG8C* (ns = not significant, Welch's unpaired two-tailed t-test), *ATG8F* (*P= 0.005850, Welch's unpaired two-tailed t-test), *ATG8H* (*P<0.000001 , Welch's unpaired two-tailed t-test) gene loci (N=2, n=6 technical replicates). (B) Graph representing 2-fold *ATG8F* gene upregulation after cycloheximide (CHX) treatment in WT; *p35S::PLT7:GR* (*P=0.0152, Welch's two-tailed t-test). (C) Graph representing *ATG8B*, *ATG8C*, *ATG8H* gene expression after cycloheximide (CHX) treatment in WT; *p35S::PLT7:GR* (ns=not significant, Welch's two-tailed t-test). (D) Rapid surge in *ATG8* gene expression in WT; *p35S::PLT7:GR* leaves after 4H DMSO or DEX induction post 12H with contact on normal 1/2MS media (*P<0.05, Welch's two-tailed t-test). (E) Graph representing decreased de novo root regeneration frequency in *plt7-1* T-DNA mutant

(***P=0.0006, Welch's two-tailed t-test, N=4, n>30 leaves per replicate)) compared to WT. (F) Graph representing total loss of de novo root regeneration in the *plt7-cr* mutant (**P=0.0059, Welch's two-tailed t-test, N=3, n>20 leaves per replicate). (G) Graph of *ATG8* gene expression in *plt7-1* and *plt7-cr* mutant leaves after 48H with contact showing significant downregulation of *ATG8F* in both *plt7-1* (*=0.0486, Welch's two-tailed t-test) and *plt7-cr* (*P=0.0258, Welch's two-tailed t-test) compared to WT (ns=not significant, Welch's two-tailed t-test). Data shown as mean ± s.e.m.

I next checked if the *plt7-1* loss of function mutant is defective in *de novo* root regeneration. This mutant displayed a ~40% reduction in root regeneration compared to WT, phenocopying the *atg8f* mutant (Figure 4.2E, 3.5A). I further validated this phenotype in a CRISPR-Cas engineered *plt7-cr* knockout mutant where strikingly, *de novo* root regeneration was severely impaired (Figure 4.2F) (140). In line with this phenotype, *ATG8F* transcript levels were significantly reduced in both *plt7-1* and *plt7-cr* mutants (Figure 4.2G). Taken together, these results indicate that PLT7 is essential for transcriptionally activating *ATG8F* mediated autophagy during *de novo* root regeneration.

4.2.2 PLT7 expression pattern recapitulates *ATG8F* during *de novo* root regeneration, and remains unchanged by loss of *ATG8F*

Given the role of PLT7 in *ATG8F* mediated autophagy regulation, I next examined its expression patterns in WT leaves using the PLT-vYFP translational reporter (WT; *pPLT7::gPLT7:vYFP*). At 0H post cut, PLT7-vYFP was undetectable across the leaf (Figure 4.3 A, A'). Subsequently with contact, I observed PLT7 expression at 1DPC in a field of cells near the cut end of the petiole (Figure 4.3 B, B'). In the following timepoints, this PLT7-vYFP expression domain expanded into the endogenous healing callus and surrounding tissues, eventually spreading from the petiole into the leaf blade during *de novo* root regeneration (Figure 4.3 C-E, C'-E'). Notably, this PLT7 expression pattern closely resembles the progressive increase of *ATG8F* transcriptional reporter activity shown in the previous chapter (Figure 3.4). Moreover, the widespread PLT7-vYFP expression pattern in the *atg8f* mutant (*atg8f*; *pPLT7::gPLT7:vYFP*) resembled the WT reporter, thus confirming that *ATG8F* mediated autophagy functions downstream of PLT7 during *de novo* root regeneration (Figure 4.3 J-N, J'-N'). Without contact, the PLT7-vYFP expression domain remained confined to the petiole and was seen only in the proliferating wound-callus cells at the cut end (Figure 4.3 F-I, F'-I').

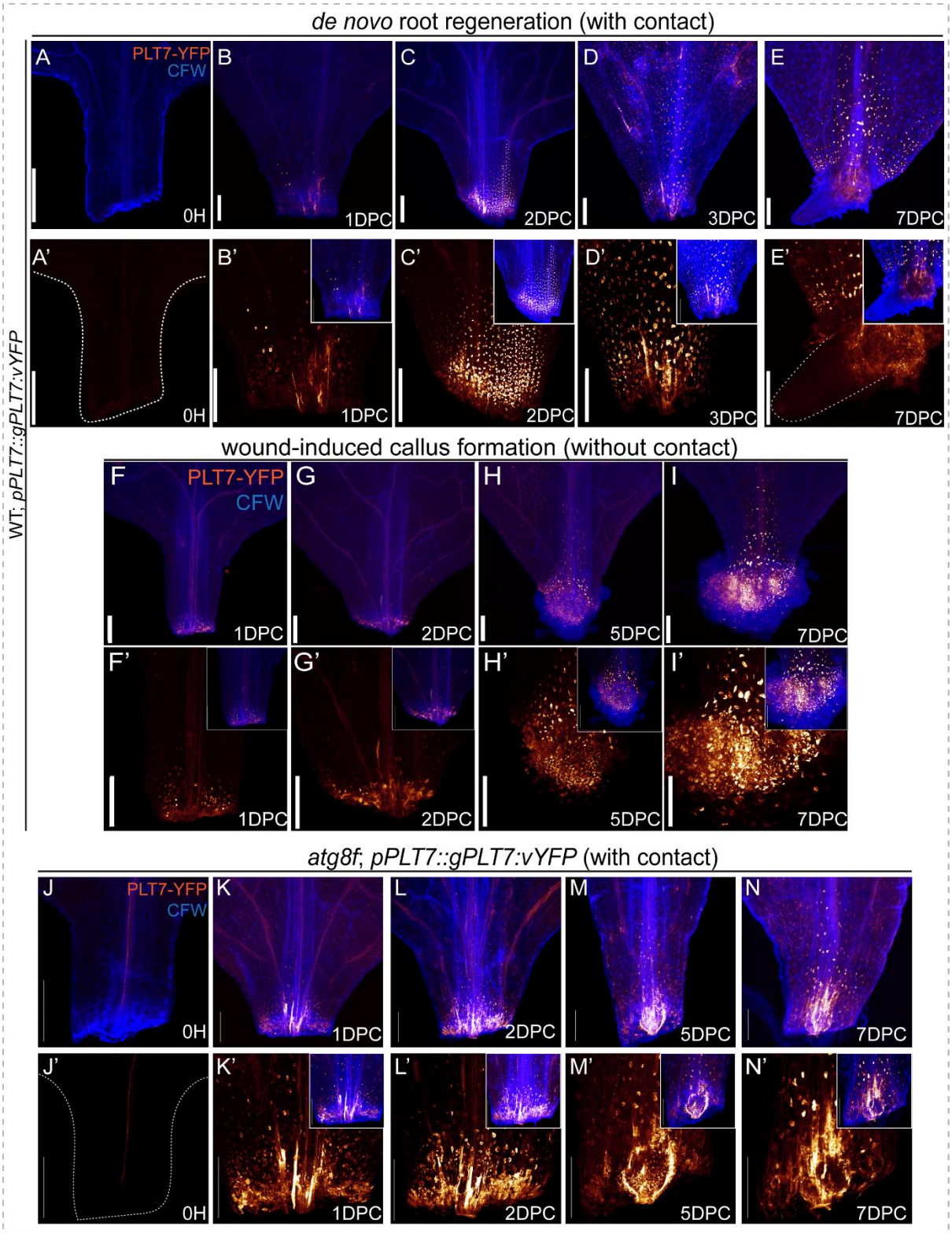

Figure 4.3 PLT7 reporter expression resembles the *ATG8F* promoter pattern during *de novo* root regeneration. (A-E, A'-E') Representative confocal projections of PLT7-vYFP expression at 10x and 20x magnification during *de novo* root regeneration (WT; *pPLT7::gPLT7:vYFP*). At 0H (A, A'), no PLT7-vYFP was seen across the petiole. At 1DPC, there is a rapid increase in PLT7 expressing cells near the cut end (B, B'). Over successive timepoints, PLT7-vYFP domain expands across the leaf in a pattern similar to the *ATG8F* promoter (C-E, C'-E') (n>18 leaves per timepoint). Dotted white line in E': emerged adventitious root. (F-I, F'-I') Representative confocal images of leaves at both 10x and 20x magnification showing restricted PLT7-vYFP

domain in leaves without contact from 1DPC till 7DPC. (J-N, J'-N') PLT7-vYFP expression pattern in the *atg8f* mutant with contact was similar to WT across all timepoints. Figure insets: PLT7-vYFP (orange LUT) and Calcofluor White (CFW) (blue channel). Scale bars: 200 µm.

In summary, these findings demonstrate that PLT7 directly activates *ATG8F* transcription by binding its promoter and indirectly upregulates other *ATG8* genes during *de novo* root regeneration. These results highlight the critical role of PLT7 in the transcriptional activation of genes encoding specific *ATG8* isoforms for a global autophagic response during *de novo* root regeneration.

4.2.3 PLT3 and PLT7 have novel, non-redundant functions during *de novo* root regeneration

Single and double *plt* mutant combinations have so far been analyzed for tissue-culture mediated shoot regeneration as well as vascular regeneration, where the loss-of-regeneration phenotype was absent or minimal (16, 17). However, no single or double combination *plt* mutants have been analyzed during *de novo* root regeneration (9, 18). Given the significant loss of root regeneration in *plt7* single mutants, I examined if other single or double *plt* T-DNA mutants – *plt3-1*, *plt5-2, plt3;5*, *plt5;7*, and *plt3;7* – showed similar effects. Surprisingly, the *plt3-1* single mutant exhibited a total loss of *de novo* root regeneration (Figure 4.4A). This phenotype was fully rescued by a functional PLT3 translational fusion construct (*plt3-1*; *pPLT3::gPLT3:vYFP*), thus confirming that loss of *PLT3* alone was responsible for the mutant phenotype (Figure 4.4C). Similar to the *plt3-1* T-DNA mutant, the CRISPR-Cas engineered *plt3-cr* knockout mutant exhibited a complete loss of root regeneration (Figure 4.4B). The *plt5-2* single mutant showed only a slight reduction in root regeneration (~20%), and consistent with the single mutant phenotype, *plt3;5* and *plt3;7* double mutants did not regenerate any *de novo* roots (Figure 4.4D). The *plt5;plt7* double mutant exhibited similar reduction (~30%) as seen in the *plt7-1* single mutant (Figure 4.4D, 4.2E). Importantly, all the single and double mutant combinations showed no change in wound-induced callus formation compared to WT, and only the triple mutant showed callus formation defects, in line with previous findings (Figure 4.4 E, G) (9). Moreover, like *plt3;plt5;plt7*, *plt3-1* single mutant did not form any detectable root primordia and only repaired the wound site with an endogenous wound callus (Figure 4.4F) (9).

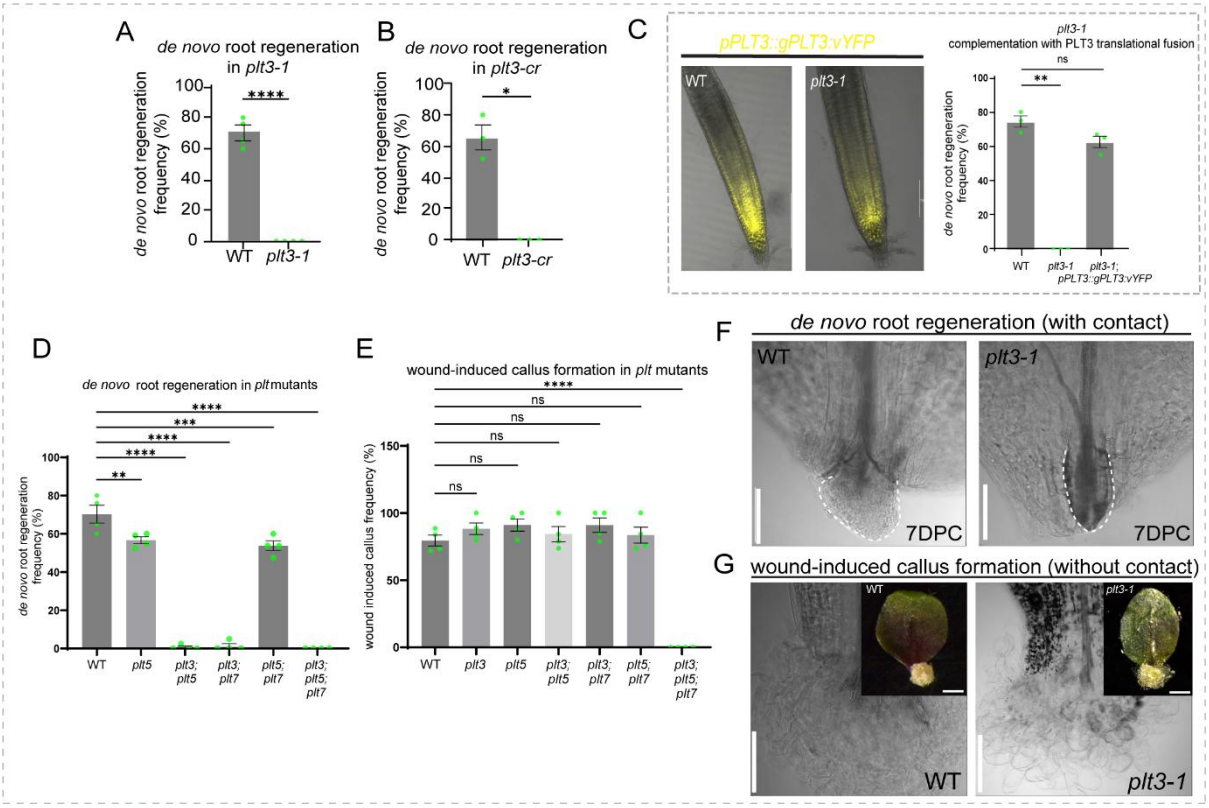

Figure 4.4 PLT3 is both necessary and sufficient for *de novo* root regeneration. (A) Graph representing loss of root regeneration in plt3-1 T-DNA mutant (****P<0.0001, ordinary one-way ANOVA) compared to WT (N=4, n>30 leaves per replicate). (B) Graph representing loss of root regeneration in plt3-cr mutant (*P=0.0148, Welch's two-tailed t-test) compared to WT (N=3, n>20 leaves per replicate). **(**C) Representative confocal images of *pPLT3::gPLT3:vYFP* reporter in WT and *plt3-1* mutant primary root tips. Graph shows rescue of *de novo* root regeneration in *plt3-1*; *pPLT3::gPLT3:vYFP* to WT levels as compared to *plt3-1* mutant (**P = 0.0022, Welch's two-tailed t-test). **(**D) Graph representing *de novo* root regeneration frequency of WT, *plt5* (**P = 0.0013, ordinary one-way ANOVA), *plt3;plt5* (**** P<0.0001, ordinary one-way ANOVA), *plt3;plt7* (****P<0.0001, ordinary one-way ANOVA), *plt5;plt7* (***P = 0.0001, ordinary one-way ANOVA), and *plt3;plt5;plt7* (****P<0.0001, ordinary one-way ANOVA). (E) Graph representing wound-induced callus frequency of WT, *plt3* (ns, ordinary one-way ANOVA), *plt5* (ns, ordinary one-way ANOVA), *plt3;plt5* (ns, ordinary one-way ANOVA), *plt3;plt7* (ns, ordinary one-way ANOVA), *plt5;plt7* (ns, ordinary one-way ANOVA), and *plt3;plt5;plt7* (****P<0.0001, ordinary one-way ANOVA). (F) Representative brightfield images of cleared WT and plt3-1 leaves at 7DPC with contact. Where WT has a visible adventitious root, plt3-1 exhibits only an endogenous callus. Dashed white line outlines regenerated root in WT and endogenous callus in plt3-1. However, no visible difference can be seen in wound-induced callus formation between the two backgrounds (G). Scale bars: 2 mm. Data shown as mean ± s.e.m.

Next, I analyzed the progression of procambium activity and founder cell specification in the *plt3* mutant. The *plt3-1* mutant showed interrupted vascular reprogramming as observed from *PXY* reporter activity (*plt3-1*; *pPXY::erYFP*) (Figure 4.5 A-B, A'-B'). Notably, *plt3-1* endogenous callus (with contact) expressed WOX11-GFP marked founder cells (*plt3-1*; *pWOX11::H2B:GFP*) similar to WT (Figure 4.5 C-D, C'-D'). Taken together, these results indicate that loss of PLT3 interrupts normal procambial reprogramming at the site of injury but

founder cell specification remains unaffected, which phenocopies the genetic and pharmacological disruption of autophagy during *de novo* root regeneration.

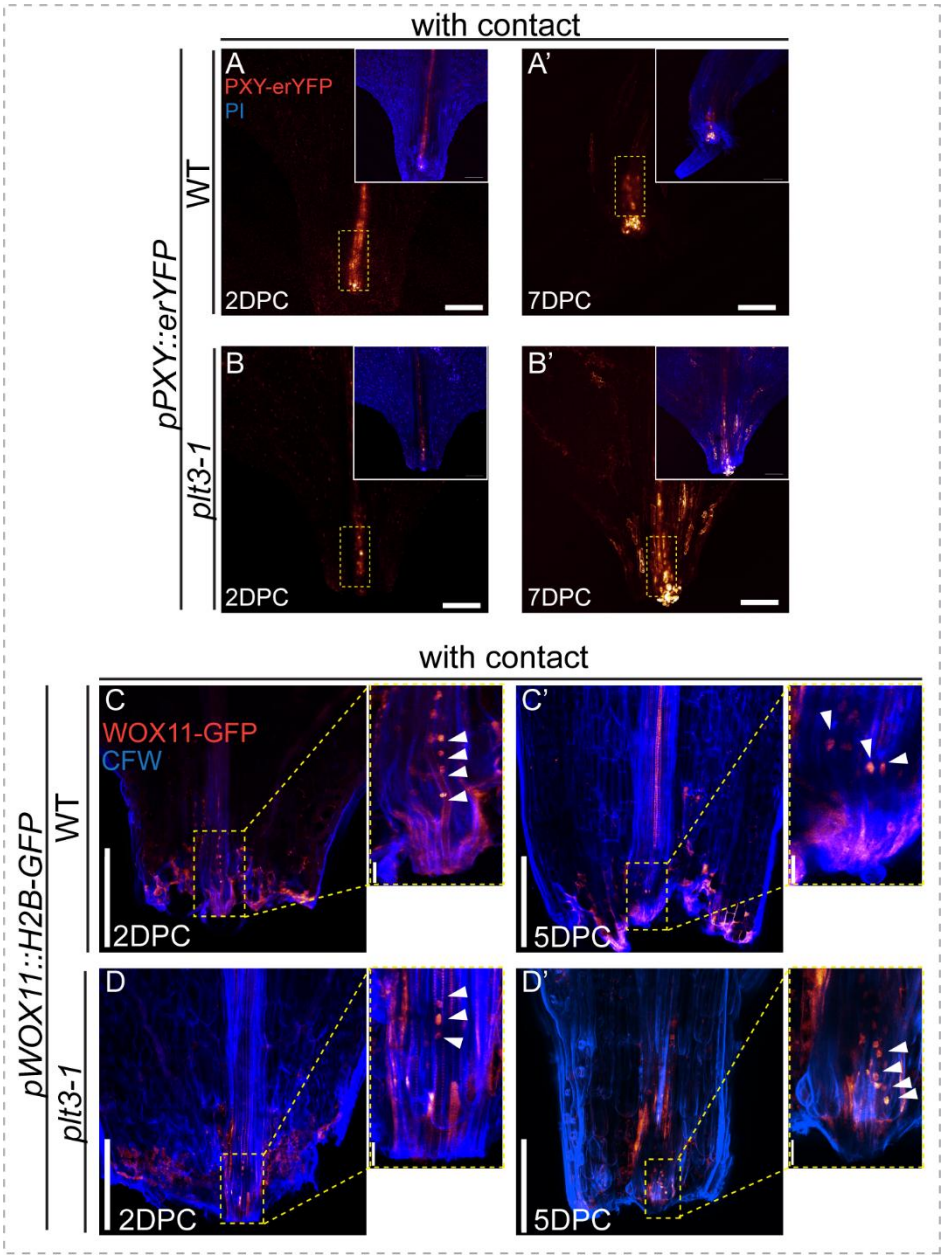

Figure 4.5 Loss of PLT3 does not affect founder cell identity, but interferes with procambium activity during de novo root regeneration. (A-B, A'-B') Representative confocal images of *PXY* promoter activity (orange LUT channel) in WT and *plt3-1* backgrounds (n>10 leaves per timepoint). While at 2DPC, procambium activity is similar between WT and *plt3-1* (A, B), at 7DPC, WT PXY-erYFP is visibly reduced within the reprogramming zone (A', yellow dashed box), whereas expression is significantly high in *plt3-1* (B'). (C-D, C'-D') Representative confocal projections of WOX11-GFP (orange LUT channel) in WT and plt3-1 mutant at 2DPC and 5DPC with contact (n>10 leaves per timepoint). Boxed-insets: endogenous callus at the cut end around the vascular bundle. Note that the orange striations and blotches are not true signal, but autofluorescence from cell damage and fixation. Scale bars: 200 µm.

In summary, these findings reveal a previously unrecognized, non-redundant role of PLT3 during *de novo* root regeneration from excised leaves, where PLT3 is both necessary and sufficient to promote this process.

4.2.4 PLT3 is an upstream regulator of PLT7 during *de novo* root regeneration

In the context of tissue culture induced shoot regeneration, PLT3 and PLT7 show overlapping expression patterns across explants, both during pluripotent callus induction and shoot regeneration (16). On the other hand, when the midvein of a 4–5-day old growing leaf is wounded near the petiole, both PLT3 and PLT7 are activated around the wound, although their expression patterns during normal leaf development show some variation (17). Aside from these, PLT3 and PLT7 expression domains also overlap during embryogenesis, at the shoot apical meristem (SAM), and in lateral root primordia (LRP) during normal development; however, PLT3 is also expressed in the primary root meristem, unlike PLT7 which is restricted to the LRP (132, 188). Since PLT3 and PLT7 are members of the same TF family, it is probable that functional redundancy would exist in both expression domains and downstream regulatory networks. The contact-mediated regeneration assay is done on 10-11-day old leaves where PLT7 expression is undetectable at the 0H timepoint (Figure 4.3 A, A'), which indicates the PLT expression domains operate in a defined developmental regime. Given the finding that PLT3 is both necessary and sufficient for *de novo* root regeneration, I next examined if the PLT3 expression pattern during *de novo* root regeneration showed any overlap with PLT7. Monitoring the PLT3 translational reporter construct in WT (WT; *pPLT3::gPLT3:vYFP*) in leaves post excision showed that at the 0H timepoint, PLT3-vYFP expression was already visible in the procambium layer of the vascular bundle (Figure 4.6 A, A'). Moreover, unlike the expansion of PLT7-vYFP from 1DPC onwards, PLT3-vYFP remained confined to the procambium throughout all timepoints during *de novo* root regeneration (Figure 4.6 B-E, B'-E'). However, like PLT7, PLT3-vYFP was actively expressed within the endogenous callus cell mass formed at the cut end post injury, and was also expressed in proliferating callus cells in without contact leaves (Figure E-I, E'-I'). Therefore, PLT3 and PLT7 expression domains overlap partially at the endogenous callus formed during *de novo* root regeneration, aside from which, PLT7-vYFP shows broad expansion across the leaf and PLT3-vYFP remains restricted to a vascular domain compared to PLT7.

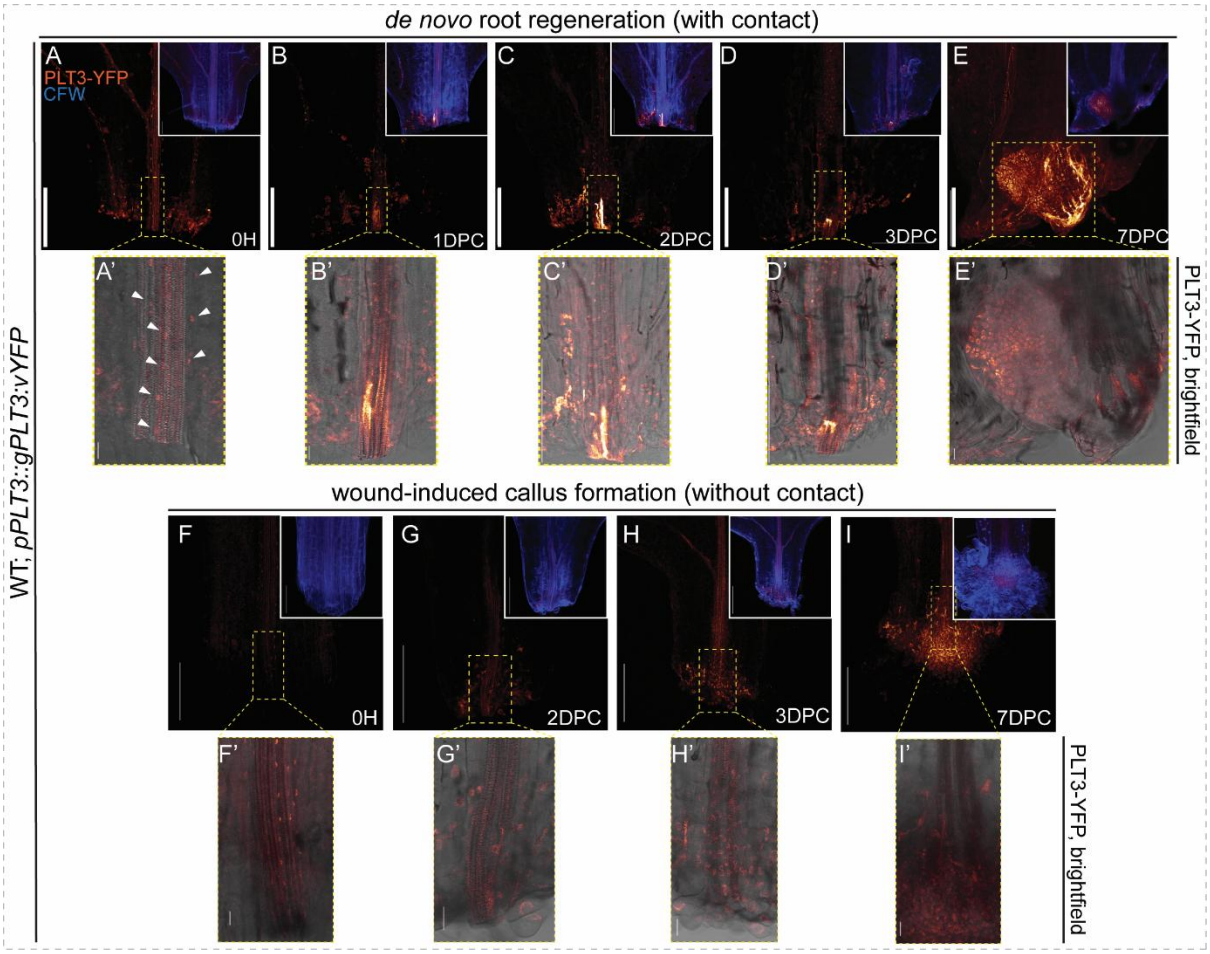

Figure 4.6 PLT3 expression domain is restricted to the procambium and the endogenous callus during de novo root regeneration. (A-E, A-E') Representative confocal projections of WT; *pPLT3::gPLT3:vYFP* leaves during *de novo* root regeneration (n>18 leaves per timepoint). Unlike PLT7-vYFP, the PLT3-vYFP signal is already present within the procambium layer. (A'-E') dashed yellow box insets of PLT3-vYFP with brightfield channel show the PLT3 domain during *de novo* root regeneration. Unlike PLT7, PLT3-vYFP remains confined to the procambium and the endogenous callus. (F-I, F'I') PLT3-vYFP is also expressed in the proliferating wound-induced callus cells emerging from the cut end of the leaf. Scale bars: 200 µm.

The data so far indicates that loss of either PLT3 or PLT7, that are plant-specific double AP2-domain transcription factors, impairs *de novo* root regeneration. Furthermore, unlike in the other regeneration scenarios, their expression domains are mostly disparate during *de novo* root regeneration from excised leaves. These findings prompted an essential question – are there potential regulatory interactions between PLT3 and PLT7 during *de novo* root regeneration? Using genetic and molecular tools, I investigated whether PLT3 and PLT7 influence each other's expression levels in excised leaves kept with contact. In the inducible PLT7-GR background, *PLT3* transcript levels remained unchanged after 4 hours of PLT7 induction (Figure 4.7A). *PLT7* transcript levels also increased after 8 hours of PLT3 induction using an inducible *p35S::PLT3:GR* construct (WT; *p35S::PLT3:GR*), and were significantly reduced in both the *plt3-1* and *plt3-cr* mutants (Figure 4.7 B-D); interestingly, *PLT3* transcript levels

remained unchanged in both *plt7-1* and *plt7-cr* mutants (Figure 4.7E). No significant change in *PLT7* transcript levels were detected 4 hours post PLT3 induction when combined with CHX treatment to block protein synthesis, indicating indirect regulation of PLT7 by PLT3 during *de novo* root regeneration (Figure 4.7F). Additionally, the PLT7 translational fusion construct showed significantly lower expression in *plt3-1* (*plt3-1*; *pPLT7::gPLT7:vYFP*) compared to WT, both in developing lateral root primordia (Figure 4.7G), as well as in excised leaves kept with contact (Figure 4.7H). Taken together, these results establish transcriptional upregulation of *PLT7* by PLT3, and reveal a previously unrecognized regulatory crosstalk between closely related members of the PLT family during *de novo* root regeneration.

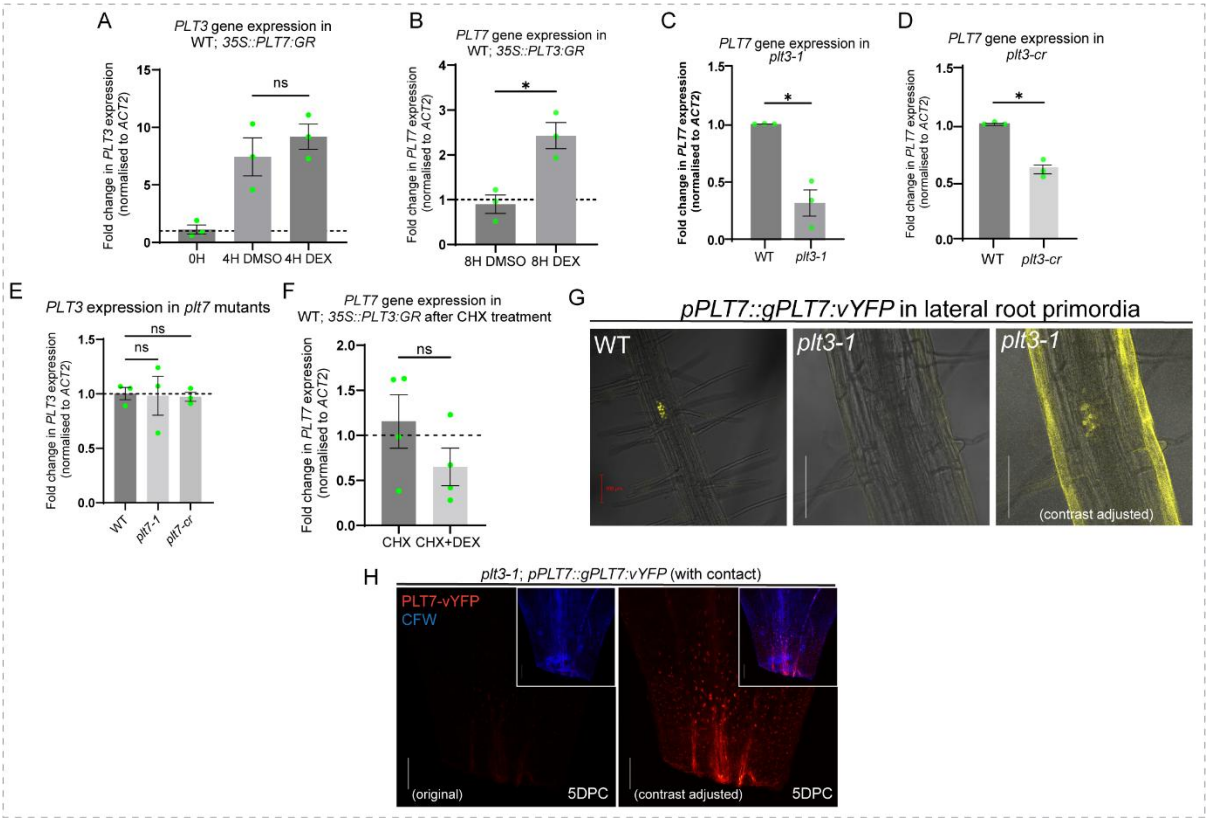

Figure 4.7 PLT3 transcriptionally activates PLT7 during de novo root regeneration, but not vice-versa. (A) Graph representing *PLT3* gene expression in WT; *35S::PLT7:GR* after 4 hours of DEX or DMSO induction. Gene expression levels of *PLT3* are unchanged upon inducible PLT7 overexpression during *de novo* root regeneration (ns, Welch's two-tailed t-test). (B) Graph representing increased *PLT7* expression in WT; *p35S::PLT3:GR* post 8 hours of DEX induction (*P=0.0161, Welch's two-tailed t-test). (*C*) Graph showing decreased *PLT7* expression in the *plt3-1* mutant (*P= 0.0185, Welch's two-tailed t-test) after 48H with contact. (*D*) Graph showing decreased *PLT7* expression in the *plt3-cr* mutant (*P= 0.0154, Welch's two-tailed t-test) after 48H with contact. (*E*) Graph showing unchanged gene expression levels of *PLT3* in *plt7* mutants after 48H with contact when compared to WT (ns=not significant, Welch's two-tailed t-test). **(F)** Graph showing no significant difference in *PLT7* expression in WT; *35S::PLT7:GR* after 4 hours of cycloheximide (CHX) treatment (ns=not significant, Welch's two-tailed t-test). (G) Representative confocal images of WT and *plt3-1* roots expressing *pPLT7::gPLT7:vYFP* reporter in the lateral root primordia (LRP). Note that in the *plt3-1* mutant, expression is significantly reduced but not completely lost (contrast adjustment shows PLT7-vYFP expression). Similarly, in (H), PLT7-vYFP marked nuclei are present in *plt3-1* leaves at 5DPC with contact, but reporter intensity is visibly reduced. As noted in Materials and Methods

(Chapter 2), image acquisition parameters for each reporter were kept constant across genetic backgrounds. Scale bars: 200 μm. Data shown as mean ± s.e.m.

In light of all results so far, PLT3 functions upstream of PLT7 during *de novo* root regeneration from excised leaves in different expression domains, showing a non-redundant interaction among these factors not observed previously. To further resolve the extent of this non-redundancy, I next examined if PLT7 could rescue *de novo* root regeneration in *plt3* mutant when expressed under the *PLT3* promoter. Towards this, I investigated the root regeneration phenotype of *plt3-1* expressing PLT7 driven under *PLT3* promoter (*pPLT3::gPLT7:vYFP*), and also of PLT3 driven under *PLT7* promoter (*pPLT7::gPLT3:vYFP*) in *plt3-1*, after confirming both factors were expressed in the requisite promoter domains in the young primary roots of *plt3-1* (Figure 4.8A). PLT7 partially rescued root regeneration under the *PLT3* promoter (*plt3-1*; *pPLT3::gPLT7:vYFP*), thus reinforcing that PLT3 is an upstream regulator of PLT7 during this process (Figure 4.8B). Strikingly, PLT3 fully rescued the *plt3-1* phenotype even when driven under the *PLT7* promoter, similar to the full complementation of *plt3-1*; *pPLT3::gPLT3:vYFP* compared to WT seen previously (Figure 4.8B, 4.4C). Monitoring the expression patterns of both heterologous PLT reporters in leaves with contact revealed that both PLT3 and PLT7 fusion proteins were localized in their native promoter domains during *de novo* root regeneration, i.e. *pPLT3::gPLT7:vYFP* domain gradually expanded throughout the leaf like the native PLT7 translational construct and *pPLT7::gPLT3:vYFP* was confined to the vascular layer as observed for *pPLT3::gPLT3:vYFP* (Figure 4.8C). Moreover, the expression intensity of PLT7 driven under PLT3 promoter was visibly reduced, similar to the native PLT7 translational construct expression in *plt3-1* seen earlier (Figure 4.8 A, C, 4.7 G, H).

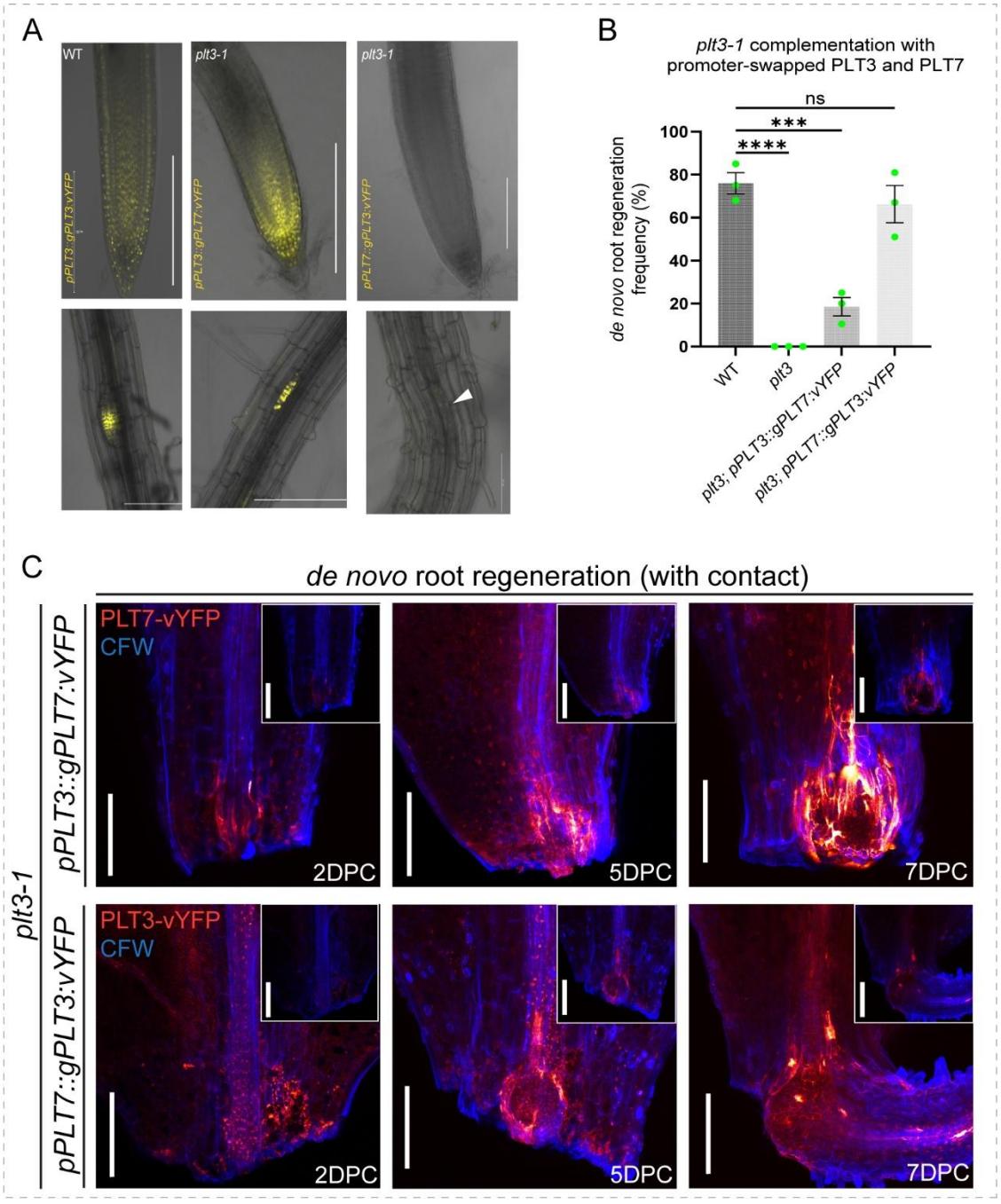

Figure 4.8 PLT3 and PLT7 retain their wound-induced expression patterns with high fidelity even under heterologous PLT promoters. (A) Representative confocal images of primary root tip and LRPs in WT and *plt3-1* mutant, with WT expressing fully functional PLT3 complement *pPLT3::gPLT3:vYFP* (left panels), *plt3-1* expressing *pPLT3::gPLT7:vYFP* (middle panels) or *pPLT7::gPLT3:vYFP* (right panels). Note that PLT3-vYFP expression under *PLT7* promoter is significantly reduced in the *plt3-1* mutant LRP and absent in the primary root meristem, which also confirms *PLT7* downregulation in the *PLT3* loss-of-function background. (B) Graph of *de novo* root regeneration frequency of promoter-swapped PLT3 and PLT7 complementation in *plt3-1.* While *pPLT3::gPLT7:vYFP* partially rescues root regeneration (***P=0.0002, ordinary one-way ANOVA) compared to the severe loss in *plt3-1* alone (****P<0.0001, ordinary one-way ANOVA), *pPLT7::gPLT3:vYFP* shows a complete rescue of *de novo* root regeneration frequency up to WT (ns= not significant, ordinary one-way ANOVA). (C) Representative contrast-adjusted confocal images of *plt3-1; pPLT3::gPLT7:vYFP* and *plt3-1; pPLT7::gPLT3:vYFP* in excised leaves at 2DPC, 5DPC, and &DPC with contact. Images show PLT7-vYFP or PLT3-vYFP (orange LUT channel) with CFW (blue channel). Insets: original images without contrast adjustment

of reporter. Note that both PLT3 and PLT7 reporter intensities were low when expressed under heterologous promoters, as compared to their native promoter driven expression patterns shown previously. Scale bars: 200 µm. Data shown as mean ± s.e.m.

Based on these intriguing results, I propose the following hypothesis– novel interactions of PLT3 and PLT7 during *de novo* root regeneration are possibly orchestrated by wound-activated intragenic *cis*-regulatory elements, that spatiotemporally activate and regulate these *PLT* genes specifically during wound repair and organ regeneration. Importantly, these *cis*-regulatory elements do not appear to affect the normal developmental programs of the PLT factors; rather, they modulate the very same *PLT* genes towards a regeneration-specific program post wounding. For PLT3 in particular, future studies could test this claim by using a synthetic promoter designed to drive *PLT3* gene expression in its own domain and test its effect on diverse regeneration contexts.

4.2.5 PLT3 both directly and indirectly activates *ATG8* genes during *de novo* root regeneration

Given my findings so far, I next sought to confirm whether PLT3 also regulates *ATG8F* transcript levels, either through PLT7 or directly, during *de novo* root regeneration. *ATG8F* transcript levels were increased after 8 hours of PLT3 induction in the inducible PLT3-GR background (Figure 4.9A). Conversely, *ATG8F* levels were reduced across both *plt3-1* and *plt3-cr* mutants (Figure 4.9 B, C). Additionally, *ATG8F* levels were unchanged after CHX treatment given during 4 hours of PLT3 induction, thus indicating indirect regulation of *ATG8F* by PLT3 during *de novo* root regeneration (Figure 4.9D). However, *ATG8H* transcript levels were significantly increased after PLT3 induction in the presence of CHX, indicating that *ATG8H* may be directly activated by PLT3 (Figure 4.9D). To confirm this, I carried out ChIP and ChIP-qPCR in WT PLT3-vYFP reporter leaves with contact against different regions of the *ATG8H* promoter (Figure 4.9E). Here, PLT3 showed nearly 8-fold direct binding to the 0-200 bp region of *ATG8H* promoter, directly upstream of the transcription start site (Figure 4.9E'). *In toto*, these findings highlight both direct and indirect regulation by PLT3 in the transcriptional control of autophagy through the *ATG8* genes during *de novo* root regeneration.

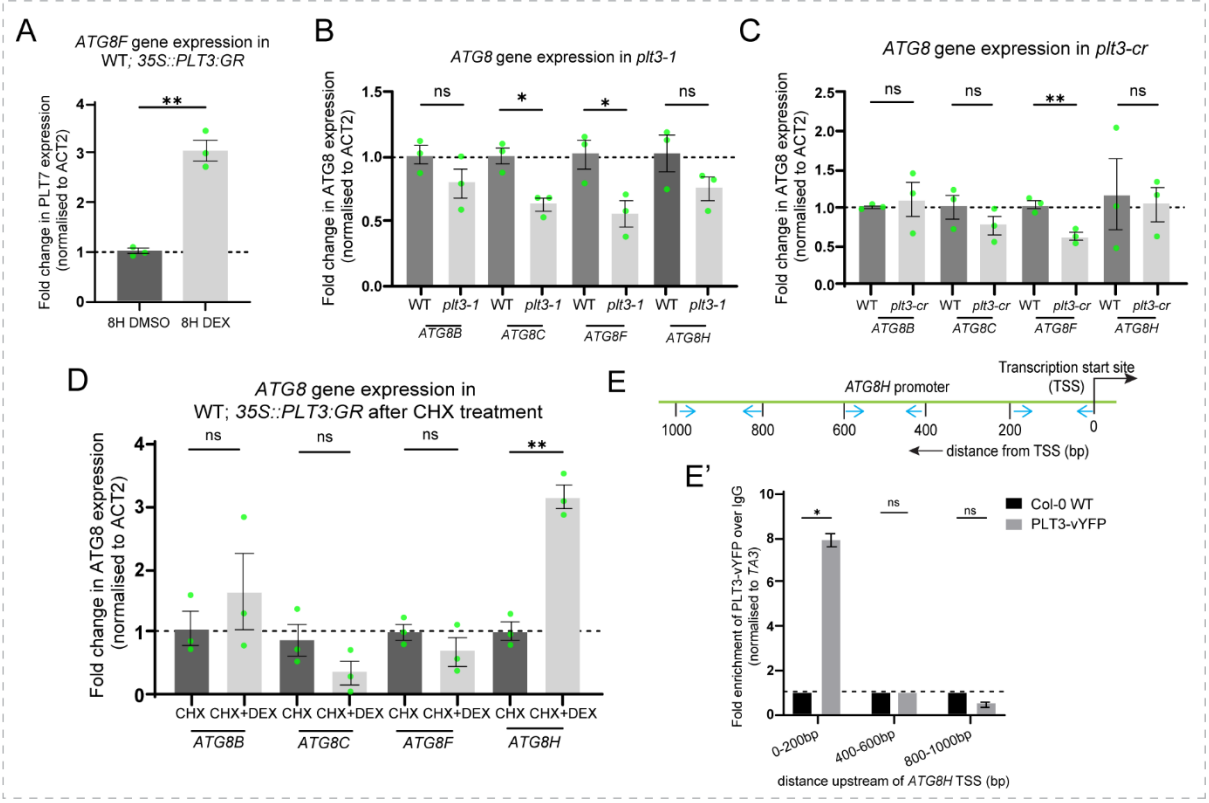

Figure 4.9 PLT3 directly upregulates *ATG8H* and indirectly activates *ATG8F* during *de novo* root regeneration. (A) Graph representing increased *ATG8F* gene expression (**P=0.0076, Welch's two-tailed t-test) in WT; *35S::PLT3:GR* after 8 hours of DEX induction. (B) Graph representing gene expression levels of *ATG8B* (ns, Welch's two-tailed t-test), *ATG8C* (*P=0.0130, Welch's two-tailed t-test), *ATG8F* (*P=0.0364, Welch's two tailed t-test), and *ATG8H* (ns= not significant, Welch's two-tailed t-test) in the *plt3-1* mutant after 48H with contact. (C) Graph representing gene expression levels of *ATG8B* (ns, Welch's two-tailed t-test), *ATG8C* (ns, Welch's two-tailed t-test), *ATG8F* (*P=0.0062, Welch's two tailed t-test), and *ATG8H* (ns= not significant, Welch's two-tailed t-test) in the *plt3-cr* mutant after 48H with contact. (D) Graph representing increased gene expression levels of *ATG8H* (**P=0.0013, Welch's two-tailed t-test) in WT; *p35S::PLT3:GR* after CHX treatment, indicating possibly direct transcriptional regulation of *ATG8H* by PLT3. Other *ATG8s* remain unchanged post treatment (ns= not significant, Welch's two-tailed t-test). (E) Schematic of *ATG8H* gene promoter upstream of TSS. Blue arrows mark the three regions, 0-200, 400-600, and 800-1000 bp of the promoter analyzed for PLT3-YFP fold enrichment. (E') Graph of ChIP-qPCR showing ~8-fold PLT3-YFP fold enrichment (*P=0.002216, Welch's two-tailed t-test) in the 0-200 bp promoter region upstream of TSS in the *ATG8H* promoter (N=2, n=6 technical replicates). Data shown as mean ± s.e.m.

PLT3 being an important plant developmental regulator, would undoubtedly regulate a large number of genes both during normal development and regeneration, aside from the *ATG8* genes characterised during this study. Indeed, PLT3 is known to directly bind to the promoter of *PLT1* in leaves during *de novo* root regeneration, another important root meristem regulator(18). Hence it would be logical to assume that the loss of *PLT3* would compromise the function of other significant downstream targets along with the *ATG8* genes, which may have a stronger phenotype in *de novo* root regeneration than the isoforms analyzed here. Nevertheless, I checked if the constitutive expression of a single *ATG8* gene could rescue the loss-of-

regeneration phenotype of *plt3*. This experiment was approached through two ways – moderately constitutive *ATG8F* expression (*plt3-1*; *pUBQ10::NG-ATG8F*) with contact (Figure 4.10 A, B), as well as estradiol induced *ATG8F* ectopic overexpression (*plt3-1*; *pG1090.XVE::ATG8F*) without contact (Figure 4.10 C, D). Remarkably, both methods of ATG8F expression partially rescued the loss of *PLT3* and restored root regeneration, to levels similar to the partial rescue by PLT7 driven under PLT3 promoter in the same mutant background (Figure 4.8xxx). Notably, inducible *ATG8F* overexpression in wildtype background (WT; *pG1090.XVE::ATG8F*) leaves did not significantly affect *de novo* root regeneration frequency, timing, or morphology (Figure 4.10 E, F), indicating that in the tested physiological conditions, *ATG8F* overexpression does not enhance root regeneration, and is unlikely to be a rate-limiting factor in wildtype plants.

(figure on next page)

Figure 4.10 Constitutive ATG8F can partially rescue *de novo* root regeneration in *plt3* loss-of-function mutant. (A) Representative stereomicroscope images of *de novo* root regeneration phenotype in WT and *plt3-1*; *pUBQ10::NG-ATG8F* lines at 15DPC with contact. (B) Graph representing a partial rescue of *plt3-1* root regeneration by the *pUBQ10::NG-ATG8F* construct (*plt3-1; UBQ10::NG-ATG8F*) for constitutive ATG8F expression (*P=0.016, Welch's two-tailed t-test). (C) Representative stereozoom images showing wound-induced callus formation without contact in *plt3-1* and *plt3-1*; *pG1090.XVE::ATG8F* with DMSO, and *de novo* root regeneration with wound-induced callus in *plt3-1*; *pG1090.XVE::ATG8F* with estradiol. Numbers written at the top right of images refers to the number of leaves with *de novo* roots seen in the total experiment set. (F) Graph of experiment shown in (E) representing partial rescue of *plt3-1 de novo* root regeneration by ectopic overexpression of ATG8F driven under an estradiol-inducible constitutive promoter (*plt3-1*; *pG1090.XVE::ATG8F*) even in leaves kept without contact (n=20 leaves in 2 biological replicates). (E) Representative stereozoom images of WT and estradiol induced WT; *pG1090.XVE::ATG8F* leaves kept with contact till 15DPC. (F) Graph of experiment images shown in (A) from n=10 leaves for each background. No statistical test was done for this dataset due to limited sample numbers. Scale bars: 2 mm. Data shown as mean ± s.e.m.

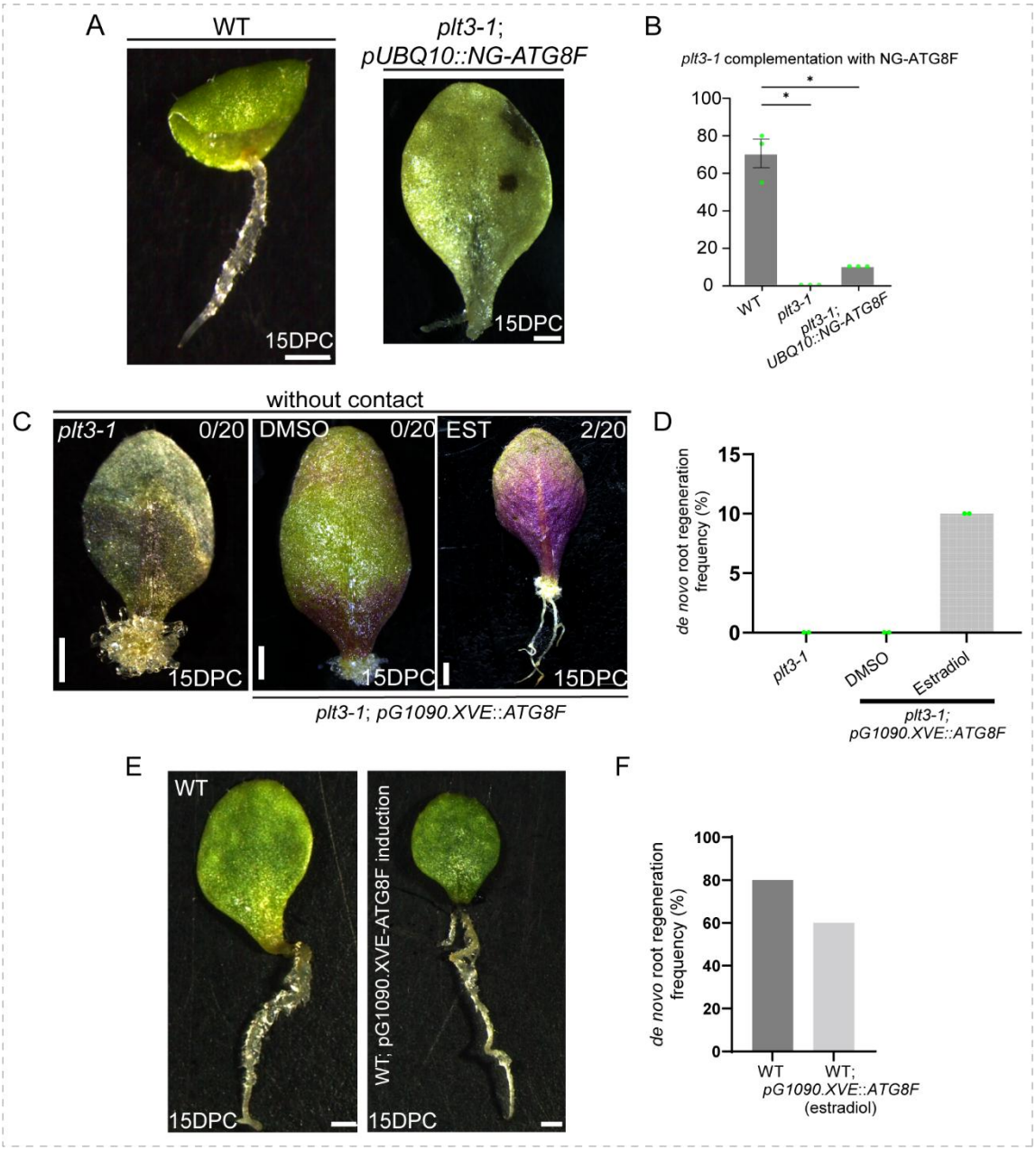

In summary, my findings demonstrate that PLT3, PLT7, and *ATG8* genes are not restricted to the site of root stem-cell fate activation in the petiole but are expressed across a broader field of cells in the excised leaf during *de novo* root regeneration. Furthermore, extensive genetic and molecular analyses reveal that PLT3 and PLT7 act in non-redundant domains during this process, with PLT3 indirectly regulating PLT7 and broadly influencing *ATG8* gene expression through both indirect and direct transcriptional activation.

4.3 DISCUSSION

Regulation of gene expression is a pivotal mechanism guiding myriad biological phenomena in living cells. This is largely controlled by transcription factors that are grouped into families

depending on their sequence and biochemical interactions. Most TFs function in a bipartite manner with one subunit designed for DNA binding, and another for interaction with protein complexes required to initiate and control transcriptional events (189). Indeed, common TF families between plants and animals are classified per ancient DNA binding motifs, such as zinc-finger domain proteins, basic helix-loop-helix (bHLH) factors, homeodomain proteins, MYB-domain, WRKY-, and MADS-box proteins, among many (190, 191). This conservation of TF sequence-structure further extends to their functional output during normal development. For e.g. homeodomain factors such as the *HOX* gene family in animals are crucial regulators of animal body plan and segmentation post embryogenesis, while their plant counterparts *WUSCHEL* (*WUS*) and *WUS-HOMEOBOX* (*WOX*) genes are master regulators of plant root and shoot meristems that are reservoirs of continuous aerial and ground tissue outgrowth in a plant's lifespan (192–194).

However, plant transcription factors have also evolved significant differences from their animal counterparts, that include novel *cis*-regulatory DNA motifs, expanded TF family homologs, and novel plant-specific TF families (195). Beyond the role of transcription factors in developmental programs, what is striking is the evolutionary emergence of plant-specific TF families tailored towards hormone-signaling and response to abiotic stresses (196). These include AP2/ERF, GRAS, WRKY, bHLH, bZIP, MYB, and NAC families that play critical roles in modulating or diverting normal developmental gene programs in response to external environmental cues (197–200). The advantage conferred by this diversification of plant regulators and their complex molecular networks is evident by the developmental plasticity that is a defining characteristic of the plant kingdom. This plasticity is what allows for the finely calibrated activation and control over common cellular processes such as cell death, autophagy, or cell-fate reprogramming in a tissue-specific output. Within the plant TF repertoire, the *PLETHORA* gene family are double AP2-domain containing factors that have been extensively characterised in various developmental and regenerative processes. Herein, the findings of my study illustrate how members of the PLETHORA family, are recruited post wounding to activate specific *ATG8* genes, that allows for the sustained output of autophagy to promote *de novo* root regeneration in excised leaves.

But given that plant TF families operate across diverse development programs, an essential question arises – how do the same factors regulating developmental phases also activate specific transcriptional programs during wound repair and regeneration? One answer is the fine-tuning of gene expression by *cis*-regulatory elements that control the spatiotemporal

output of the developmental regulators and also initiate transcriptional networks unique to the regeneration context (201). Along these lines, a landmark study done in zebrafish shows the gain or loss of regeneration capacity in vertebrates to be causally linked with changes in regeneration-responsive enhancers (202). *Cis*-regulatory elements and their regulators have also been identified for developmental processes in plants, but whether injury-induced reprogramming depend on the similar regulatory principles remains unclear (203). Moreover, genomic regulatory sequences do not follow conserved principles between plants and animals. Animal enhancers are position independent and can be found several thousand base-pairs away from the gene locus, while plant enhancers are position dependent, and frequently found downstream of the TSS (204). A recent report discovered conserved *cis*-regulatory elements within the *PLT1/2* promoters, that were necessary to maintain accurate *PLT* expression during embryogenesis and root development (182). An intriguing discovery from my study was the conserved injury-induced expression patterns of PLT3 and PLT7 factors in excised leaves with contact, even when expressed under heterologous promoters. Given that both PLT3 and PLT7 were expressed in the promoter specific domains during normal development, my findings lead me to speculate that the spatiotemporal specificity of PLT3 and PLT7 regulation during *de novo* root regeneration can be partly attributed to novel, unrecognized intragenic elements that are activated exclusively in response to injury, that drive PLT activation and function in domains independent of the promoter.

In summary, this chapter highlights how plant specific developmental regulators such as the PLT factors can transcriptionally regulate specific members of the *ATG8* gene family to activate *de novo* root regeneration post injury. Moreover, these related members of the same TF family show unique, context-specific interactions during this process, where PLT3 functions upstream of PLT7 and both factors directly and indirectly regulate different *ATG8* genes. Lastly, the non-overlapping TF activity is possibly driven by unmapped intragenic *cis*-regulatory elements within the *PLT* genes themselves that spatiotemporally drive PLT expression in a regeneration-responsive program not observed during normal plant development.

CHAPTER 5

The PLT-ATG8 axis is essential to coordinate organelle turnover and modulate ROS levels during de novo root regeneration

Results from this chapter have been published in:

Ganguly, A., Humnabadkar, A., Gautam, K., Willemsen, V., Xu, L., Dagdas, Y., & Prasad, K. (2026). PLETHORA–autophagy axis activates organ regeneration through ROS modulation. *Proceedings of the National Academy of Sciences*, *123*(6), e2513954123. (Featured on Cover)

"Chance is all-powerful. Always cast your fishing hook; in the pond where you least expect it, you'll find a fish."

– Murasaki Shikibu

5.1 INTRODUCTION

Autophagy broadly operates under two modalities across eukaryotes: macroautophagy and microautophagy. Macroautophagy, or canonical autophagy, involves engulfing of entire organelles and cytoplasmic debris within membrane bound autophagosomes, that eventually fuse with the lysosome (in animals) or the lytic vacuole (in plants) for enzymatic breakdown and organelle turnover (19, 128). Microautophagy involves selective degradation of damaged components in organelles or protein aggregates by close association with the lysosome or the vacuole tonoplast, which directly engulf the cargo by membrane invagination to form a microautophagic body that is degraded within the lumen. While each pathway involves dedicated cargo receptors and enzymes with process-specific post-translational modifications, the end-point of all autophagy is the lytic vacuole in plants and the lysosome in animals (205). In plants, the lytic vacuole is the largest organelle of the cell, roughly ~90% of the total cell volume, where during autophagy, damaged cellular components are encapsulated and transported into the vacuole lumen, where these are degraded and recycled to maintain cellular homeostasis (169, 205). The breakdown of cytosolic parts during autophagy serves a dual function – firstly, it ensures cellular homeostasis is maintained by ridding the cell of damaged or defective organelles and protein complexes, and secondly, recycling of the organic constituents ensures a reservoir of energy for the cell to undergo metabolic reprogramming (130, 169).

Given that wounding is a crucial signal to activate tissue regeneration in both plants and animals, how does wounding activate autophagy is not yet well understood (10, 12, 206–208). In the biphasic model of autophagy, transcriptional networks are activated in the second phase after the existing autophagy proteome helps restore cellular homeostasis immediately post wounding. Herein there are two essential questions to explore – what are the wound-induced signals that first activate autophagy, and what are the sources of these signals (209, 210)? Wound-induced signals such as ROS and RNS are also byproducts of essential catalytic processes in mitochondria, chloroplasts, and peroxisomes during normal plant development. Balancing the intracellular redox environment when exposed to sudden stress therefore is crucial to cell function, as excess amounts of these molecules damages organelles and cell health, while sub-optimal levels may hinder with essential metabolic processes and

compromise cellular homeostasis (211). The activation of wound-induced autophagy may very well be the pivotal mechanism to balance this conundrum, where damaged organelles would be degraded to avoid buildup of metabolic stress. In plants autophagy is known to be activated by ROS, and autophagy defective mutants can accumulate ROS under normal development or when exposed to abiotic stressors like UV damage and flooding (212–216). The regulation of cell stress by autophagy would thus necessitate careful coordination of cytoplasmic events with the activation of gene regulatory networks to maintain those processes.

The findings of the previous chapters showed that PLT factors transcriptionally activate *ATG8*-mediated autophagy in excised leaves to promote *de novo* root regeneration. However, autophagy involves active encapsulation and movement of cell debris from the cytoplasm to the lytic vacuole, that would involve different cytosolic complexes at each step. Therefore, it was necessary to understand the cellular consequences of disrupting the PLT-*ATG8* regulatory axis, especially in the context of cells exposed at the site of injury that must undertake rapid reprogramming events for cell survival and wound repair. The results of this chapter demonstrate the role of the PLT-*ATG8* genetic module in facilitating coordinated organelle turnover in the cells of excised leaves, the loss of which leads to the build-up of intracellular stress. Herein my findings strongly indicate that the PLT-autophagy axis modulates wound induced ROS to the optimal levels required to promote stem cell regulators for successful *de novo* root regeneration.

5.2 RESULTS

5.2.1 Autophagy activation leads to coordinated organelle turnover during *de novo* root regeneration

Autophagy is a catabolic pathway that involves various protein complexes and intermediates within the cytosol. The previous chapters of this thesis established that *de novo* root regeneration requires PLT-regulated transcriptional activation of *ATG8* genes for autophagy mediated cellular reprogramming. In this chapter, I first examined the cellular consequence, if any, of disrupting the PLT-*ATG8* axis within cells of the excised leaves. Towards this, I monitored organelle turnover using chlorophyll autofluorescence for chloroplasts, along with a constitutive reporter tagging the lytic vacuole tonoplast with the aquaporin gene *GAMMA-TIP1* (*pUBQ10::GTIP1:TagRFP*; GTIP1-RFP henceforth) in wild type mesophyll cells adjacent to the cut end in leaves with contact.

Immediately post excision, the GTIP1-RFP tagged vacuole in WT cells were immobile, with the chloroplasts arranged uniformly around the vacuole periphery (Figure 5.1A). At 1DPC and 2DPC with contact, I observed GTIP1-RFP tagged intravacuolar strands and invaginations originating from the tonoplast, indicative of tonoplast remodelling (Figure 5.1 B, C). Interestingly, the chloroplasts in the WT mesophyll showed rapid aggregative movements on the tonoplast and inside the vacuole. Moreover, some chloroplasts were localized on rapidly moving GTIP1-RFP marked transvacuolar strands within the lumen, suggesting eventual degradation for organelle turnover (Figure 5.1 B-D) (22). By 5DPC, mesophyll chloroplasts were majorly aggregated inside the vacuole and not in the cytoplasm (Figure 5.1 E). Collectively, these data showed that post injury, the mesophyll chloroplasts were actively transported from the cytoplasm into the lytic vacuole for eventual degradation, that is a central hallmark of chloroplast autophagy (Figure 5.1 A-E, K) (20–22, 217, 218).

(figure on next page)

Figure 5.1 *De novo* root regeneration necessitates autophagy for coordinated organelle turnover in cells post wounding. (A-E) Representative confocal images of the tonoplast marker GTIP1-RFP and chloroplasts (autofluorescence) in WT mesophyll cells with contact at 0H-1DPC-2DPC-3DPC-5DPC. Images depict the mid-section of the lytic vacuole of a mesophyll cell adjacent to the cut end of the excised leaf. (F-J) Representative confocal images of the tonoplast marker GTIP1-RFP and chloroplasts (autofluorescence) in WT mesophyll cells without contact at 0H-1DPC-2DPC-3DPC-5DPC. Note that (H) shows two asymmetrical wound-callus daughter cells from a cylindrical mesophyll parent cell. (B-E) In the WT cells with contact, the tonoplast undulates and forms transvacuolar strands and invaginations, and the chloroplasts at the periphery begin to stream within the cell and over time, enter the vacuole lumen through tonoplast strands where they aggregate for further degradation. (K) Kymographs of WT; *GTIP1-RFP* with contact taken through the sagittal plane of the vacuole. At 0DPC the lumen is clear. From 1DPC to 5DPC, the tonoplast is actively mobile and forms invaginations and transvacuolar strands inside the lumen. The chloroplasts actively aggregate within the lumen for recycling and show streaming movements. (L) Kymographs of WT without contact show a clear vacuole lumen with chloroplasts at periphery, across all timepoints. Scale bars: 20 μm.

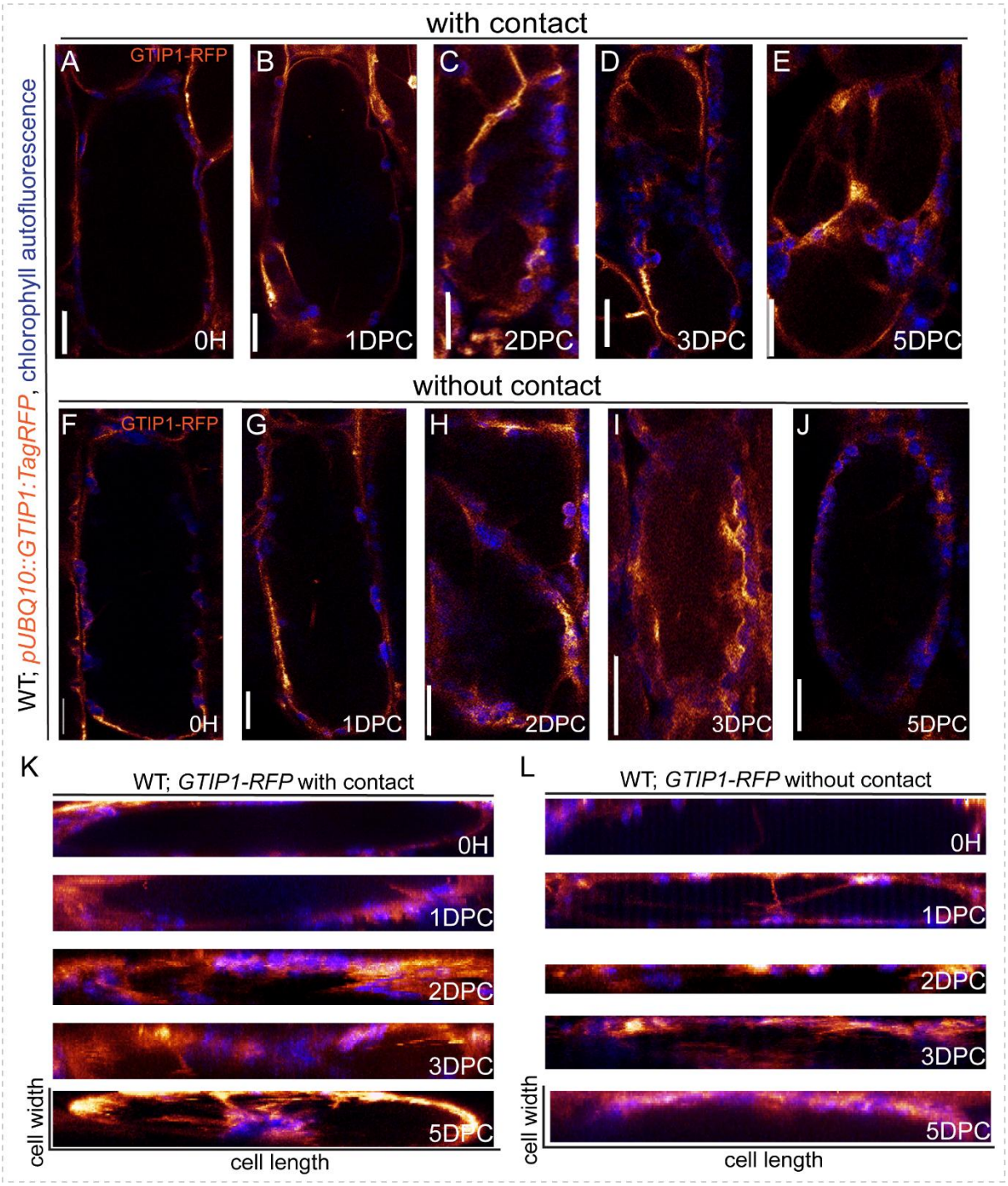

Next, I looked at the chloroplast-vacuole dynamics in leaves without contact. Strikingly, in these cells, mesophyll cell chloroplasts remained external to the lytic vacuole across all timepoints from 0H to 5DPC, and the tonoplast did not show intravacuolar remodelling (Figure 5.1 F-J, L). These intracellular patterns of chloroplasts in the WT cells with and without contact were also conspicuous in kymograph analysis (Figure 5.1 K, L). The lack of chloroplast motion and vacuolar remodelling confirmed the lack of autophagy mediated organelle turnover in

leaves without contact, and further validated the genetic and molecular results observed in the previous chapters of this thesis at the cellular scale.

5.2.2 Disrupting the PLT-*ATG8* axis severely compromises organelle turnover and impairs *de novo* root regeneration

Given the visible differences in chloroplast recycling and spatial localization between mesophyll cells with contact or without contact in WT, I next examined the chloroplast-vacuole dynamics of the *atg8f* and *plt3* mutants. In *atg8f* (*atg8f*; GTIP1-RFP), at 0H, the vacuole and chloroplast behavior were similar to WT (Figure 5.2 A, A'). However, from 1DPC to 3DPC, the chloroplasts of *atg8f* mesophyll cells remained static in the cytoplasm even at 3DPC and showed no aggregative, intravacuolar localization (Figure 5.2 B'-D', 5.3 B, D). There were no internalized chloroplasts within the vacuole indicating severely impaired organelle turnover in the mutant. At 5DPC, there were aggregated chloroplasts within the *atg8f* vacuole, that suggests a partial restoration of organelle turnover within the mutant at the later timepoints (Figure 5.2 E'). It is important to note here, that chloroplast compartmentalization in the vacuole is also known to occur through autophagy-independent mechanisms, albeit under different stress conditions (219). These intravacuolar patterns in *atg8f* cells with contact were also conspicuous in kymograph analysis (Figure 5.3B, D). The loss of chloroplast aggregation and intravacuolar organelle turnover in the *atg8f* mutant reveals a lack of coordinated organelle sorting and clearance, that is crucial to maintain cellular homeostasis.

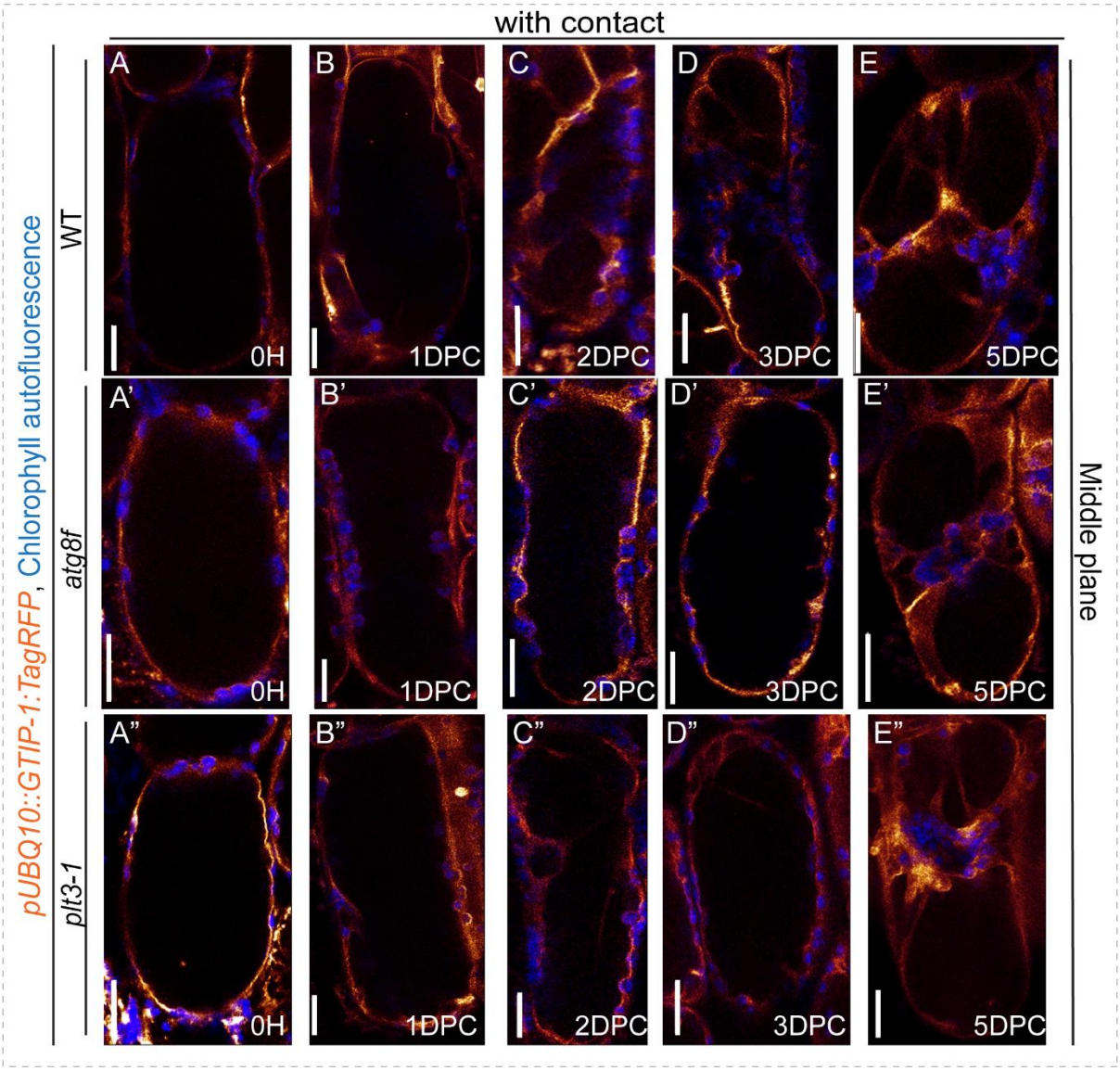

Figure 5.2 Genetic disruption of the PLT-*ATG8* axis severely compromises organelle turnover in cells post wounding. (A-E) Representative confocal images of the tonoplast marker GTIP1-RFP and chloroplasts (autofluorescence) in WT mesophyll cells with contact at 0H-1DPC-2DPC-3DPC-5DPC. Images have been previously used in Figure 5.1 (A-E). (A'-E') Representative confocal images of GTIP1-RFP and chloroplasts in *atg8f* mutant with contact at the same timepoints as WT. (A"-E") Representative confocal images of GTIP1-RFP and tonoplasts in plt3-1 mutant with contact at the same timepoints as WT. All images are single optical slices of the central plane of each cell as determined during image acquisition. (A, A', A") At 0H tonoplast-chloroplast dynamics are similar in WT and the mutants. (B-E) In the WT cells with contact, the tonoplast undulates and forms transvacuolar strands and invaginations, and the chloroplasts at the periphery begin to stream within the cell and over time, enter the vacuole lumen through tonoplast strands where they aggregate for further degradation. (B'-E') GTIP1-tonoplast movement is compromised in *atg8f* mutant and remains at the periphery even at 3DPC. The chloroplasts are static and do not localize inside the vacuole lumen. At 5DPC, the chloroplasts have aggregated within the lumen in *atg8f*. (B"-E") Tonoplast-chloroplast dynamics in *plt3-1* mesophyll cells during *de novo* root regeneration resemble *atg8f.* The lack of tonoplast remodelling is accompanied by the absence of chloroplast streaming and aggregation within the lumen for degradation and recycling. Scale bars: 20 µm.

The *plt3-1* mutant mesophyll cells also exhibited vacuole-chloroplast dynamics similar to the *atg8f* mutant (*plt3-1*; GTIP1-RFP). Mesophyll chloroplasts in *plt3-1* did not aggregate or show

any spatial difference in response to injury from 0H till 3DPC, as compared to the WT (Figure 5.2 A''-E''). Moreover, the tonoplast in *plt3-1* cells was less dynamic than in WT at both early and later timepoints despite normal vacuole morphology post excision (Figure 5.3 A, C, E).

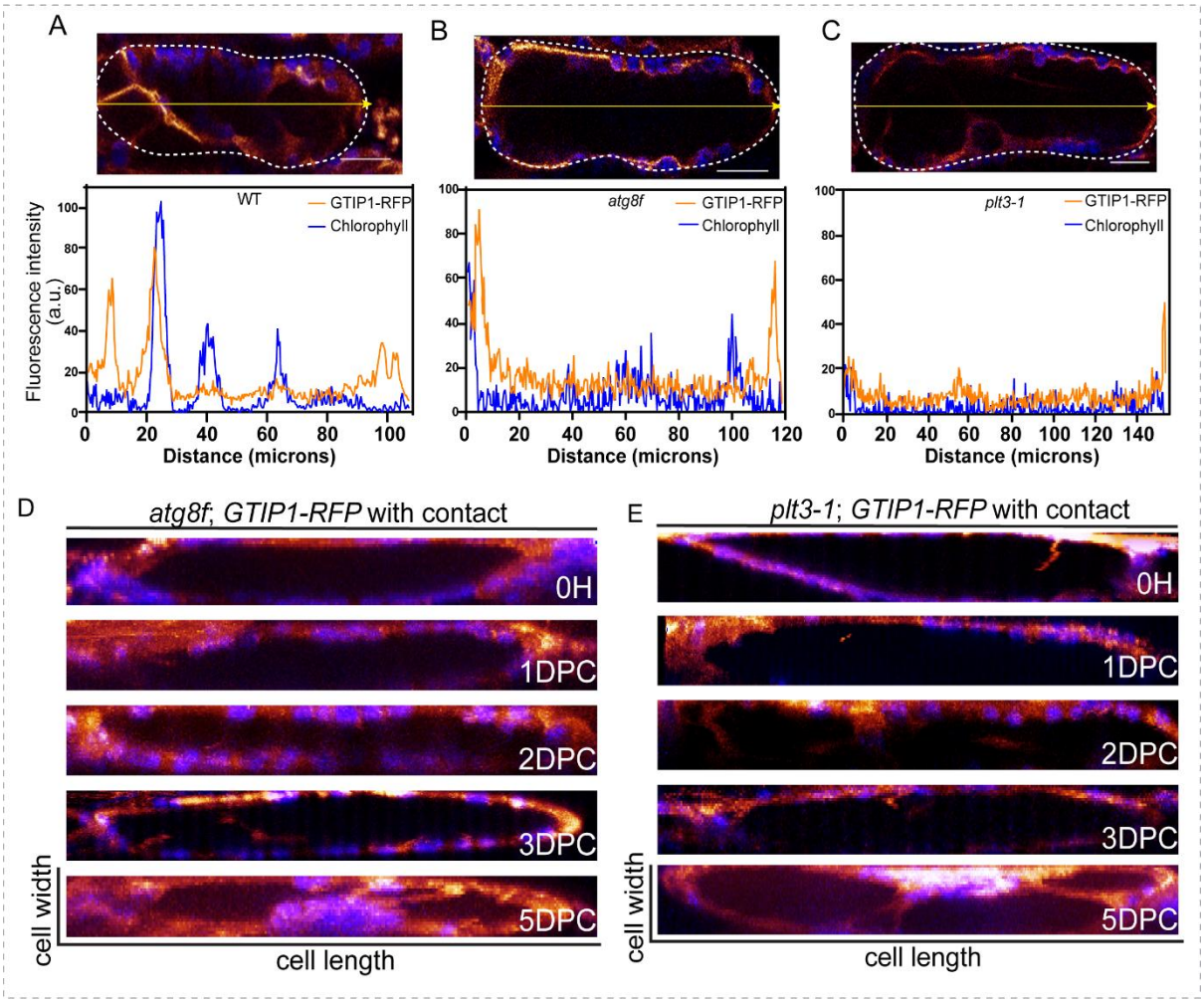

Figure 5.3 Analysis of intravacuolar chloroplast localization and turnover during *de novo* root regeneration. (A) Line-scan graph of GTIP1-RFP (orange) and chloroplast (blue) fluorescence intensity across the yellow line (image inset) within the WT vacuole at 2DPC with contact. (B) Line-scan graph of GTIP1-RFP (orange) and chloroplast (blue) fluorescence intensity across the yellow line (image inset) within the *atg8f* vacuole at 2DPC with contact. (C) Line-scan graph of GTIP1-RFP (orange) and chloroplast (blue) fluorescence intensity across the yellow line (image inset) within the *plt3-1* vacuole at 2DPC with contact. (D) Kymographs of *atg8f; GTIP1-RFP* show a loss of internalized tonoplast remodelling and chloroplast aggregation over 1-, 2-, and 3-DPC. At 5DPC, some partial aggregation of chloroplasts is seen. (E) Kymographs of *plt3; GTIP1-RFP* mesophyll cells from 0H to 5DPC. Like in *atg8f*, *plt3* mesophyll cells are unable to remodel the lytic vacuole tonoplast and chloroplast movement within the lumen is absent.

In summary, these findings highlight the necessity of a functional PLT-*ATG8* module to restore cellular homeostasis in excised leaves by promoting organelle turnover and maintaining organelle quality control mechanisms in the cells at the site of active cellular reprogramming during *de novo* root regeneration.

5.2.3 Wound-induced ROS is spatiotemporally stabilized during *de novo* root regeneration and not during wound-induced callus formation

Given the conspicuous lack of organelle turnover and vacuolar remodelling, I speculated that the lack of a functional PLT-*ATG8* module would lead to the buildup of intracellular stress within the reprogramming cells post injury. One of the canonical markers of cell stress are reactive oxygen species (ROS), that serve as important signals for activating cell repair pathways, including autophagy (220). In the context of injury, ROS serve as both a source as well as an output of stress response, thereby underscoring their necessity for cell survival and healing (221). Autophagy deficient mutants in plants are known to accumulate ROS in aerial organs during normal development (214, 222); this prompted me to investigate ROS levels in WT leaves with and without contact. Towards this, I stained the excised leaves at different timepoints with 2',7'-dichlorofluorescin diacetate (H_2DCFDA), an ROS-sensitive fluorescent probe (223). DCFDA-marked ROS intensities were quantified against unstained leaves incubated in v/v DMSO to normalize the background tissue autofluorescence (Figure 5.4J, also see Chapter 2).

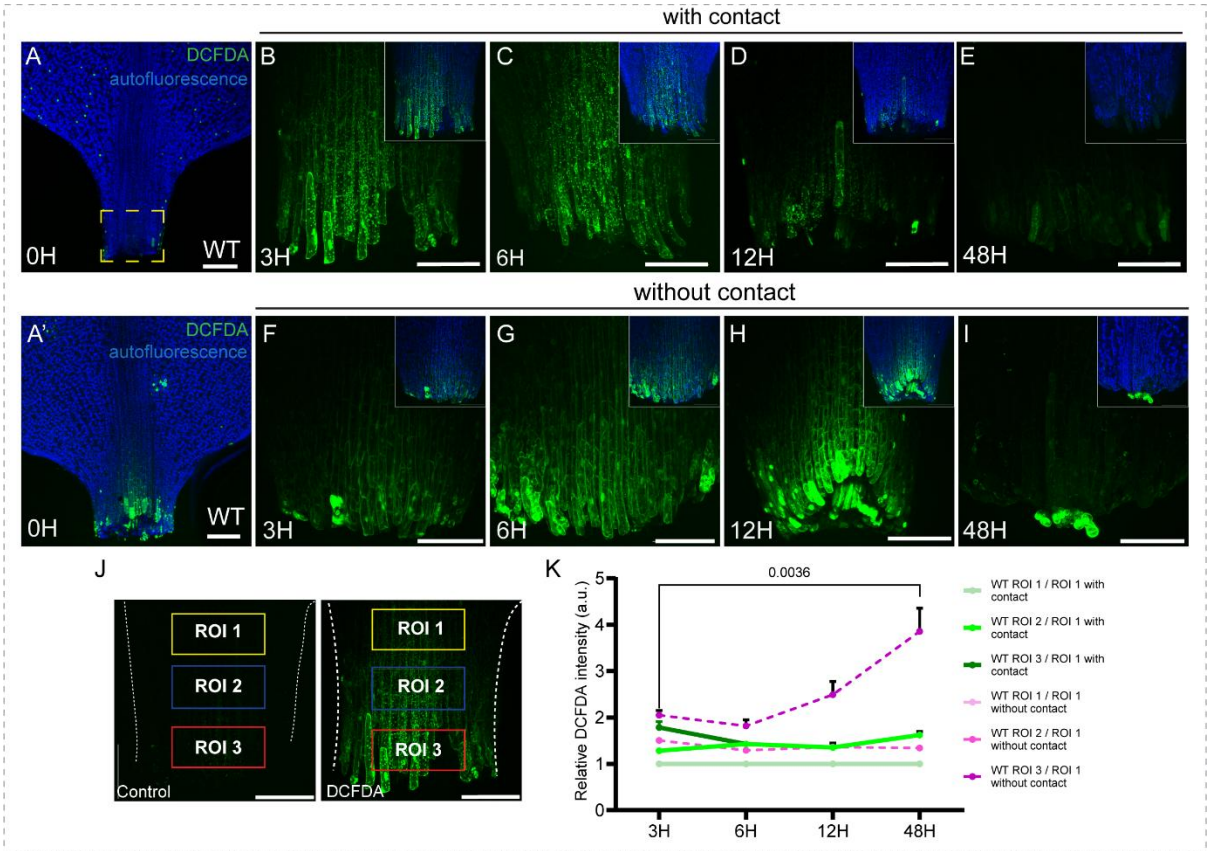

Figure 5.4 Wound-induced ROS accumulates in cells at the cut end of excised leaves and is spatiotemporally regulated during *de novo* root regeneration. (A-E, A') Representative maximum intensity projections of DCFDA-ROS signal intensity in WT excised leaves at different timepoints post excision with contact. DCDFA

signal showed a rapid ROS surge at 3H post cut (B), which gradually reduced over time with contact (E) (n >10 leaves per timepoint). (F-I) Representative maximum intensity projections of DCFDA-ROS in WT leaves kept without contact (n>10 leaves per timepoint). Note the increasing intensity of the DCFDA signal within the cells adjacent to the cut end till 12H (F-H), and the sequestration of DCFDA-ROS signals in the newly formed wound-induced callus cells at 48H (I). (J) Representative image of unstained and DCFDA stained petioles showing different regions designated as ROI 1, ROI 2, ROI 3 based on proximity to cut end for DCFDA signal intensity quantification. (K) Graph depicting relative DCFDA intensity across each ROI in 3H-, 6H- 12H-, and 48H leaves with and without contact. After the initial surge at 3H post cut, relative ROS signal intensity stabilizes in leaves with contact, while it significantly increases over time without contact at the cut end (P= 0.0036, Welch's two-tailed t-test). Note that the signal intensity ratio for ROI 1 / ROI 1 of both with and without contact is 1. Scale bars: 200 μm. Data shown as mean ± s.e.m.

DCFDA-marked ROS showed an early surge at 3H in the petiole cells of excised leaves with contact (Figure 5.4 A, A'). In the subsequent timepoints of 6-12-48H, this surge was spatially reduced and confined to the cells adjacent to the cut end at 48H (Figure 5.4 B-E, K). From these observations, I inferred that the cells in the vicinity of the injury displayed a rapid surge of wound-induced ROS post excision. However, with time, there was a gradual reduction and spatial confinement of these ROS signals for *de novo* root regeneration (Figure 5.4 J, K). The ROS intensity at 48H was confined to cells adjacent to the cut end, where previously dynamic organelle clearing was observed (Figure 5.4E, 5.1 A-E, K). Notably, in leaves without contact, the ROS levels did not go down; rather, the levels kept increasing in the cells adjacent to the cut end over time (Figure 5.4 F-I, K); eventually these ROS signals were sequestered inside the wound-induced callus cells, which remained ROS-saturated through all timepoints examined (Figure 5.4I).

Taken together, these results establish that *de novo* root regeneration is facilitated by the spatiotemporal regulation of wound-induced ROS, while wound-induced callus cells exhibit prolonged, near saturating levels of ROS.

5.2.4 PLT-*ATG8* axis mediated modulation of ROS levels is essential for *de novo* root regeneration

I next checked how does compromised autophagy impact ROS levels during *de novo* root regeneration. H_2DCFDA staining of *atg8f* mutant showed that intracellular ROS was significantly elevated ectopically across the petiole in *atg8f* compared to WT in the 3H-12H interval (Figure 5.5 A, B, A', B', F). Strikingly, the *atg8f*;*atg8h* double mutant showed increased ROS accumulation at 48H, at which time WT leaves show a confined low ROS near the cut end (Figure 5.5 C, C', G 5.4E). Next, I examined if loss of function of PLT3 or PLT7 had similar effects on ROS levels during *de novo* root regeneration. Similar to the *atg8f* and *atg8f*;*atg8h* mutants, both *plt3-1* and *plt7-1* showed ectopically elevated ROS levels across the

petiole over time in leaves with contact (Figure 5.5 D, E, D', E', H, I). Collectively, these findings strongly suggest that PLT-regulated autophagic activation is essential for stabilizing wound-induced ROS to the optimal levels necessary for promoting *de novo* root regeneration.

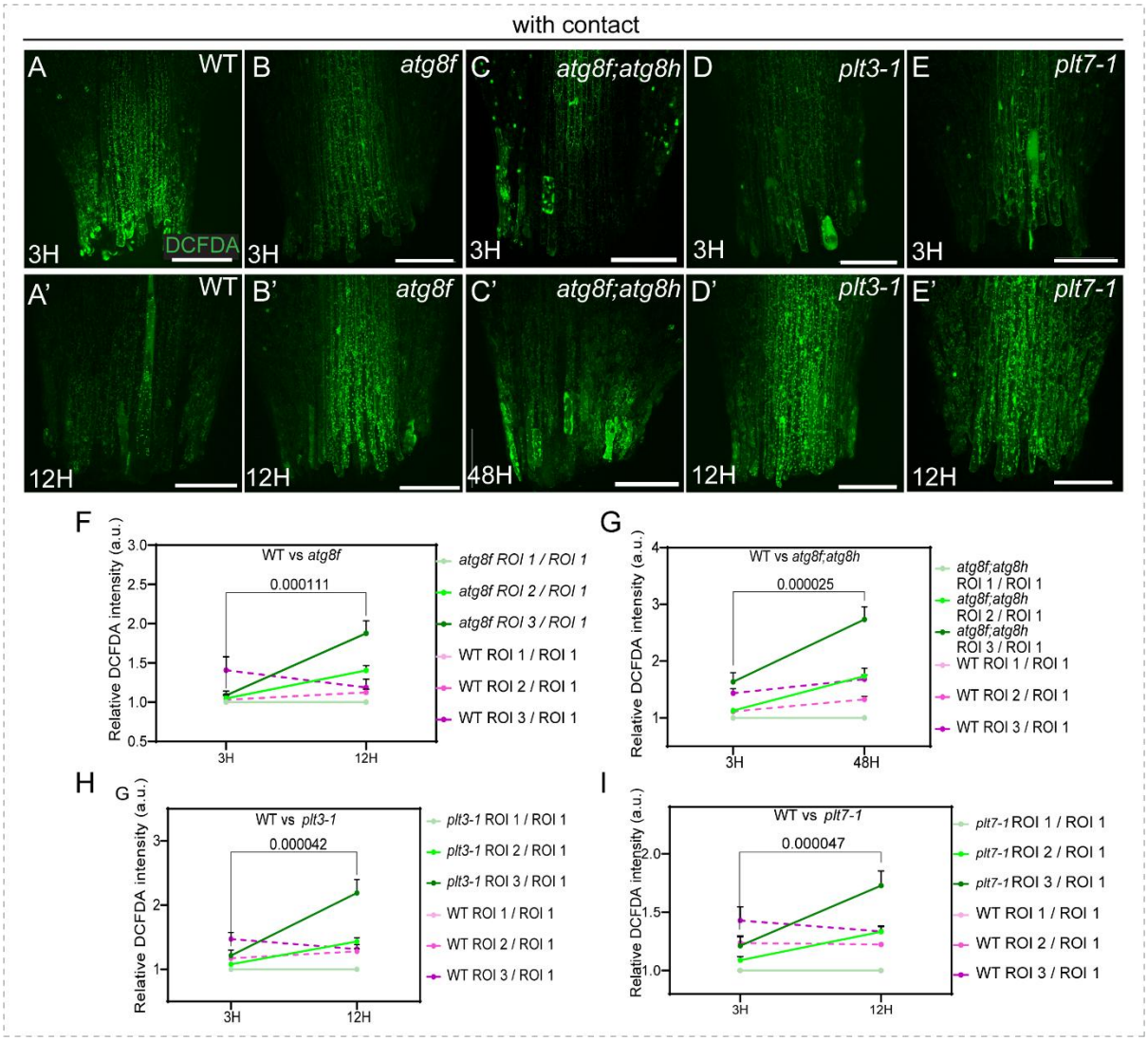

Figure 5.5 Disrupting the PLT-*ATG8* regulatory axis leads to ectopic accumulation of ROS. (*A*, *A'*) Representative maximum intensity projections of DCFDA-stained WT excised leaves at different timepoints post excision with contact. DCDFA signal showed a rapid ROS surge at 3H post cut (*A*), which was spatiotemporally reduced later at 12H post cut (*A'*) (n >10 leaves per timepoint). (*B, B'*) Representative confocal images of stronger DCFDA intensity in *atg8f* mutant at 12H compared to WT at 12H with contact. (*C, C'*) Representative confocal images of stronger DCFDA intensity in *atg8f;atg8h* mutant at a later timepoint compared to WT at 12H with contact. (*D, D'*) Representative confocal images of stronger DCFDA intensity in *plt3-1* mutant at 12H compared to WT at 12H with contact. (*E*, *E'*) Representative confocal images of stronger DCFDA intensity in *plt7-1* mutant at 12H compared to WT at 12H with contact. While there is an equivalent surge of wound induced ROS at 3H across WT and all mutants, the ROS levels in WT significantly reduce over time whereas there is ectopic ROS increase in the mutants at the same timepoint. (F-I) Graphs showing normalized DCFDA intensities in WT compared with *atg8f*, atg8f*;atg8h*, *plt3-1* and *plt7-1* mutants between 3H and 12H timepoints (48H for *atg8f;atg8h*). DCFDA intensities were analyzed using Fiji and normalized both against unstained controls and ROI 1 (farthest from the cut end) and plotted. All mutants tested showed higher ROS intensities near the cut end (ROI 3/ ROI 1) at the later timepoints when normalized against ROI 1 (*atg8f* P= 0.000111, Welch's two-tailed t-

test; *atg8f;atg8h* P= 0.000025, Welch's two-tailed t-test; *plt3-1* P= 0.000042, Welch's two-tailed t-test; *plt7-1* P= 0.000047, Welch's two-tailed t-test). Note that the signal intensity for ROI 1 / ROI 1 of both WT and the mutants is 1. Data shown as mean ± s.e.m. Scale bars: 200 µm.

Since the data so far showed elevated levels of ROS accumulation in the *plt3-1*, *plt7-1*, *atg8f*, and *atg8f*;atg8*h* mutant leaves which are unable to regenerate *de novo* roots, I next examined if externally induced high ROS affected *de novo* root regeneration. To address this, I added hydrogen peroxide (H_2O_2) to the regeneration media as an ROS inducer, and kept excised leaves with contact on media supplemented with different concentrations of H_2O_2 (0.1 mM, 0.5 mM, 1 mM). Here, *de novo* root regeneration at 0.1 mM H_2O_2 was similar to WT control (Figure 5.6A). However, 0.5 mM reduced, and 1 mM H_2O_2 completely abolished *de novo* root regeneration (Figure 5.6A). This complete loss of *de novo* root regeneration with excess ROS phenocopies the *plt3-1*, *plt7-1*, *atg8f*, and *atg8f*;*atg8h* mutants and 3-MA mediated autophagy inhibition, thereby affirming the necessity of the PLT-*ATG8* axis in modulating wound induced ROS levels during *de novo* root regeneration.

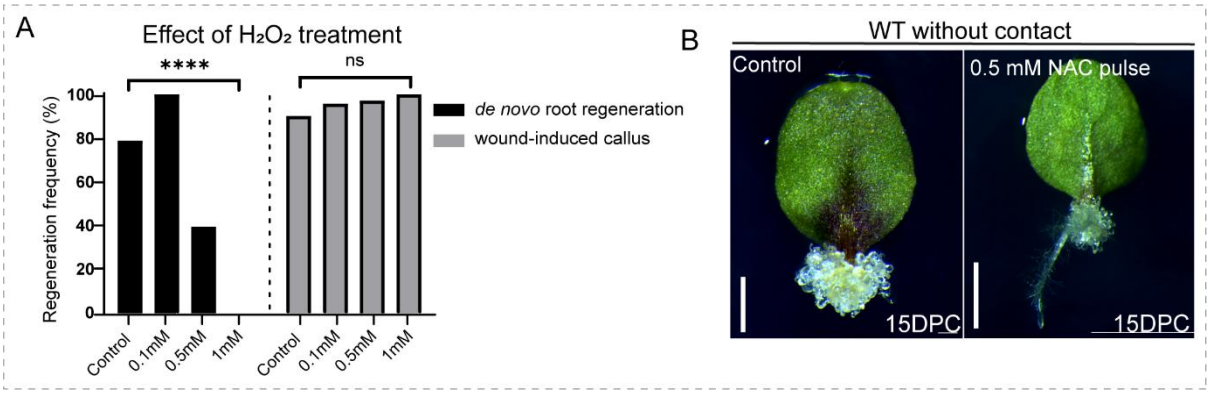

Figure 5.6 Excessive ROS impairs *de novo* root regeneration, while optimal ROS levels boost *de novo* root regeneration. (A) Graph representing *de novo* root regeneration frequency of WT leaves after ROS induction treatment using hydrogen peroxide (H_2O_2). ROS manipulation reveals that low ROS induction can activate and high ROS accumulation can impair *de novo* root regeneration, with no effect on the wound healing response (****P<0.0001, Pearsons's χ^2 test) (n=20 leaves per group). (B) Representative stereozoom images showing *de novo* rooting in WT leaf without contact treated with 0.5 mM NAC as compared to the untreated control. NAC treatment induces *de novo* root regeneration in WT leaf kept without contact. The leaf regenerates both a wound-induced callus and an adventitious root from the cut end. Scale bars: 2 mm.

The necessity of finely tuned ROS modulation during *de novo* root regeneration evoked an interesting question – could reduction of ROS by external means reactivate organ regeneration fate? Towards this, I used a pharmacological approach for ROS inhibition using a well-known ROS scavenger, N-acetylcysteine (NAC in text) (224, 225). Initial optimization experiments of inhibitor concentrations were done with wildtype leaves kept without contact, with the aim of regenerating *de novo* roots. Remarkably, a 12H pulse treatment of 0.5 mM NAC immediately post excision led to *de novo* root regeneration in leaves even without contact (Figure 5.6B).

Given these data, I further investigated the importance of ROS modulation using NAC as an ROS scavenging reagent in the *plt-atg8* mutants.

In collaboration with Aabha and Komal, I next optimized the treatment period for NAC induced root regeneration on the *plt3-1* mutant. Here, after testing different time periods of NAC pulses in different leaf orientations (protocol written in Chapter 2), we observed that a transient 12H pulse of NAC both at 0.25 mM with contact and 1 mM without contact successfully rescued *de novo* root regeneration in *plt3-1* (Figure 5.7 A, B). Indeed, transient 12H pulse treatment of NAC successfully rescued *de novo* root regeneration across *plt3*, *plt7*, *atg8f*, and *atg8f;atg8h* mutants both with and without contact (Figure 5.7 A-F). These findings reinforce the necessity of ROS reduction to optimal levels necessary for *de novo* root regeneration. Importantly, in the WT leaves with contact where ROS levels are endogenously optimized, further reduction by NAC treatment actually reduced the root regeneration frequency compared to the untreated control (Figure 5.7A). These results, together with the detrimental effects of excess ROS (Figure 5.6A), highlight the importance for optimal ROS levels during organ regeneration. Collectively, my findings suggest that the spatiotemporal suppression of excessive ROS accumulation through the PLT-autophagy axis restores proper redox balance and promotes successful *de novo* root regeneration.

(*figure on next page*)

Figure 5.7 ROS quenching by external means successfully boosts *de novo* root regeneration across *PLT* and *ATG8* mutants irrespective of contact. Representative stereozoom images of WT (A), *plt3-1* (B), *atg8f;atg8h* (C), *plt3-cr* (D), *plt7-cr* (E) and *atg8f* (F) leaves pulsed with suboptimal concentrations of N-acetylcysteine for 12H post excision, then transferred to ½ MS media with contact (after 0.25 mM NAC pulse) or without contact (after 1 mM NAC pulse). Samples were pooled from 3 separate experiment sets. Numbers at the top right corner of each image indicate number of leaves showing the representative phenotype (wound-induced callus, *de novo* root, wound-induced callus + *de novo* root, or no regeneration) out of the total sample set examined. ROS quenching by NAC rescued *de novo* root regeneration in both *plt* and *atg8* mutants kept with or without contact. Lower concentration of NAC (0.25mM) failed to rescue *plt3-cr* (D), possibly due to the severity of the mutant phenotype. Scale bars: 2 mm.

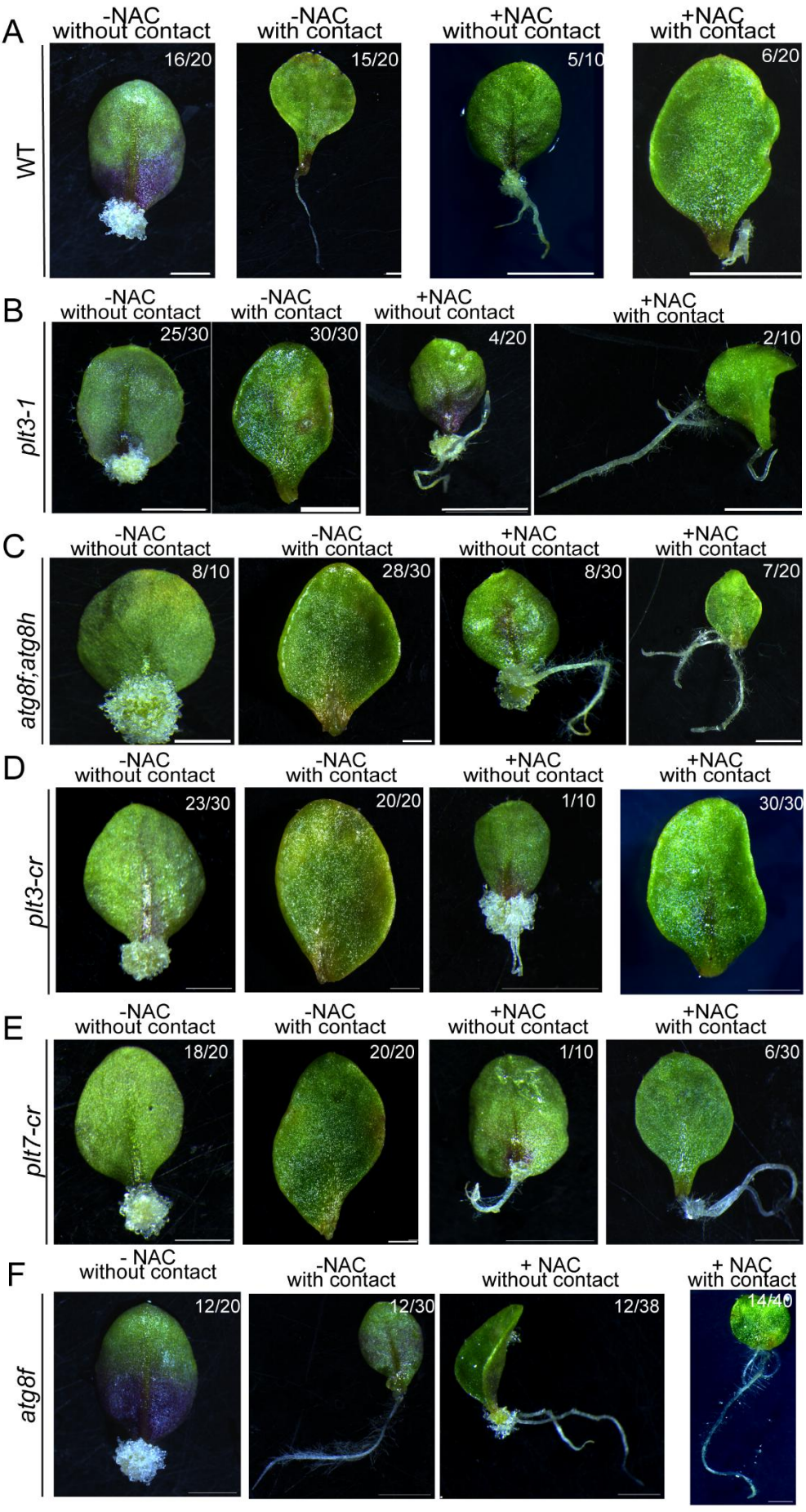
A
-NAC without contact
-NAC with contact
+NAC without contact
+NAC with contact
WT
16/20
15/20
5/10
6/20
B
-NAC without contact
-NAC with contact
+NAC without contact
+NAC with contact
plt3-1
25/30
30/30
4/20
2/10
C
-NAC without contact
-NAC with contact
+NAC without contact
+NAC with contact
atg8f;atg8h
8/10
28/30
8/30
7/20
D
-NAC without contact
-NAC with contact
+NAC without contact
+NAC with contact
plt3-cr
23/30
20/20
1/10
30/30
E
-NAC without contact
-NAC with contact
+NAC without contact
+NAC with contact
plt7-cr
18/20
20/20
1/10
6/30
F
- NAC without contact
-NAC with contact
+ NAC without contact
+ NAC with contact
atg8f
12/20
12/30
12/38
14/40

5.2.5 PLT-autophagy-ROS module promotes stem cell activation during *de novo* root regeneration

The observations of Chapter 3 and 4 suggested that the PLT-*ATG8* axis were necessary for vascular reprogramming but did not impact founder cell identity. I next checked root stem cell expression in the excised leaves under different conditions using a translational fusion reporter of WOX5 (WOX5-RFP), an essential root stem cell regulator, in WT (WT; *pWOX5::gWOX5:mRFP*) (83). In WT leaves with contact, WOX5-RFP expressing cells were visible at 5DPC, in line with previous reports (Figure 5.8A) (81, 83), indicative of root primordium cell activation (82). Strikingly, WOX5-RFP expression was undetectable in leaves kept without contact, and also during excess ROS or 3-MA autophagy inhibitor treatment (Figure 5.8 B-D). WOX5-RFP marked cells were also absent across both *plt3-cr* and *plt7-cr* mutants (*plt3-cr*; *pWOX5::gWOX5:mRFP*; *plt7-cr*; *pWOX5::gWOX5:mRFP*) (Figure 5.8 E, F). Strikingly, a 12H pulse of 1 mM NAC successfully restored WOX5-RFP expression in *plt3-cr* even without contact, which reinforces the necessity of ROS modulation to activate root stem cell regulators during *de novo* root regeneration (Figure 5.8G). Taken together, the findings of this study indicate that the PLT-autophagy regulatory module stabilizes wound-induced ROS surge in cells post wounding, that allows these cells to rejuvenate and progress towards stem cell regulator activation for successful *de novo* root regeneration.

(*figure on next page*)

Figure 5.8 Regulation of ROS levels by the PLT-autophagy module activates root stem regulator expression and drives *de novo* root regeneration. (A-B) Representative confocal images of WOX5-RFP (orange LUT channel) (WT; *pWOX5::gWOX5:*mRFP) in WT leaves with (A) and without (B) contact at 5DPC (n= 10-12 leaves per condition). Dashed yellow box: zoomed-in image of endogenous callus area at the cut end. White arrowheads in (A) inset mark WOX5-RFP expressing nuclei. No detectable WOX5-RFP seen in leaves under autophagy inhibitor 3-MA treatment (C), or under external ROS induction (D) (n= 8-10 leaves per treatment). No detectable WOX5-RFP seen in *PLT* gene mutants *plt3-cr* (E) and *plt7-cr* (F) at 5DPC with contact (n=10-12 leaves). However, a 12H pulse of 1mM NAC was sufficient to induce WOX5-RFP expression in *plt3-cr* (indicated by white arrowhead in G-inset) kept without contact post treatment (G). (G) inset – Orange LUT channel was contrast adjusted for better visibility of WOX-RFP signal within the leaf tissue. Scale bars: 200 µm.

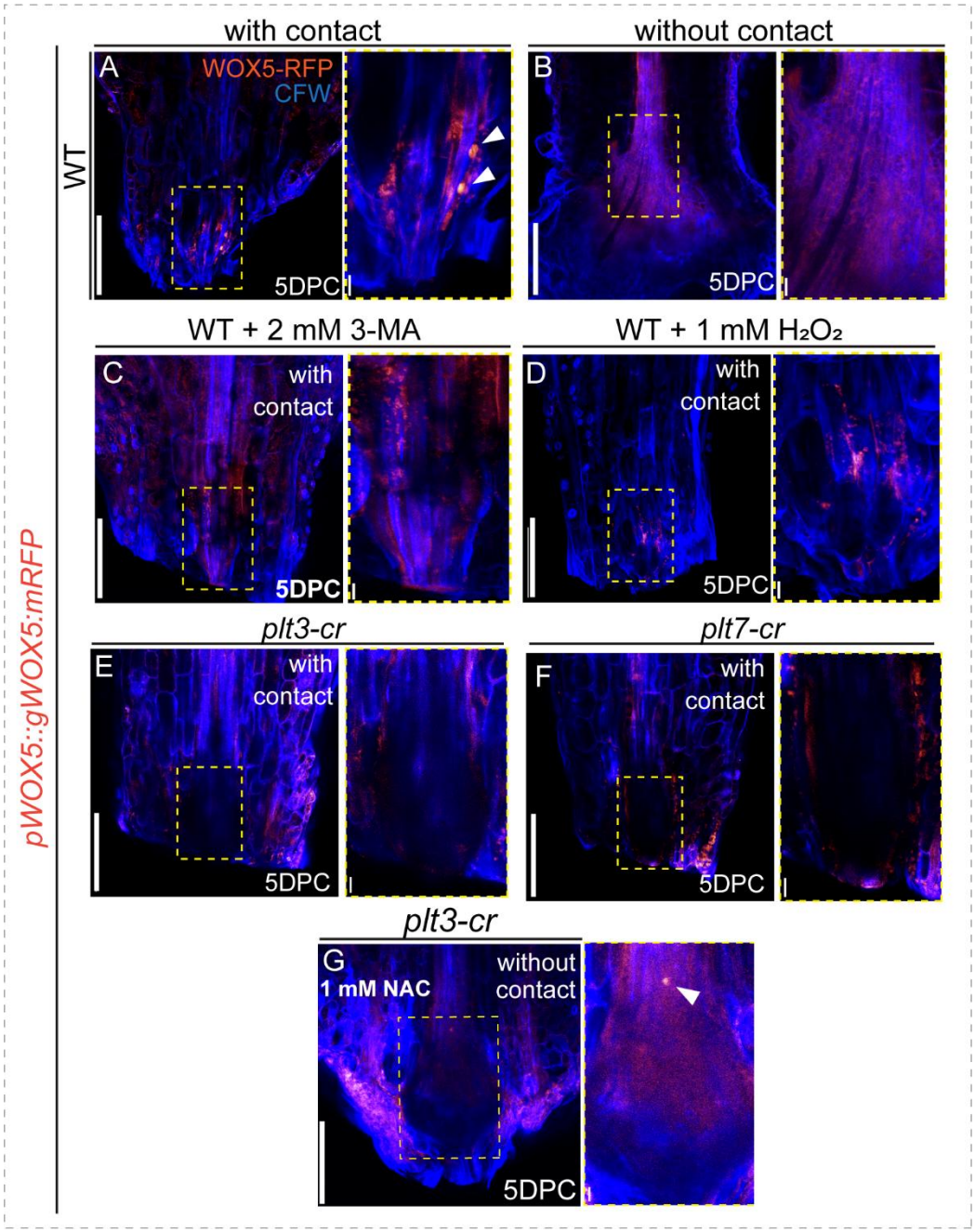
pWOX5::gWOX5:mRFP
WT
with contact
without contact
A
WOX5-RFP
CFW
5DPC
B
5DPC
WT + 2 mM 3-MA
WT + 1 mM H₂O₂
C
with contact
5DPC
D
with contact
5DPC
plt3-cr
plt7-cr
E
with contact
5DPC
F
with contact
5DPC
plt3-cr
G
1 mM NAC
without contact
5DPC

5.3 DISCUSSION

Irrespective of the cause, the basic principles of wound induced signalling are common to most multicellular lifeforms. Cellular damage leads to an immediate release of Ca2+ waves from the site of injury into the tissue that activate both short- and long-range signalling cascades through gap junctions in animals and plasmodesmata in plants (118). These calcium signals then induce an ROS response in the surrounding tissue through rapid NADPH oxidase activity (39, 226). These ROS signals trigger downstream cascades essential to wound repair, that include programmed cell death, autophagy, stress hormone pathways such as ethylene or jasmonate in plants and Wnt-beta-catenin in animals (31, 39). In animal models, autophagy and ROS exist in a feedback loop: ROS can induce autophagy, while autophagy clears ROS-producing organelles and proteins to restore redox balance (227–229). Indeed, autophagy has been shown to support tissue regeneration in invertebrates and vertebrates by modulating ROS, such as in irradiation-induced intestinal regeneration in *Drosophila* (227, 230). Whether a similar autophagy-ROS principle operates in plants to support regeneration was unclear.

Herein this study shows that the precise spatiotemporal modulation of wound-induced ROS in excised leaves is crucial to promote *de novo* root regeneration over simple wound healing and wound callus proliferation. While this work does not explore the physiological source of the wound-induced ROS signals, it is necessary to note that both mitochondria and chloroplasts are sites of active ROS production in plant cells, either by oxidative phosphorylation in the former, or the photooxidation of chloroplast protein complexes in the latter (119). Regardless of the source, these wound-induced ROS rapidly surge in cells post wounding, which must be controlled to ensure cell survival and wound repair. Post excision, leaves experience a rapid ROS surge irrespective of the contact pose. However, the ROS dynamics diverge over time with a distinct signature for each final outcome. In the process of root regeneration, ROS levels decline and become spatially confined near the wound, whereas during wound-callus proliferation they remain elevated within the amorphous callus cells throughout. This makes it evident that ROS is tuned within the regeneration competent cells to create an optimal redox state that permits *de novo* rooting. The PLT-autophagy axis ensures this very purpose. The PLTs activate *ATG8* genes that provides a steady transcriptional output for autophagy mediated turnover of defective proteins and organelles in the lytic vacuole of cells near the wound, that in turn reduces the initial ROS burst. These cellular events eventually buffer ROS levels at the steady state required to promote root stem cell differentiation from the cohort of founder cells reprogrammed during wound healing. The necessity of a balanced redox state to support this

outcome is reinforced by the observation that ROS quenching in normal WT leaves with contact (with a functioning PLT-*ATG8* axis) reduced *de novo* root regeneration compared to the untreated group (Figure 5.7A).

Another interesting aspect of this study was the direct effect of genetic disruption of the PLT-*ATG8* module on cellular behaviour. The conspicuous lack of chloroplast internalization and tonoplast remodelling in the lytic vacuole in both *atg8f* and *plt3* mesophyll cells provided robust experimental validation of this specific transcriptional network at the cellular scale for reestablishing cellular homeostasis for a prolonged period. Whether a similar axis operates during stem cell differentiation for lateral roots or other secondary aerial organs remains to be seen. Notwithstanding the importance of both the PLT factors or normal autophagy pathways during plant development, my findings prove how these networks come together in plant tissues post injury to stabilize ROS levels, and create an optimal cellular redox balance that enables stem-cell differentiation for *de novo* root regeneration.

CHAPTER 6

Conclusions and broader perspectives of this thesis

"We shall not cease from exploration, and the end of all our exploring will be to arrive where we started and know the place for the first time."

– T.S. Eliot

6.1 Thesis Summary

The near ubiquitous ability of plants to repair and regenerate lost/damaged tissue is central to their historical use for breeding and propagation practices. Post injury, plants can initiate wound repair, local cell proliferation to seal the wound, and even regenerate new organs *de novo*. This evokes an essential question – what are the processes that determine the regenerative fate? This thesis uses contact-mediated regeneration from excised *Arabidopsis thaliana* leaves as a facile binary system to explore how cell survival and homeostasis processes are directed post injury to activate *de novo* organ regeneration over wound-induced callus proliferation in plants. Here I found that autophagy, an ancient cellular quality control pathway across lifeforms, is activated during *de novo* root regeneration and not wound-induced callus formation. This activation is sustained throughout by regulated transcriptional output of specific autophagy related genes (*ATG*s) from the *ATG8* gene family – *ATG8F* and *ATG8H*, that are essential for autophagosome biogenesis, assembly, and transport in plants. These autophagy genes are in turn, directly activated by specific members of the plant-specific PLETHORA family of transcription factors, namely PLT3 and PLT7, that show context-specific novel interactions which make them function non-redundantly during the *de novo* root regeneration process. At the cellular scale, the PLT-autophagy genetic module coordinates organelle turnover and spatiotemporal ROS stabilization post injury, thereby restoring the redox balance of cells around the wound to the optimal levels necessary to support long term cellular reprogramming for eventual root outgrowth. In summary, the findings of this thesis illustrate the ability of plants to utilize kingdom-wide conserved physiological principles through precise transcriptional feedback within injured tissue to dictate diverse regenerative fates.

6.2 Autophagy is dispensable for wound healing in plants, and activated specifically during organ regeneration

The findings of **Chapter 3** from this thesis provide insights into how the contact-mediated regeneration assay activates autophagy specifically during *de novo* root regeneration and not during wound-induced callus formation. Since the organ regeneration fate in this scenario appears dependent on direct physical contact with a substrate, it is tempting to speculate that mechanical cues at the site of injury can activate different wound signalling mechanisms that

may give rise to diverse regenerative outcomes. A recent study by Kareem *et al* supports this idea by showing how media stiffness or 'water availability' impacts *de novo* root regeneration in both *Arabidopsis* and tomato by positioning the auxin maxima at the site of root primordium initiation (70). However, the contact switching experiment shown in Chapter 3 (Figure 3.1) revealed that the external cues provided by any such substrate is relevant for organ regeneration only if provided within the initial 48 hours post injury, and does not significantly influence root regeneration at the later stages. This puts the usefulness of mechanical cues in the process of injury induced *de novo* organogenesis as an accessory rather than a primary signal, and calls for the investigation of other, more potent cellular processes that determine the regeneration response. In this context, my findings position autophagy as a key cellular process for promoting organ regeneration over wound-induced callus formation. Taken together with existing literature, the results of this study suggest that mechanosignalling inputs may support the initial activation of wound-induced autophagy, other cellular processes can take over and sustain the autophagy response at the later stages of regeneration.

While a large body of research shows how autophagy response is regulated at the post-translational-scape by enzymatic cleavage, post-translational modifications, protein flux, and catabolic turnover, studies on the transcriptional regulation of autophagy are a more recent avenue of investigation across model systems (160, 165, 180, 231–233). Autophagy related genes (*ATG*s) comprise a large family, conserved in both sequence and function across eukaryotes, bar some notable exceptions like the *ATG8* genes in plants (157, 160, 234, 235). While *ATG8*/*LC3* exists as a single gene in most animals and fungi, plants have evolved multiple orthologs of *ATG8*. Herein it becomes essential to understand why would plants generate multiple copies of a single gene to perform similar cellular functions. One explanation could be that the precise use of autophagy in a context-dependent manner rather than as a ubiquitous response would require additional transcriptional calibration (165, 236). In my study, I found that among the nine *ATG8* orthologs in *A. thaliana*, four genes *ATG8B*, *ATG8C*, *ATG8F*, and *ATG8H* were transcriptionally upregulated only with contact, while the other genes showed no significant change. Further analysis revealed that *ATG8F* and *ATG8H* significantly impacted *de novo* regeneration fate while leaving wound-induced callus formation unaffected. These data support my earlier point of plants deploying autophagy as a selective strategy rather than a ubiquitous wound response. From an evolutionary perspective, these findings align with the conserved role of autophagy in cellular regeneration across taxa. Phylogenetic analyses reveal strong homology among ATGs in vertebrates and invertebrates,

and functional studies in planarians and hydra demonstrate that autophagy genes such as *DjATG8-2* and *DjATG8-3*, linked to mTOR signaling, are indispensable for tissue regeneration (237, 238). Interestingly, while ATG8F and ATG8H are required for sustaining autophagic flux in roots under phosphate (Pi) starvation, their loss-of-function mutants do not show any difference in Pi levels compared to the wildtype under starvation stress; however, the *atg8f;atg8h* double mutant was reported to show a slight reduction of lateral root numbers compared to wildtype (239). This also suggests that these ATG8 isoforms have different functions across stress conditions, but these functions may converge at the level of organ formation and emergence irrespective of the developmental context. The molecular basis of ATG8F and ATG8H specifically impacting root regeneration may be the effect of several regulatory events, ranging from their transcriptional regulation (explored in this thesis), to tissue-specific protein interactions that remain to be discovered. Future studies can dissect this functional specificity using heterologous promoters for manipulating ATG8 expression patterns, along with investigating the biochemical interactions of different motifs within these isoforms during different physiological conditions.

Lastly, this chapter also shows that in the timeline of cell-fate reprogramming events during *de novo* root regeneration, perturbing autophagy does not impact founder cell activation, that even occurs in leaves without contact with wound-induced callus formation. $WOX11^{+}$ founder cells were seen in leaves without contact as well as after the genetic or chemical disruption of autophagy, suggesting that the initial cell reprogramming events post wounding confer preliminary competence irrespective of the final regenerative fate (Figure 6.1).

6.3 Plant-specific PLETHORA factors transcriptionally regulate autophagy genes in a non-redundant manner during *de novo* root regeneration

Chapter 4 of this thesis shows that the plant-specific PLETHORA transcription factors both directly and indirectly activate *ATG8* genes during *de novo* root regeneration. Using DAP-seq data as a starting point, this study deploys both PLT overexpression and depletion lines to establish the genetic control of autophagy through *ATG8* genes by the PLTs during *de novo* root regeneration. PLT7 directly binds to the *ATG8F* promoter directly upstream of the TSS and upregulates it in leaves kept with contact, while also indirectly activating the other *ATG8*s. Moreover, while no PLT7 activity was seen in the leaves at 0H, there is a gradual expansion over the next few days of $PLT7^{+}$ cells from the cut end of the petiole up the leaf blade, in a pattern similar to the *ATG8F* promoter activity observed in Chapter 3. Previous studies have

shown that while the *plt3;plt5-2;plt7* higher-order mutant is deficient in regenerative ability, the single or double-combination mutants are not significantly different than wildtype (16, 17). However, during the course of testing PLT7 sufficiency for organ regeneration, this study shows that during *de novo* root regeneration from excised leaves, the PLTs work in a novel, non-redundant manner, where PLT3, not PLT7, is both necessary and sufficient for this process. Moreover, PLT3 reporter activity was seen in the procambium layer around the vascular bundle even at 0H, and remained confined to this cell layer throughout all timepoints, unlike PLT7. While both PLT expression domains partially overlap in the endogenous healing callus formed at the cut end, their spatiotemporal dynamics are markedly different during the root regeneration program. Gene expression analyses revealed that PLT3 indirectly upregulated PLT7 during *de novo* root regeneration, whereas PLT7 overexpression or depletion did not affect PLT3 levels. Interestingly, PLT3 directly bound the *ATG8H* promoter, indicating both PLTs directly influence autophagy activation through their individual *ATG8* targets. Moreover, ectopic *ATG8F* expression did not adversely affect root regeneration in wildtype, but partially rescued it in the *plt3* mutant, both with and without contact. These findings prove two important points – firstly, that the sustained expression of a single *ATG8* gene is capable of partially rescuing organ regeneration in a *PLT* deficient mutant, and that this overexpression does not appear to be rate-limiting for the organ regeneration process.

The PLTs are known as master regulators of plant development as well as regeneration. Several lines of evidence demonstrate that these factors are highly conserved in function and act redundantly across tissues during development (132, 141, 182, 240, 241). This redundancy is also reflected during regeneration where single or double combination *plt* mutants are not significantly compromised either, and only higher-order mutants show significant defects (16, 17, 48). However, this redundancy of function is only partially recapitulated by their localization (138, 184, 242), the latter being dependent on their individual upstream transcriptional regulators. How do the regulatory networks of PLTs regulate their expression domains is relatively unexplored. By expressing PLT3 and PLT7 under each other's promoters in the *plt3* loss-of-function mutant, this study uncovered that surprisingly, both PLTs reverted to their native expression domains in excised leaves post injury, while being expressed under their heterologous promoter domains during normal root development. This striking fidelity of PLT3 and PLT7 strongly supports the possibility of intragenic regulatory elements within the gene loci that allows these developmental regulators to activate genetic programs exclusively in response to injury, to recalibrate the cellular state from maintaining normal development to

transition into new cell lineages. In summary, developmental regulators unique to the plant kingdom play a pivotal role in activating specific gene programs in response to injury to activate cellular responses in a precise manner. Moreover, these factors exhibit context-dependent interactions that are otherwise repressed or dormant during normal development, but essential to reprogram cells towards diverse regenerative outcomes.

6.4 The PLT-autophagy axis stabilizes wound-induced ROS and restores cellular homeostasis to the optimal levels necessary for *de novo* root regeneration

Results shown in **Chapter 5** unite the PLT-*ATG8* transcriptional module with the cellular environment in cells undergoing active reprogramming post injury. The aggregative movements of chloroplasts in wound-adjacent mesophyll cells, along with the active remodelling of their vacuoles provide qualitative evidence of sustained autophagy activation within these cells that leads to coordinated organelle compartmentalization and turnover. These cellular processes are essential to remove defective cell parts that may become cytotoxic when left unchecked. Moreover, my findings prove that the loss of the PLT-autophagy axis in the excised leaves translates into severely compromised organelle clearance and disruption of cellular homeostasis post injury. While the current study did not investigate the spatial dynamics of NG-ATG8F tagged autophagosomes with the lytic vacuole, recent evidence from other groups shows that ATG8 proteins can also conjugate to the vacuole tonoplast, that activates tonoplast invagination and maintains vacuolar integrity upon cell wall damage or ionophore treatment (243, 244). Interestingly, results of Chapters 3 and 5 strongly suggest that active ATG8F-mediated autophagy occurs concomitantly with active tonoplast remodelling in mesophyll cells with contact. Taken together, these findings open essential avenues to explore how ATG8-mediated vacuolar remodelling can also impact the mechanical homeostasis of plant cells during development or regeneration.

From these data, one can infer that in the absence of the PLT-autophagy axis, stress signals would accumulate and persist within cells post injury rather than stabilize to reestablish cellular homeostasis. Stress signals are the output of a large spectrum of molecules, ranging from cellular proteins such as DAMPs and MAP kinases, to ions such as ROS, RNS, and Ca^{2+} (107, 109, 111, 245). Among them, ROS presents a fascinating avenue of study, as it functions as a crucial signal for wound repair and pathogen defense mechanisms, and is also capable of influencing cellular reprogramming and differentiation. In animal models, autophagy and ROS exist in a feedback loop: ROS can induce autophagy, while autophagy clears ROS-producing

organelles and proteins to restore redox balance (227–229). In this study, H_2-DCFDA imaging at the early hours post cut shows a wound-induced ROS surge post wounding, regardless of the final outcome. This initial ROS burst likely activates defense and repair pathways in cells for survival and to heal the wound. During this process the cells near the wound gain regeneration competence and create a niche of founder cells essential for the next phase of reprogramming. In regeneration competent conditions, the PLT–*ATG8* axis then attenuates this wound-induced ROS signalling, ensuring optimal redox conditions for *de novo* root regeneration. The wound-induced callus cells in contrast, are ROS-saturated throughout, which shows a lack of stress remediation. Studies in planaria echo this binary outcome, where different ROS thresholds dictate wound closure versus regeneration (246).

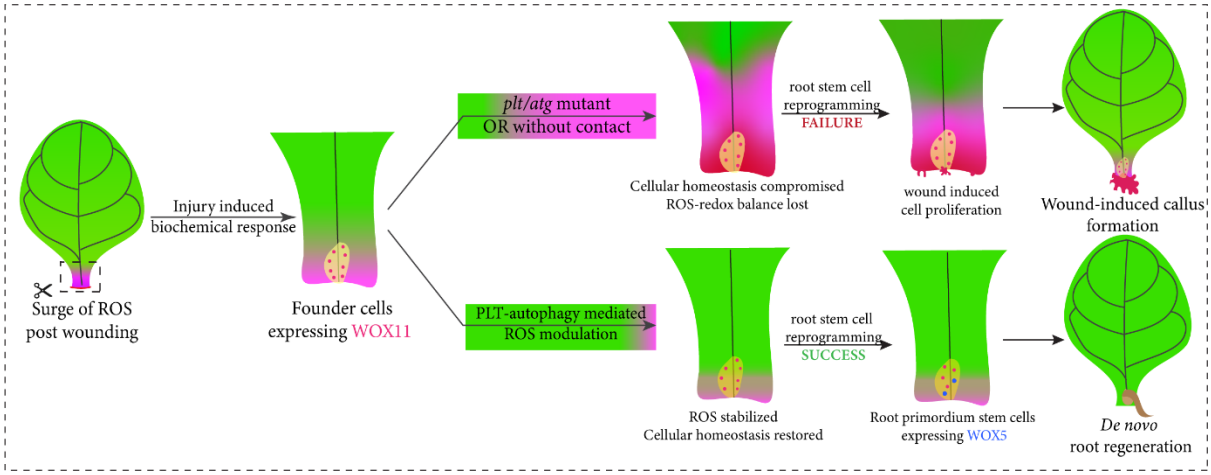

Figure 6.1 Restoration of cellular homeostasis instructs regenerative fate post wounding. An excised leaf can regenerate either a *de novo* root or a wound-induced callus at the cut end. These regenerative outcomes depend on the transcriptional activation of cellular recycling mechanisms like autophagy, which promotes cellular homeostasis and brings down wound-induced ROS to a permissive range. This cellular environment is conducive for the commitment of founder cells formed post injury into root primordium stem cells capable of organ regeneration. Using the PLETHORA factors, plants channel the autophagy-ROS biochemical feedback towards a focused regenerative fate rather than a common wound response.

These findings led to an important question – would modulation of ROS levels alone be sufficient to instruct *de novo* root regeneration? A brief 12-hour application of N-acetylcysteine, an ROS scavenger, was sufficient to promote root regeneration across both *PLT* and *ATG8* mutants, underscoring redox homeostasis as an essential determinant of cell-fate transitions during regeneration. Notably, ROS quenching reduced root regeneration in wildtype leaves with contact, indicating that further depletion of endogenously modulated ROS was also detrimental for the organ regeneration fate. These findings underscore the importance of optimal ROS levels as the fulcrum between cell proliferation and differentiation, where the latter supports necessary stem cell activity for root outgrowth. This was further supported by

restoration of WOX5-RFP expressing cells in the *plt3-cr* mutant upon ROS quenching, indicating that the PLT-autophagy-ROS axis finetunes cellular energy state to drive the critical transition of founder cells into root stem-cell primordia capable of adventitious root outgrowth. While this thesis did not touch on the genetic regulation of ROS enzymes, a previous study reported that loss-of-function mutants of RESPIRATORY BURST OXIDASE HOMOLOGS (RBOH) genes RBOHD and RBOHF showed enhanced *de novo* root regeneration compared to wildtype (76). However, during lateral root development, these mutants showed a significant delay in LR emergence and numbers, and their overexpression enhanced LR initiation (247). Moreover, external ROS inducer treatment in this thesis showed complete inhibition of root regeneration at 1 mM H2O2, whereas the same dose and higher enhanced LR emergence and density during normal development. Taken together, these findings strongly suggest that the role of ROS as a wound signal during root regeneration differs from its role as an endogenous cellular signal in root development, and open up interesting avenues of exploration into the regulatory networks surrounding ROS mediated cell-fate reprogramming in diverse physiological contexts.

6.5 Summary

Aerial organs have been used as explants for vegetative propagation and breeding practices for ages. These applications directly depend on the ability of plants to routinely heal wounds and regenerate damaged organs. Yet, regeneration is more than the activation of hormones and developmental networks. It is a multi-step process that requires cells to survive, activate defense response against pathogens, restore homeostasis, and manage stress, all the while undergoing cell-fate transitions (248). This thesis provides useful insights into how plants are capable of healing wounds and regenerating *de novo* organs by using lineage-specific transcription factors like PLTs to channel conserved cellular pathways like autophagy. By directly interfacing with a quality-control pathway, the PLT-autophagy axis becomes a metabolic switch that regulates wound-induced ROS surge into an optimal redox state conducive for stem-cell regulator activation. Importantly, the dynamics of PLTs and ROS during *de novo* organ regeneration show a marked difference from their known developmental roles, further highlighting the importance of regeneration-specific networks that are activated in response to injury. The findings of this thesis thus provide a framework to explore how cellular environment actively dictates fate transitions during regeneration, with broad implications on both convergent and divergent strategies of regeneration in eukaryotes.

CHAPTER 7

References

1. K. D. Birnbaum, A. S. Alvarado, Slicing across kingdoms: regeneration in plants and animals. *Cell* **132**, 697–710 (2008).

2. K. Sugimoto, S. P. Gordon, E. M. Meyerowitz, Regeneration in plants and animals: Dedifferentiation, transdifferentiation, or just differentiation? *Trends Cell Biol.* **21**, 212–218 (2011).

3. M. M. Mathew, K. Prasad, Model systems for regeneration: Arabidopsis. *Development (Cambridge)* **148** (2021).

4. C. Gordy, Y. W. He, The crosstalk between autophagy and apoptosis: Where does this lead? *Protein Cell* **3**, 17–27 (2012).

5. M. Dickman, B. Williams, Y. Li, P. Figueiredo, T. Wolpert, Reassessing apoptosis in plants. *Nature Plants 2017 3:10* **3**, 773–779 (2017).

6. D. V. Savatin, G. Gramegna, V. Modesti, F. Cervone, Wounding in the plant tissue: The defense of a dangerous passage. *Front. Plant Sci.* **5**, 111139 (2014).

7. R. K. Monson, A. M. Trowbridge, R. L. Lindroth, M. T. Lerdau, Coordinated resource allocation to plant growth–defense tradeoffs. *New Phytologist* **233**, 1051–1066 (2022).

8. S. A. Eming, P. Martin, M. Tomic-Canic, Wound repair and regeneration: Mechanisms, signaling, and translation. *Sci. Transl. Med.* **6**, 265sr6 (2014).

9. A. P. Shanmukhan, *et al.*, Regulation of touch-stimulated de novo root regeneration from Arabidopsis leaves. *Plant Physiol.* (2021). https://doi.org/10.1093/PLPHYS/KIAB286.

10. J. V. Kanne, *et al.*, Overexpression of ATG8/LC3 enhances wound-induced somatic reprogramming in Physcomitrium patens. *Autophagy* **18**, 1463–1466 (2022).

11. E. Rodriguez, *et al.*, Autophagy mediates temporary reprogramming and dedifferentiation in plant somatic cells. *EMBO J.* **39**, e103315 (2020).

12. K. I. Kurotani, *et al.*, Autophagy is induced during plant grafting to promote wound healing. *Nature Communications 2025 16:1* **16**, 3483- (2025).

13. L. Xu, De novo root regeneration from leaf explants: wounding, auxin, and cell fate transition. *Curr. Opin. Plant Biol.* **41**, 39–45 (2018).

14. C. Yang, M. Luo, X. Zhuang, F. Li, C. Gao, Transcriptional and Epigenetic Regulation of Autophagy in Plants. *Trends in Genetics* **36**, 676–688 (2020).

15. W. Agbemafle, M. M. Wong, D. C. Bassham, Transcriptional and post-translational regulation of plant autophagy. *J. Exp. Bot.* **74**, 6006–6022 (2023).

16. A. Kareem, *et al.*, PLETHORA genes control regeneration by a two-step mechanism. *Current Biology* **25**, 1017–1030 (2015).

17. D. Radhakrishnan, *et al.*, A coherent feed-forward loop drives vascular regeneration in damaged aerial organs of plants growing in a normal developmental context. *Development (Cambridge)* **147** (2020).

18. W. Liu, *et al.*, Transcriptional landscapes of de novo root regeneration from detached Arabidopsis leaves revealed by time-lapse and single-cell RNA sequencing analyses. *Plant Commun.* **3**, 100306 (2022).

19. K. Yoshimoto, Y. Ohsumi, Unveiling the Molecular Mechanisms of Plant Autophagy—From Autophagosomes to Vacuoles in Plants. *Plant Cell Physiol.* **59**, 1337–1344 (2018).

20. M. Izumi, H. Ishida, S. Nakamura, J. Hidema, Entire Photodamaged Chloroplasts Are Transported to the Central Vacuole by Autophagy. *Plant Cell* **29**, 377–394 (2017).

21. C. Wan, *et al.*, Selective autophagy regulates chloroplast protein import and promotes plant stress tolerance. *EMBO J.* **42** (2023).

22. H. Ishida, K. Yoshimoto, Chloroplasts are partially mobilized to the vacuole by autophagy. *Autophagy* **4**, 961–962 (2008).

23. S. Michaeli, G. Galili, Degradation of Organelles or Specific Organelle Components via Selective Autophagy in Plant Cells. *International Journal of Molecular Sciences 2014, Vol. 15, Pages 7624-7638* **15**, 7624–7638 (2014).

24. A. L. Anding, E. H. Baehrecke, Cleaning House: Selective Autophagy of Organelles. *Dev. Cell* **41**, 10–22 (2017).

25. J. Wang, Q. Zhang, Y. Bao, D. C. Bassham, Autophagic degradation of membrane-bound organelles in plants. *Biosci. Rep.* **43** (2023).

26. K. D. Birnbaum, Development: Acting your cellular age. *Nat. Plants* **1**, 15100 (2015).

27. C. Gaillochet, J. U. Lohmann, The never-ending story: From pluripotency to plant developmental plasticity. *Development (Cambridge)* **142**, 2237–2249 (2015).

28. A. N. Landge, D. Radhakrishnan, A. Kareem, K. Prasad, Intermediate Developmental Phases during Regeneration. *Plant Cell Physiol.* **59**, 702–707 (2018).

29. J. P. Brockes, A. Kumar, Comparative aspects of animal regeneration. *Annu. Rev. Cell Dev. Biol.* **24**, 525–549 (2008).

30. R. Heidstra, S. Sabatini, Plant and animal stem cells: similar yet different. *Nat. Rev. Mol. Cell Biol.* **15**, 301–312 (2014).

31. M. A. Hernández-Oñate, A. Herrera-Estrella, Damage response involves mechanisms conserved across plants, animals and fungi. *Curr. Genet.* **61**, 359–372 (2015).

32. L. Liu, *et al.*, Comparisons between Plant and Animal Stem Cells Regarding Regeneration Potential and Application. *Int. J. Mol. Sci.* **24** (2023).

33. K. Chiou, E. M. S. Collins, Why we need mechanics to understand animal regeneration. *Dev. Biol.* **433**, 155–165 (2018).

34. D. L. Bodor, W. Pönisch, R. G. Endres, E. K. Paluch, Of Cell Shapes and Motion: The Physical Basis of Animal Cell Migration. *Dev. Cell* **52**, 550–562 (2020).

35. K. Sugimoto, H. Temman, S. Kadokura, S. Matsunaga, To regenerate or not to regenerate: factors that drive plant regeneration. *Curr. Opin. Plant Biol.* **47**, 138–150 (2019).

36. A. Kareem, *et al.*, Protocol: a method to study the direct reprogramming of lateral root primordia to fertile shoots. *Plant Methods* **12**, 27 (2016).

37. C. W. Melnyk, Quantitative regeneration: Skoog and Miller revisited. *Quantitative plant biology* **4**, e10 (2023).

38. M. Ikeuchi, Y. Ogawa, A. Iwase, K. Sugimoto, Plant regeneration: cellular origins and molecular mechanisms. *Development* **143**, 1442–1451 (2016).

39. T. C. Byatt, P. Martin, Parallel repair mechanisms in plants and animals. *DMM Disease Models and Mechanisms* **16** (2023).

40. J. M. Pérez-Pérez, Anchor Root Development: A World within Worlds. *Mol. Plant* **13**, 1105–1107 (2020).

41. X. Zhang, *et al.*, Auxin transport positions stem cells in the vascular cambium during normal development and regeneration. *Proc. Natl. Acad. Sci. U. S. A.* **122**, e2511087122 (2025).

42. P. Marhava, *et al.*, Re-activation of Stem Cell Pathways for Pattern Restoration in Plant Wound Healing. *Cell* **177**, 957-969.e13 (2019).

43. J. Xu, *et al.*, A Molecular Framework for Plant Regeneration. *Science (1979).* **311**, 385–388 (2006).

44. J. Heyman, *et al.*, The heterodimeric transcription factor complex ERF115-PAT1 grants regeneration competence. *Nat. Plants* **2** (2016).

45. B. Canher, *et al.*, Rocks in the auxin stream: Wound-induced auxin accumulation and ERF115 expression synergistically drive stem cell regeneration. *Proc. Natl. Acad. Sci. U. S. A.* **117**, 16667–16677 (2020).

46. H. Iida, *et al.*, Plants monitor the integrity of their barrier by sensing gas diffusion. *Nature 2025 644:8076* **644**, 483–489 (2025).

47. G. Sena, X. Wang, H. Y. Liu, H. Hofhuis, K. D. Birnbaum, Organ regeneration does not require a functional stem cell niche in plants. *Nature* **457**, 1150–1153 (2009).

48. K. Durgaprasad, *et al.*, Gradient Expression of Transcription Factor Imposes a Boundary on Organ Regeneration Potential in Plants. *Cell Rep.* **29**, 453-463.e3 (2019).

49. Y. Liang, J. Heyman, R. Lu, L. De Veylder, Evolution of wound-activated regeneration pathways in the plant kingdom. *Eur. J. Cell Biol.* **102**, 151291 (2023).

50. L. Hoermayer, *et al.*, Wounding-induced changes in cellular pressure and localized auxin signalling spatially coordinate restorative divisions in roots. *Proc. Natl. Acad. Sci. U. S. A.* **117**, 15322–15331 (2020).

51. R. Matosevich, *et al.*, Local auxin biosynthesis is required for root regeneration after wounding. *Nat. Plants* **6**, 1020–1030 (2020).

52. I. Efroni, *et al.*, Root Regeneration Triggers an Embryo-like Sequence Guided by Hormonal Interactions. *Cell* **165**, 1721–1733 (2016).

53. L. Hoermayer, J. Friml, Targeted cell ablation-based insights into wound healing and restorative patterning. *Curr. Opin. Plant Biol.* **52**, 124–130 (2019).

54. Q. Wan, R. Yao, Y. Zhao, L. Xu, JA and ABA signaling pathways converge to protect plant regeneration in stress conditions. *Cell Rep.* **44**, 115423 (2025).

55. W. Zhou, *et al.*, A Jasmonate Signaling Network Activates Root Stem Cells and Promotes Regeneration. *Cell* **177**, 942-956.e14 (2019).

56. P. Marhavý, *et al.*, Single-cell damage elicits regional, nematode-restricting ethylene responses in roots. *EMBO J.* **38**, EMBJ2018100972- (2019).

57. Y. Zhang, X. Wang, J. Zhang, X. Q. He, Plant in situ tissue regeneration: dynamics, mechanisms and implications for forestry research. *Forestry Research* **2023** (2023).

58. J. L. Baulies, *et al.*, MicroRNA control of stem cell reconstitution and growth in root regeneration. *Nature Plants 2025 11:3* **11**, 531–542 (2025).

59. I. Cohen, *et al.*, Transient restriction of intercellular communication is required for root tip regeneration. *Current Biology* **35**, 3638-3649.e5 (2025).

60. M. M. Mathew, *et al.*, Wound repair in plants guided by cell geometry. *Current Biology* (2025). https://doi.org/10.1016/J.CUB.2025.06.072.

61. J. Shin, P. J. Seo, Varying Auxin Levels Induce Distinct Pluripotent States in Callus Cells. *Front. Plant Sci.* **0**, 1653 (2018).

62. I. M, *et al.*, Wounding Triggers Callus Formation via Dynamic Hormonal and Transcriptional Changes. *Plant Physiol.* **175**, 1158–1174 (2017).

63. J. M. Lee, *et al.*, Wounding induces multilayered barrier formation in mature leaves via phytohormone signalling and ATML1-mediated epidermal specification. *Nature Plants 2025 11:7* **11**, 1298–1315 (2025).

64. M. Ikeuchi, K. Sugimoto, A. Iwase, Plant Callus: Mechanisms of Induction and Repression. *Plant Cell* **25**, 3159–3173 (2013).

65. A. Iwase, *et al.*, The AP2/ERF Transcription Factor WIND1 Controls Cell Dedifferentiation in Arabidopsis. *Current Biology* **21**, 508–514 (2011).

66. M. Ikeuchi, *et al.*, Wound-inducible WUSCHEL-RELATED HOMEOBOX 13 is required for callus growth and organ reconnection. *Plant Physiol.* **188**, 425–441 (2022).

67. N. Ogura, *et al.*, WUSCHEL-RELATED HOMEOBOX 13 suppresses de novo shoot regeneration via cell fate control of pluripotent callus. *Sci. Adv.* **9** (2023).

68. B. Rymen, *et al.*, Histone acetylation orchestrates wound-induced transcriptional activation and cellular reprogramming in Arabidopsis. *Communications Biology 2019 2:1* **2**, 404- (2019).

69. K. Sugimoto, Y. Jiao, E. M. Meyerowitz, Arabidopsis Regeneration from Multiple Tissues Occurs via a Root Development Pathway. *Dev. Cell* **18**, 463–471 (2010).

70. A. Kareem, *et al.*, Water availability positions auxin response maxima to determine plant regeneration fates. *Nat. Plants* (2025). https://doi.org/10.1038/s41477-025-02029-2.

71. G. Kanmegne, R. S. Atchioutchoua, G. R. T. Noumbo, Combining air-layering and stem cutting techniques to optimize the production of quality planting materials for agroforestry tree

species: a case study of Canarium schweinfurthii Engl. (Burseraceae). *Forests Trees and Livelihoods* **31**, 170–183 (2022).

72. S. Tran, *et al.*, Endogenous salicylic acid suppresses de novo root regeneration from leaf explants. *PLoS Genet.* **19** (2023).

73. G. Zhang, *et al.*, Jasmonate-mediated wound signalling promotes plant regeneration. *Nat. Plants* **5**, 491–497 (2019).

74. H. Li, L. Yao, L. Sun, Z. Zhu, ETHYLENE INSENSITIVE 3 suppresses plant de novo root regeneration from leaf explants and mediates age-regulated regeneration decline. *Development (Cambridge)* **147** (2020).

75. J. Yan, *et al.*, IRR1 contributes to de novo root regeneration from Arabidopsis thaliana leaf explants. *Physiol. Plant.* **175** (2023).

76. S. Y. Shin, S. J. Park, H. S. Kim, J. H. Jeon, H. J. Lee, Wound-induced signals regulate root organogenesis in Arabidopsis explants. *BMC Plant Biol.* **22**, 1–14 (2022).

77. G. Zhang, *et al.*, Functional Analysis of CLE26 in Controlling De Novo Root Regeneration from Detached Arabidopsis Leaves. *Int. J. Mol. Sci.* **25**, 13156 (2024).

78. L. Chen, *et al.*, YUCCA-mediated auxin biogenesis is required for cell fate transition occurring during de novo root organogenesis in Arabidopsis. *J. Exp. Bot.* **67**, 4273–4284 (2016).

79. K. Lee, H. Yoon, O.-S. Park, P. J. Seo, ENHANCER OF SHOOT REGENERATION1 promotes de novo root organogenesis after wounding in Arabidopsis leaf explants. *Plant Cell* **36**, 2359–2374 (2024).

80. X. Chen, *et al.*, A simple method suitable to study de novo root organogenesis. *Front. Plant Sci.* **5**, 88651 (2014).

81. J. Liu, *et al.*, WOX11 and 12 Are Involved in the First-Step Cell Fate Transition during de Novo Root Organogenesis in Arabidopsis. *Plant Cell* **26**, 1081–1093 (2014).

82. E. Bustillo-Avendaño, *et al.*, Regulation of hormonal control, cell reprogramming, and patterning during de novo root organogenesis. *Plant Physiol.* **176**, 1709–1727 (2018).

83. X. Hu, L. Xu, Transcription factors WOX11/12 directly activate WOX5/7 to promote root primordia initiation and organogenesis. *Plant Physiol.* **172**, 2363–2373 (2016).

84. N. Zhai, *et al.*, Cytokinin facilitates the patterning of the adventitious root apical meristem from leaf cuttings. *Molecular horticulture* **4**, 11 (2024).

85. X. Chen, *et al.*, Auxin-Independent NAC pathway acts in response to explant-specific wounding and promotes root tip emergence during de novo root organogenesis in arabidopsis. *Plant Physiol.* **170**, 2136–2145 (2016).

86. J. Pan, *et al.*, Control of de novo root regeneration efficiency by developmental status of Arabidopsis leaf explants. *Journal of Genetics and Genomics* **46**, 133–140 (2019).

87. E. Larriba, M. Nicolás-Albujer, A. B. Sánchez-García, J. M. Pérez-Pérez, Identification of Transcriptional Networks Involved in De Novo Organ Formation in Tomato Hypocotyl Explants. *Int. J. Mol. Sci.* **23** (2022).

88. S. Asghar, *et al.*, De novo root regeneration from leaf explant: a mechanistic review of key factors behind cell fate transition. *Planta* **261**, 33 (2025).

89. J. Duclercq, B. Sangwan-Norreel, M. Catterou, R. S. Sangwan, De novo shoot organogenesis: From art to science. *Trends Plant Sci.* **16**, 597–606 (2011).

90. A. Iwase, *et al.*, WIND1-based acquisition of regeneration competency in Arabidopsis and rapeseed. *Journal of Plant Research 2015 128:3* **128**, 389–397 (2015).

91. A. Iwase, *et al.*, WIND1 Promotes Shoot Regeneration through Transcriptional Activation of ENHANCER OF SHOOT REGENERATION1 in Arabidopsis. *Plant Cell* **29**, 54–69 (2017).

92. A. O. Kshetry, *et al.*, A synthetic transcription cascade enables direct in planta shoot regeneration for transgenesis and gene editing in multiple plants. *Mol. Plant* **18**, 2066–2081 (2025).

93. C. Nishitani, T. Demura, H. Fukuda, Analysis of Early Processes in Wound-Induced Vascular Regeneration using TED3 and ZeHB3 as Molecular Markers. *Plant Cell Physiol.* **43**, 79–90 (2002).

94. T. Sachs, The induction of transport channels by auxin. *Planta* **127**, 201–206 (1975).

95. J. Benayoun, R. Aloni, T. Sachs, Regeneration Around Wounds and the Control of Vascular Differentiation. *Ann. Bot.* **39**, 447–454 (1975).

96. T. Sachs, The Control of the Patterned Differentiation of Vascular Tissues. *Adv. Bot. Res.* **9**, 151–262 (1981).

97. A. Zhang, *et al.*, Cell-wall damage activates DOF transcription factors to promote wound healing and tissue regeneration in Arabidopsis thaliana. *Current Biology* **32**, 1883-1894.e7 (2022).

98. D. Radhakrishnan, *et al.*, Age, Wound Size, and Position of Injury - Dependent Vascular Regeneration Assay in Growing Leaves. *Bio. Protoc.* **11**, e4010 (2021).

99. E. E. Kuchen, *et al.*, Generation of leaf shape through early patterns of growth and tissue polarity. *Science (1979).* **335**, 1092–1096 (2012).

100. J. Zhang, *et al.*, Molecular features of secondary vascular tissue regeneration after bark girdling in Populus. *New Phytologist* **192**, 869–884 (2011).

101. J. J. Chen, *et al.*, Differential regulation of auxin and cytokinin during the secondary vascular tissue regeneration in Populus trees. *New Phytologist* **224**, 188–201 (2019).

102. P. T. Serivichyaswat, *et al.*, High temperature perception in leaves promotes vascular regeneration and graft formation in distant tissues. *Development (Cambridge)* **149** (2022).

103. N. Kral, A. Hanna Ougolnikova, G. Sena, C. Giovanni Sena, Externally imposed electric field enhances plant root tip regeneration. *Regeneration* **3**, 156–167 (2016).

104. J. B. Reid, J. J. Ross, Regulation of tissue repair in plants. *Proc. Natl. Acad. Sci. U. S. A.* **108**, 17241–17242 (2011).

105. Z. W, *et al.*, A Jasmonate Signaling Network Activates Root Stem Cells and Promotes Regeneration. *Cell* **177**, 942-956.e14 (2019).

106. X. Ma, *et al.*, Ca2+ waves and ethylene/JA crosstalk orchestrate wound responses in Arabidopsis roots. *EMBO Reports 2025 26:12* **26**, 3187–3203 (2025).

107. G. De Lorenzo, S. Ferrari, F. Cervone, E. Okun, Extracellular DAMPs in Plants and Mammals: Immunity, Tissue Damage and Repair. *Trends Immunol.* **39**, 937–950 (2018).

108. M. Toyota, *et al.*, Glutamate triggers long-distance, calcium-based plant defense signaling. *Science (1979).* **361**, 1112–1115 (2018).

109. H. Suda, M. Toyota, Integration of long-range signals in plants: A model for wound-induced Ca2+, electrical, ROS, and glutamate waves. *Curr. Opin. Plant Biol.* **69**, 102270 (2022).

110. A. P. Shanmukhan, M. M. Mathew, D. Radhakrishnan, M. Aiyaz, K. Prasad, Regrowing the damaged or lost body parts. *Curr. Opin. Plant Biol.* **53**, 117–127 (2020).

111. Y. Fichman, R. Mittler, Integration of electric, calcium, reactive oxygen species and hydraulic signals during rapid systemic signaling in plants. *Plant Journal* **107**, 7–20 (2021).

112. S. A. R. Mousavi, A. Chauvin, F. Pascaud, S. Kellenberger, E. E. Farmer, GLUTAMATE RECEPTOR-LIKE genes mediate leaf-to-leaf wound signaling. *Nature* **500**, 422–426 (2013).

113. Q. Shao, Q. Gao, D. Lhamo, H. Zhang, S. Luan, Two glutamate- and pH-regulated Ca2+ channels are required for systemic wound signaling in Arabidopsis. *Sci. Signal.* **13** (2020).

114. M. Hernández-Coronado, *et al.*, Plant glutamate receptors mediate a bet-hedging strategy between regeneration and defense. *Dev. Cell* **57**, 451-465.e6 (2022).

115. T. Li, *et al.*, Calcium signals are necessary to establish auxin transporter polarity in a plant stem cell niche. *Nature Communications 2019 10:1* **10**, 726- (2019).

116. A. Modrego, *et al.*, Mapping of the Classical Mutation rosette Highlights a Role for Calcium in Wound-Induced Rooting. *Plant Cell Physiol.* **64**, 152–164 (2023).

117. S. Zhang, *et al.*, The calcium signaling module CaM–IQM destabilizes IAA–ARF interaction to regulate callus and lateral root formation. *Proc. Natl. Acad. Sci. U. S. A.* **119** (2022).

118. S. Gilroy, *et al.*, A tidal wave of signals: calcium and ROS at the forefront of rapid systemic signaling. *Trends Plant Sci.* **19**, 623–630 (2014).

119. G. Noctor, J. P. Reichheld, C. H. Foyer, ROS-related redox regulation and signaling in plants. *Semin. Cell Dev. Biol.* **80**, 3–12 (2018).

120. Y. Fichman, R. J. Myers, D. A. G. Grant, R. Mittler, Plasmodesmata-localized proteins and ROS orchestrate light-induced rapid systemic signaling in Arabidopsis. *Sci. Signal.* **14** (2021).

121. S. I. Zandalinas, Y. Fichman, R. Mittler, Vascular Bundles Mediate Systemic Reactive Oxygen Signaling during Light Stress. *Plant Cell* **32**, 3425–3435 (2020).

122. R. Schmidt, J. H. M. Schippers, ROS-mediated redox signaling during cell differentiation in plants. *Biochimica et Biophysica Acta (BBA) - General Subjects* **1850**, 1497–1508 (2015).

123. S. Yang, *et al.*, ROS: The Fine-Tuner of Plant Stem Cell Fate. *Trends Plant Sci.* **23**, 850–853 (2018).

124. F. Valandro, P. K. Menguer, C. Cabreira-Cagliari, M. Margis-Pinheiro, A. Cagliari, Programmed cell death (PCD) control in plants: New insights from the Arabidopsis thaliana deathosome. *Plant Science* **299**, 110603 (2020).

125. M. C. Maiuri, E. Zalckvar, A. Kimchi, G. Kroemer, Self-eating and self-killing: crosstalk between autophagy and apoptosis. *Nat. Rev. Mol. Cell Biol.* **8**, 741–752 (2007).

126. N. C. Chang, Autophagy and Stem Cells: Self-Eating for Self-Renewal. *Front. Cell Dev. Biol.* **8**, 138 (2020).

127. G. Tettamanti, E. Carata, A. Montali, L. Dini, G. M. Fimia, Autophagy in development and regeneration: role in tissue remodelling and cell survival. *European Zoological Journal* **86**, 113–131 (2019).

128. X. Ding, X. Zhang, M. S. Otegui, Plant autophagy: new flavors on the menu. *Curr. Opin. Plant Biol.* **46**, 113–121 (2018).

129. S. Signorelli, Ł. P. Tarkowski, W. Van den Ende, D. C. Bassham, Linking Autophagy to Abiotic and Biotic Stress Responses. *Trends Plant Sci.* **24**, 413–430 (2019).

130. M. Petersen, E. Ebstrup, E. Rodriguez, Going through changes – the role of autophagy during reprogramming and differentiation. *J. Cell Sci.* **137** (2024).

131. C. Galinha, *et al.*, PLETHORA proteins as dose-dependent master regulators of Arabidopsis root development. *Nature* **449**, 1053–1057 (2007).

132. K. Prasad, *et al.*, Arabidopsis PLETHORA transcription factors control phyllotaxis. *Current Biology* **21**, 1123–1128 (2011).

133. M. Kerstens, *et al.*, Nature and nurture: Genotype-dependent differential responses of root architecture to agar and soil environments. *Genes (Basel).* **12**, 1028 (2021).

134. N. Zhai, L. Xu, Pluripotency acquisition in the middle cell layer of callus is required for organ regeneration. *Nat. Plants* **7**, 1453–1460 (2021).

135. O. Smetana, *et al.*, High levels of auxin signalling define the stem-cell organizer of the vascular cambium. *Nature 2019 565:7740* **565**, 485–489 (2019).

136. R. Siligato, *et al.*, Multisite gateway-compatible cell type-specific gene-inducible system for plants. *Plant Physiol.* **170**, 627–641 (2016).

137. Y. Long, *et al.*, Optimizing FRET-FLIM labeling conditions to detect nuclear protein interactions at native expression levels in living Arabidopsis roots. *Front. Plant Sci.* **9**, 334379 (2018).

138. M. Aida, *et al.*, The PLETHORA genes mediate patterning of the Arabidopsis root stem cell niche. *Cell* **119**, 109–120 (2004).

139. M. Kerstens, *et al.*, PLETHORA transcription factors promote early embryo development through induction of meristematic potential. *Development (Cambridge)* **151** (2024).

140. M. Kerstens, *et al.*, Nature and nurture: Genotype-dependent differential responses of root architecture to agar and soil environments. *Genes (Basel).* **12** (2021).

141. L. Santuari, *et al.*, The PLETHORA Gene Regulatory Network Guides Growth and Cell Differentiation in Arabidopsis Roots. *Plant Cell* **28**, 2937–2951 (2016).

142. S. J. Clough, A. F. Bent, Floral dip: A simplified method for Agrobacterium-mediated transformation of Arabidopsis thaliana. *Plant Journal* **16**, 735–743 (1998).

143. D. Kurihara, Y. Mizuta, Y. Sato, T. Higashiyama, ClearSee: A rapid optical clearing reagent for whole-plant fluorescence imaging. *Development (Cambridge)* **142**, 4168–4179 (2015).

144. W. G. Choi, *et al.*, Orchestrating rapid long-distance signaling in plants with Ca2+, ROS and electrical signals. *Plant Journal* **90**, 698–707 (2017).

145. R. Rahni, I. Efroni, K. D. Birnbaum, A Case for Distributed Control of Local Stem Cell Behavior in Plants. *Dev. Cell* **38**, 635–642 (2016).

146. E. Larriba, *et al.*, Dynamic hormone gradients regulate wound-induced de novo organ formation in tomato hypocotyl explants. *Int. J. Mol. Sci.* **22** (2021).

147. T. Zhang, Y. Ge, G. Cai, X. Pan, L. Xu, WOX-ARF modules initiate different types of roots. *Cell Rep.* **42**, 112966 (2023).

148. L. Chen, B. Sun, L. Xu, W. Liu, Wound signaling: The missing link in plant regeneration. *Plant Signal. Behav.* **11** (2016).

149. Z. Wang, *et al.*, Salicylic acid promotes quiescent center cell division through ROS accumulation and down-regulation of PLT1, PLT2, and WOX5. *J. Integr. Plant Biol.* **63**, 583–596 (2021).

150. E. W. Chehab, C. Yao, Z. Henderson, S. Kim, J. Braam, Arabidopsis touch-induced morphogenesis is jasmonate mediated and protects against pests. *Current Biology* **22**, 701–706 (2012).

151. A. G. R. Jacobsen, G. Jervis, J. Xu, J. F. Topping, K. Lindsey, Root growth responses to mechanical impedance are regulated by a network of ROS, ethylene and auxin signalling in Arabidopsis. *New Phytologist* **231**, 225–242 (2021).

152. Y. Wang, L. Sun, R. Wang, H. Li, Z. Zhu, The AP2 transcription factors TOE1/TOE2 convey Arabidopsis age information to ethylene signaling in plant de novo root regeneration. *Planta* **257** (2023).

153. S. Y. Shin, *et al.*, Submergence promotes auxin-induced callus formation through ethylene-mediated post-transcriptional control of auxin receptors. *Mol. Plant* **15**, 1947–1961 (2022).

154. S. I. Zandalinas, R. Mittler, Vascular and nonvascular transmission of systemic reactive oxygen signals during wounding and heat stress. *Plant Physiol.* **186**, 1721–1733 (2021).

155. R. S. Marshall, R. D. Vierstra, Autophagy: The Master of Bulk and Selective Recycling. *Annu. Rev. Plant Biol.* **69**, 173–208 (2018).

156. Y. Wu, R. Xu, X. Zhuang, Multifaceted Roles of the ATG8 Protein Family in Plant Autophagy: From Autophagosome Biogenesis to Cargo Recognition. *J. Mol. Biol.* 168981 (2025). https://doi.org/10.1016/J.JMB.2025.168981.

157. F. Bu, M. Yang, X. Guo, W. Huang, L. Chen, Multiple Functions of ATG8 Family Proteins in Plant Autophagy. *Front. Cell Dev. Biol.* **8**, 532931 (2020).

158. T. N. Nguyen, M. Lazarou, A unifying model for the role of the ATG8 system in autophagy. *J. Cell Sci.* **135** (2022).

159. D. C. Bassham, Methods for analysis of autophagy in plants. *Methods* **75**, 181–188 (2015).

160. S.-H. Kim, C. Kwon, J.-H. Lee, T. Chung, Genes for Plant Autophagy: Functions and Interactions. *Mol. Cells* **34**, 413 (2012).

161. E. A. Allen, E. H. Baehrecke, Autophagy in animal development. *Cell Death Differ.* **27**, 903–918 (2020).

162. L. J. Restrepo, E. H. Baehrecke, Regulation and Functions of Autophagy During Animal Development. *J. Mol. Biol.* **436**, 168473 (2024).

163. A. Del Chiaro, *et al.*, An A. thaliana mutant lacking all nine ATG8 isoforms provides genetic evidence for functional specialization of ATG8 in plants. *J. Cell Sci.* **138** (2025).

164. J. L. Nieto-Torres, A. M. Leidal, J. Debnath, M. Hansen, Beyond Autophagy: The Expanding Roles of ATG8 Proteins. *Trends Biochem. Sci.* **46**, 673–686 (2021).

165. K. Dong, *et al.*, Comprehensive genetic analyses of Arabidopsis autophagy-related 8 family reveal redundant regulatory roles during autophagy. *New Phytologist* (2025). https://doi.org/10.1111/NPH.70418;WGROUP:STRING:PUBLICATION.

166. C. Takatsuka, Y. Inoue, K. Matsuoka, Y. Moriyasu, 3-Methyladenine Inhibits Autophagy in Tobacco Culture Cells under Sucrose Starvation Conditions. *Plant Cell Physiol.* **45**, 265–274 (2004).

167. T. Su, *et al.*, Autophagy: An Intracellular Degradation Pathway Regulating Plant Survival and Stress Response. *Front. Plant Sci.* **11**, 164 (2020).

168. M. Yagyu, K. Yoshimoto, New insights into plant autophagy: molecular mechanisms and roles in development and stress responses. *J. Exp. Bot.* **75**, 1234–1251 (2024).

169. M. Petersen, *et al.*, Autophagy in plants. *Autophagy Reports* **3** (2024).

170. T. Avin-Wittenberg, A. Honig, G. Galili, Variations on a theme: plant autophagy in comparison to yeast and mammals. *Protoplasma 2011 249:2* **249**, 285–299 (2011).

171. E. Millard, S. A. Tooze, ATG9 Not Just an Autophagy Related Protein. *J. Mol. Biol.* **437**, 169288 (2025).

172. S. Cheng, Q. Wang, H. Manghwar, F. Liu, Autophagy-Mediated Regulation of Different Meristems in Plants. *Int. J. Mol. Sci.* **23**, 6236 (2022).

173. L. Huang, *et al.*, Autophagy regulates glucose-mediated root meristem activity by modulating ROS production in Arabidopsis. *Autophagy* **15**, 407 (2019).

174. C. Giannini, *et al.*, Nuclear auxin signalling induces autophagy for developmental reprogramming. *bioRxiv* 2025.11.04.686542 (2025). https://doi.org/10.1101/2025.11.04.686542.

175. C. Yang, *et al.*, HY5-HDA9 Module Transcriptionally Regulates Plant Autophagy in Response to Light-to-Dark Conversion and Nitrogen Starvation. *Mol. Plant* **13**, 515–531 (2020).

176. F. Pietrocola, *et al.*, Regulation of autophagy by stress-responsive transcription factors. *Semin. Cancer Biol.* **23**, 310–322 (2013).

177. J. Füllgrabe, D. J. Klionsky, B. Joseph, The return of the nucleus: transcriptional and epigenetic control of autophagy. *Nature Reviews Molecular Cell Biology 2013 15:1* **15**, 65–74 (2013).

178. A. S. Gross, M. Raffeiner, Y. Zeng, S. Üstün, Y. Dagdas, Autophagy in Plant Health and Disease. *Annu. Rev. Plant Biol.* (2025). https://doi.org/10.1146/ANNUREV-ARPLANT-060324-094912.

179. P. Wang, T. M. Nolan, Y. Yin, D. C. Bassham, Identification of transcription factors that regulate ATG8 expression and autophagy in Arabidopsis. *Autophagy* **16**, 123–139 (2020).

180. W. J. Shu, M. J. Zhao, D. J. Klionsky, H. N. Du, Old factors, new players: transcriptional regulation of autophagy. *Autophagy* **16**, 956–958 (2020).

181. J. W. Kim, P. J. Seo, The early hormone signaling network underlying wound-induced de novo root regeneration. *J. Exp. Bot.* **76**, 1996–2004 (2025).

182. M. Kerstens, *et al.*, Two deeply conserved non-coding sequences control PLETHORA1/2 expression and coordinate embryo and root development. *Plant Commun.* **6** (2025).

183. A. Horstman, V. Willemsen, K. Boutilier, R. Heidstra, AINTEGUMENTA-LIKE proteins: hubs in a plethora of networks. *Trends Plant Sci.* **19**, 146–157 (2014).

184. Y. Du, B. Scheres, PLETHORA transcription factors orchestrate de novo organ patterning during Arabidopsis lateral root outgrowth. *Proc. Natl. Acad. Sci. U. S. A.* **114**, 11709–11714 (2017).

185. A. Bartlett, *et al.*, Mapping genome-wide transcription-factor binding sites using DAP-seq. *Nature Protocols 2017 12:8* **12**, 1659–1672 (2017).

186. T. Aoyama, N. H. Chua, A glucocorticoid-mediated transcriptional induction system in transgenic plants. *Plant Journal* **11**, 605–612 (1997).

187. N. Yamaguchi, C. M. Winter, F. Wellmer, D. Wagner, Identification of Direct Targets of Plant Transcription Factors Using the GR Fusion Technique. *Methods in Molecular Biology* **1284**, 123–138 (2015).

188. H. Hofhuis, *et al.*, Phyllotaxis and rhizotaxis in Arabidopsis are modified by three plethora transcription factors. *Current Biology* **23**, 956–962 (2013).

189. B. Deplancke, D. Alpern, V. Gardeux, The Genetics of Transcription Factor DNA Binding Variation. *Cell* **166**, 538–554 (2016).

190. S. Gundu, N. Tabassum, I. Blilou, Moving with purpose and direction: transcription factor movement and cell fate determination revisited. *Curr. Opin. Plant Biol.* **57**, 124–132 (2020).

191. S. Jeong, M. Volny, W. Lukowitz, Axis formation in Arabidopsis - transcription factors tell their side of the story. *Curr. Opin. Plant Biol.* **15**, 4–9 (2012).

192. E. van der Graaff, T. Laux, S. A. Rensing, The WUS homeobox-containing (WOX) protein family. *Genome Biology 2009 10:12* **10**, 248- (2009).

193. T. R. Bürglin, Analysis of TALE superclass homeobox genes (MEIS, PBC, KNOX, Iroquois, TGIF) reveals a novel domain conserved between plants and animals. *Nucleic Acids Res.* **25**, 4173–4180 (1997).

194. P. W. H. Holland, Evolution of homeobox genes. *Wiley Interdiscip. Rev. Dev. Biol.* **2**, 31–45 (2013).

195. S. H. Shiu, M. C. Shih, W. H. Li, Transcription Factor Families Have Much Higher Expansion Rates in Plants than in Animals. *Plant Physiol.* **139**, 18–26 (2005).

196. X. L. T. Hoang, D. N. H. Nhi, N. B. A. Thu, N. P. Thao, L.-S. P. Tran, Transcription Factors and Their Roles in Signal Transduction in Plants under Abiotic Stresses. *Curr. Genomics* **18**, 483 (2017).

197. T. Javed, S. J. Gao, WRKY transcription factors in plant defense. *Trends in Genetics* **39**, 787–801 (2023).

198. Y. Yoon, *et al.*, The Role of Stress-Responsive Transcription Factors in Modulating Abiotic Stress Tolerance in Plants. *Agronomy 2020, Vol. 10,* **10** (2020).

199. J. Mizoi, K. Shinozaki, K. Yamaguchi-Shinozaki, AP2/ERF family transcription factors in plant abiotic stress responses. *Biochimica et Biophysica Acta (BBA) - Gene Regulatory Mechanisms* **1819**, 86–96 (2012).

200. T. A. Meraj, *et al.*, Transcriptional Factors Regulate Plant Stress Responses Through Mediating Secondary Metabolism. *Genes (Basel).* **11**, 346 (2020).

201. A. M. Rodriguez, J. Kang, Regeneration enhancers: Starting a journey to unravel regulatory events in tissue regeneration. *Semin. Cell Dev. Biol.* **97**, 47 (2019).

202. W. Wang, *et al.*, Changes in regeneration-responsive enhancers shape regenerative capacities in vertebrates. *Science (1979).* **369** (2020).

203. A. P. Marand, A. L. Eveland, K. Kaufmann, N. M. Springer, cis-Regulatory Elements in Plant Development, Adaptation, and Evolution. *Annu. Rev. Plant Biol.* **74**, 111–137 (2023).

204. Y. Voichek, G. Hristova, A. Mollá-Morales, D. Weigel, M. Nordborg, Widespread position-dependent transcriptional regulatory sequences in plants. *Nature Genetics 2024 56:10* **56**, 2238–2246 (2024).

205. M. S. Otegui, *et al.*, Vacuolar degradation of plant organelles. *Plant Cell* **36**, 3036–3056 (2024).

206. D. Mijaljica, F. Spada, D. J. Klionsky, I. P. Harrison, Autophagy is the key to making chronic wounds acute in skin wound healing. *Autophagy* **19**, 2578–2584 (2023).

207. D. Moreno-Blas, T. Adell, C. González-Estévez, Autophagy in Tissue Repair and Regeneration. *Cells 2025, Vol. 14,* **14** (2025).

208. K. Sylakowski, A. Wells, ECM-regulation of autophagy: The yin and the yang of autophagy during wound healing. *Matrix Biology* **100–101**, 197–206 (2021).

209. L. Chen, B. Sun, L. Xu, W. Liu, Wound signaling: The missing link in plant regeneration. *Plant Signal. Behav.* **11** (2016).

210. S. A. Eming, P. Martin, M. Tomic-Canic, Wound repair and regeneration: Mechanisms, signaling, and translation. *Sci. Transl. Med.* **6** (2014).

211. L. A. Del Río, ROS and RNS in plant physiology: an overview. *J. Exp. Bot.* **66**, 2827–2837 (2015).

212. T. Avin-Wittenberg, Autophagy and its role in plant abiotic stress management. *Plant Cell Environ.* **42**, 1045–1053 (2019).

213. S. Magen, H. Seybold, D. Laloum, T. Avin-Wittenberg, Metabolism and autophagy in plants—a perfect match. *FEBS Lett.* **596**, 2133–2151 (2022).

214. S. Yamauchi, *et al.*, Autophagy controls reactive oxygen species homeostasis in guard cells that is essential for stomatal opening. *Proc. Natl. Acad. Sci. U. S. A.* **116**, 19187–19192 (2019).

215. K. Yoshimoto, *et al.*, Processing of ATG8s, Ubiquitin-Like Proteins, and Their Deconjugation by ATG4s Are Essential for Plant Autophagy. *Plant Cell* **16**, 2967–2983 (2004).

216. K. Yoshimoto, *et al.*, Organ-specific quality control of plant peroxisomes is mediated by autophagy. *J. Cell Sci.* **127**, 1161–1168 (2014).

217. M. Izumi, *et al.*, Autophagosome development and chloroplast segmentation occur synchronously for piecemeal degradation of chloroplasts. *Elife* **12** (2024).

218. H. Ishida, *et al.*, Mobilization of Rubisco and stroma-localized fluorescent proteins of chloroplasts to the vacuole by an ATG gene-dependent autophagic process. *Plant Physiol.* **148**, 142–155 (2008).

219. S. Wang, E. Blumwald, Stress-Induced Chloroplast Degradation in Arabidopsis Is Regulated via a Process Independent of Autophagy and Senescence-Associated Vacuoles. *Plant Cell* **26**, 4875–4888 (2015).

220. R. Scherz-Shouval, Z. Elazar, Regulation of autophagy by ROS: Physiology and pathology. *Trends Biochem. Sci.* **36**, 30–38 (2011).

221. V. Petrov, J. Hille, B. Mueller-Roeber, T. S. Gechev, ROS-mediated abiotic stress-induced programmed cell death in plants. *Front. Plant Sci.* **6** (2015).

222. K. Oikawa, *et al.*, Pexophagy suppresses ROS-induced damage in leaf cells under high-intensity light. *Nature Communications 2022 13:1* **13**, 1–17 (2022).

223. S. Chhajed, Y. Y. Li, S. Chen, Reactive Oxygen Species (ROS) Measurement in Arabidopsis Guard Cells in Response to Biotic and Abiotic Stresses. *Methods in Molecular Biology* **2832**, 205–212 (2024).

224. S. Y. Sun, N-acetylcysteine, reactive oxygen species and beyond. *Cancer Biol. Ther.* **9**, 109 (2010).

225. M. Zafarullah, W. Q. Li, J. Sylvester, M. Ahmad, Molecular mechanisms of N-acetylcysteine actions. *Cellular and Molecular Life Sciences* **60**, 6–20 (2003).

226. S. Gilroy, *et al.*, ROS, calcium, and electric signals: key mediators of rapid systemic signaling in plants. *Plant Physiol* **171**, 1606–1615 (2016).

227. H. Nagai, H. Tatara, K. Tanaka-Furuhashi, S. Kurata, T. Yano, Homeostatic Regulation of ROS-Triggered Hippo-Yki Pathway via Autophagic Clearance of Ref(2)P/p62 in the Drosophila Intestine. *Dev. Cell* **56**, 81-94.e10 (2021).

228. Y. Cao, *et al.*, ROS functions as an upstream trigger for autophagy to drive hematopoietic stem cell differentiation. *Hematology* **21**, 613–618 (2016).

229. R. Scherz-Shouval, Z. Elazar, Regulation of autophagy by ROS: Physiology and pathology. *Trends Biochem. Sci.* **36**, 30–38 (2011).

230. C. Lennicke, *et al.*, Enhancing autophagy by redox regulation extends lifespan in Drosophila. *Nature Communications* **16**, 1–13 (2025).

231. O. Kapuy, M. Holczer, M. Márton, T. Korcsmáros, Autophagy-dependent survival is controlled with a unique regulatory network upon various cellular stress events. *Cell Death Dis.* **12**, 1–11 (2021).

232. M. C. Gómez-Puerto, *et al.*, Activation of autophagy by FOXO3 regulates redox homeostasis during osteogenic differentiation. *Autophagy* **12**, 1804–1816 (2016).

233. C. Yang, M. Luo, X. Zhuang, F. Li, C. Gao, Transcriptional and Epigenetic Regulation of Autophagy in Plants. *Trends in Genetics* **36**, 676–688 (2020).

234. S. P. Metur, Y. Lei, Z. Zhang, D. J. Klionsky, Regulation of autophagy gene expression and its implications in cancer. *J. Cell Sci.* **136**, jcs260631 (2023).

235. H. Zhang, The Genetics of Autophagy in Multicellular Organisms. *Annu. Rev. Genet.* **56**, 17–39 (2022).

236. A. Del Chiaro, *et al.*, An A. thaliana mutant lacking all nine ATG8 isoforms provides genetic evidence for functional specialization of ATG8 in plants. *J. Cell Sci.* **138** (2025).

237. Q. Song, H. Liu, H. Zhen, B. Zhao, Autophagy and its role in regeneration and remodeling within invertebrate. *Cell Biosci.* **10** (2020).

238. J. Kang, Z. Dong, J. Wang, G. Chen, D. Liu, Autophagy-related Djatg8 is required for remodeling in planarian Dugesia japonica. *Biol. Open* **8** (2019).

239. L. Y. Lin, *et al.*, Role of autophagy-related proteins ATG8f and ATG8h in the maintenance of autophagic activity in Arabidopsis roots under phosphate starvation. *Front. Plant Sci.* **14**, 1018984 (2023).

240. J. S. Mudunkothge, B. A. Krizek, Three Arabidopsis AIL/PLT genes act in combination to regulate shoot apical meristem function. *The Plant Journal* **71**, 108–121 (2012).

241. S. Nole-Wilson, T. L. Tranby, B. A. Krizek, AINTEGUMENTA-like (AIL) genes are expressed in young tissues and may specify meristematic or division-competent states. *Plant Mol. Biol.* **57**, 613–628 (2005).

242. A. P. Mähönen, *et al.*, PLETHORA gradient formation mechanism separates auxin responses. *Nature* **515**, 125–129 (2014).

243. J. Julian, *et al.*, ATG8ylation of vacuolar membrane protects plants against cell wall damage. *Nature Plants 2025 11:2* **11**, 321–339 (2025).

244. X. Zheng, *et al.*, ATG8ylation-mediated tonoplast invagination mitigates vacuole damage. *Nature Communications 2025 16:1* **16**, 6621- (2025).

245. S. Di Meo, T. T. Reed, P. Venditti, V. M. Victor, Role of ROS and RNS Sources in Physiological and Pathological Conditions. *Oxid. Med. Cell. Longev.* **2016**, 1245049 (2016).

246. A. V. Van Huizen, S. J. Hack, J. M. Greene, L. J. Kinsey, W. S. Beane, Reactive Oxygen Species Signaling Differentially Controls Wound Healing and Regeneration. *bioRxiv* 2022.04.05.487111 (2022). https://doi.org/10.1101/2022.04.05.487111.

247. B. Orman-Ligeza, *et al.*, RBOH-mediated ROS production facilitates lateral root emergence in Arabidopsis. *Development (Cambridge)* **143**, 3328–3339 (2016).

248. J. Xu, More than a blueprint: Developmental regulators secure the cellular environment for regeneration. *Proceedings of the National Academy of Sciences* **123**, e2600463123 (2026).